

~~UNCLASSIFIED~~Copy
RM E51B07

MAY 21 1951



RESEARCH MEMORANDUM

ALTITUDE-PERFORMANCE AND REYNOLDS
NUMBER INVESTIGATION OF CENTRIFUGAL
FLOW-COMPRESSOR TURBOJET ENGINE

By H. D. Wilsted and R. E. Grey

Lewis Flight Propulsion Laboratory
Cleveland, Ohio

FOR REFERENCE

NOT TO BE TAKEN FROM THIS ROOM

CLASSIFIED DOCUMENT

This document contains classified information affecting the National Defense of the United States within the meaning of the Espionage Act, USC 50:31 and 32. Its transmission or the revelation of its contents in any manner to an unauthorized person is prohibited by law.

Information so classified may be imparted only to persons in the military and naval services of the United States, appropriate civilian officers and employees of the Federal Government who have a legitimate interest therein, and to United States citizens of known loyalty and discretion who of necessity must be informed thereof.

CLASSIFICATION CHANGED

UNCLASSIFIED UNAVAILABLE

To

Naca Rec'd. Effective
By authority of 4 RN-118 Date 3-19-57
NB 4-4-57

NATIONAL ADVISORY COMMITTEE FOR AERONAUTICS

WASHINGTON

NACA LIBRARY

LANGLEY AERONAUTICAL LABORATORY

May 15, 1951

Langley Field, Va.

~~CONFIDENTIAL~~~~UNAVAILABLE~~



3 1176 01435 2182

1

NACA RM E51B07

2113

NATIONAL ADVISORY COMMITTEE FOR AERONAUTICS

RESEARCH MEMORANDUMALTITUDE-PERFORMANCE AND REYNOLDS NUMBER INVESTIGATION
OF CENTRIFUGAL-FLOW-COMPRESSOR TURBOJET ENGINE

By H. D. Wilsted and R. E. Grey

SUMMARY

The performance of a centrifugal-flow-compressor turbojet engine was investigated in an altitude chamber over a range of simulated-flight conditions from sea level to 65,000 feet at flight Mach numbers from 0.27 to 1.25. In addition to showing altitude performance characteristics, the effect of Reynolds number on altitude engine performance, corrected to standard sea-level conditions, is presented.

Engine performance data could be generalized at altitudes to 30,000 feet by conventional methods but could not be generalized for higher altitudes. At an altitude of 30,000 feet, performance data could also be generalized for varying flight Mach number over the range of engine speeds at which critical flow existed in the jet nozzle. At altitudes above 30,000 feet, engine performance was correlated with Reynolds number index based on engine-inlet stagnation conditions. This correlation was independent of flight Mach number for the engine speeds investigated (90 and 100 percent of rated speed). An empirical correlation parameter for combustion efficiency was presented, which was a function of engine operating conditions and correlated all of the data except at fuel-air ratios below 0.007.

INTRODUCTION

The design and the tactical use of aircraft for ever increasing altitudes and flight speeds demands an accurate method for predicting engine performance at these flight conditions. Altitude-chamber and wind-tunnel investigations of the performance of turbojet engines such as those reported in references 1 to 4 have shown that the conventional correction factors fail to generalize the engine performance variables at high altitudes. An investigation was therefore made at the NACA Lewis laboratory to determine the altitude performance of the

J33-A-23 turbojet engine and to demonstrate the magnitude of departure of actual altitude performance from that predicted from sea-level performance.

The investigation was conducted in two parts; the first phase consisted of a conventional engine performance investigation with engine speed as the primary variable and with flight Mach number and altitude held constant at each of several values. In this phase, altitude was varied from sea level to 50,000 feet and the flight Mach number was varied from 0.27 to 1.25. In the second phase of the investigation, pressure altitude was the primary variable with flight Mach number and engine speed held constant at each of several values. In this phase of the investigation, pressure altitude was varied from 10,000 to 65,000 feet while flight Mach number was held constant at 0.37, 0.62, and 0.91 at each of two constant engine speeds, 90 and 100 percent of rated speed. Engine-inlet-air temperature was also held constant so that each engine speed resulted in a constant compressor Mach number.

S113

APPARATUS AND PROCEDURE

Engine

Two J33-A-23 turbojet engines were used in this investigation. The engines have a centrifugal-flow-type compressor, 14 through-flow tubular combustors, and a single-stage impulse turbine. The engine had a sea-level thrust rating of 4600 pounds at a turbine-outlet temperature of 1265° F at rated speed (11,750 rpm). At this condition, the engine fuel flow was approximately 4830 pounds per hour. The engine weight less starter, generator, and tachometer generator was 1795 pounds and the maximum diameter was $50\frac{1}{2}$ inches. A J33-A-23 engine-bearing serial number A-071878 was used in phase I of the investigation. This engine was destroyed by fire of unknown origin near the end of the first phase of the investigation. An engine bearing serial number A-074460 was used for phase II of the investigation.

Altitude Chamber

The altitude chamber in which the engine was installed is schematically shown in figure 1. The chamber was 10 feet in diameter and 60 feet long. Air could be supplied to the chamber at temperatures between 90° and -40° F and pressures could be varied to simulate altitudes from sea level to about 65,000 feet. The engine was mounted on a thrust frame that was connected through linkage to a thrust-measuring cell. The thrust cell was a null-type pressure-balanced diaphragm. The thrust

apparatus was calibrated by the dead-weight method with the engine and all fuel and instrumentation connections in place.

The inlet or ram-pressure section of the chamber was separated from the exhaust or altitude-pressure section of the chamber by a bulkhead. The seal between the tail pipe and the bulkhead consisted of three asbestos board rings. These rings were installed so as to avoid interference with axial movement required by engine expansion and thrust measurement and to allow approximately 1 inch lateral movement to prevent binding.

Instrumentation

Engine instrumentation locations, before and after each of the principal components of the engine, are shown in figure 2. The details of the instrumentation for stations 1 to 7 are shown in figure 3. Engine-inlet temperature was measured by eight iron-constantan thermocouples at the cowl inlet (fig. 3(a)). Engine-inlet pressure was measured by five total-pressure tubes on both the front and rear compressor-inlet screens (fig. 3(b)). Details of the compressor-outlet rakes, burner-outlet probes (used to detect blow-out), diffuser thermocouples supplied with the engine and used for engine-temperature indication, and tail-pipe probes and rakes used to obtain pressures and temperatures for computing engine air flow are shown in figures 3(c) to 3(h). The simulated altitude pressure was measured by two probes located near the jet-nozzle outlet in the exhaust portion of the chamber. In the first phase of the investigation, fuel flow was measured by a remote-reading, variable-area orifice meter, and engine speed was measured by an electrical frequency-impulse counter. In order to improve accuracy of data and ease of operation in the second phase of the investigation, the remote-reading fuel-flow meter was replaced with calibrated rotameters; altitude-chamber pressure gages were replaced with calibrated absolute manometers, whose greater scale length allowed more accurate pressure readings; and an electrically operated strobotac was installed to assist in maintaining constant engine-speed settings.

Procedure

The investigation was conducted in two phases: (1) a conventional engine performance investigation; and (2) an evaluation of the effects of inlet-air density on engine performance. In the first phase of the investigation, a desired flight condition was maintained while the engine speed was varied. Simulated-flight conditions were varied over a range of

2113

altitudes from sea level to 50,000 feet at a Mach number of 0.67 and at an altitude of 30,000 feet the simulated flight Mach number was varied from 0.27 to 1.25. The compressor-inlet pressure and temperature settings were held at NACA standard altitude pressures and temperatures corresponding to the particular flight Mach number assuming 100-percent ram pressure recovery. The flight Mach number is based on ratio of inlet to exhaust pressure. In the second phase of the investigation, the compressor-inlet temperature, engine speed, and flight Mach number were maintained while the altitude was varied. The pressure altitude was varied from 10,000 to 65,000 feet, corresponding to an exhaust pressure of about 1460 to 119 pounds per square foot. The inlet temperature was held constant at 520° R. Two engine speeds, 90 and 100 percent of rated, were investigated for each of three flight Mach numbers, 0.37, 0.62, and 0.91. The symbols used in this report and the methods used in computing engine performance variables are presented in the appendix.

RESULTS AND DISCUSSION

A summary of the performance and operational data obtained during the first phase of the investigation at various simulated-altitude conditions is presented in table I. Altitude data corrected for small variations in compressor-inlet pressure, inlet temperature, and exhaust-pressure settings are summarized in table II. Table II also includes the data corrected to conditions of NACA standard sea-level static pressure and temperature at the compressor inlet.

Simulated-Flight Performance

Effect of altitude. - Altitude performance data from table II obtained at a flight Mach number of 0.67 and simulated altitudes from sea level to 50,000 feet are presented in figures 4 to 9 to show the effect of altitude on the engine performance. Jet thrust, net thrust, air flow, and fuel flow (figs. 4, 5, 6, and 7, respectively) rapidly decreased with increasing altitude as would be expected because of the accompanying decrease in engine inlet-air density. The net-thrust specific fuel consumption (fig. 8) decreased with increasing altitude until 30,000 feet was reached and then increased with further increase in altitude. These trends result from the combined effects of (1) an increase in cycle efficiency with decreasing inlet temperatures, and (2) a reduction in component efficiency at high altitude. The tail-pipe indicated temperature (fig. 9) decreased with increasing altitude at the low engine speeds as a direct effect of reduced inlet-air temperature on operating temperatures and on the effective compressor Mach number. At the higher engine speeds, there was a slight rise in tail-pipe temperature with increasing

altitude, which is attributed to a reduction in component efficiencies at high altitudes. Similar tail-pipe-temperature trends are shown and explained in reference 1.

Effect of flight Mach number. - Performance data, obtained at an altitude of 30,000 feet for flight Mach numbers from 0.27 to 1.25, are presented in figures 10 to 15 to show the effects of flight Mach number on the engine performance parameters. Jet thrust, air flow, and fuel flow (figs. 10, 12, and 13, respectively) generally increased as would be expected with the increasing inlet-air density resulting from the increased flight Mach number. The net thrust (fig. 11) increased with increasing flight Mach number at high engine speeds, but decreased at low engine speeds. The net-thrust specific fuel consumption (fig. 14) generally increased with increasing flight Mach number. The tail-pipe indicated temperatures (fig. 15) decreased with increasing flight Mach number; this trend was most pronounced at the low engine speeds.

Generalized Performance

Performance data were corrected to standard sea-level static conditions in the conventional manner (reference 5). The development of this method for generalizing turbine-engine performance parameters assumes flow similarity throughout the engine for any particular compressor-tip Mach number. In this development, the flow characteristics were assumed to be insensitive to Reynolds number effects and the efficiencies of the engine components were assumed to be unaffected by changes in altitude and flight Mach number.

Effect of altitude. - The corrected engine performance data (from table II) obtained at a flight Mach number of 0.67 and simulated altitudes from sea level to 50,000 feet are presented in figures 16 to 22 to show the effect of altitude on the corrected engine performance variables. The corrected values of jet thrust (fig. 16) generalized to an altitude of 30,000 feet. There was a decrease in corrected jet thrust at 40,000- and 50,000-foot altitudes. The apparent equality of the corrected jet thrust at 40,000- and 50,000-foot altitudes probably results from an insensitivity of the thrust mechanism to the small thrust measurements at 50,000 feet. Corrected net thrust (fig. 17) and corrected air flow (fig. 18) also generalized to 30,000 feet and showed reductions at altitudes above 30,000 feet. These reductions in corrected air flow are attributed to the internal losses associated with the lower Reynolds number existing in the engine flow passages at high altitude. The reduction in corrected air flow with increasing altitude causes the corrected jet and net thrust to decrease in a similar manner. The corrected fuel flow

(fig. 19) and the corrected net-thrust specific fuel consumption (fig. 20) generally increased with increasing altitude except at the high engine speeds where generalization was obtained to 30,000 feet and thereafter an increase with altitude occurred for altitudes above 30,000 feet. These trends in corrected fuel consumption and corrected specific fuel consumption are the result of lower combustion efficiencies (fig. 21) associated with the lower combustor pressure existing at the low engine speeds and high altitudes. At low corrected engine speeds, there is a rapid decrease in combustion efficiency with increasing altitude, but at high engine speeds where the compressor pressure ratio is high there is no apparent loss in combustion efficiency until altitudes greater than 30,000 feet are reached. The corrected tail-pipe indicated temperature (fig. 22) generalized to 40,000 feet but increased at higher altitudes.

Effect of flight Mach number. - In general, at a particular corrected engine speed, the increased inlet pressure with increasing Mach number raises the total expansion ratio of the engine (from turbine inlet to exhaust-nozzle throat) until critical flow is established in the jet nozzle. After critical flow is established, the expansion pressure ratio of the engine remains constant with increasing flight Mach number. With critical flow in the jet nozzle, generalization of flow characteristics throughout the engine should be possible unless engine-inlet pressures are low enough to adversely affect engine-component efficiencies, as discussed in connection with altitude effects. When the jet nozzle is choked, corrected pressures, temperatures, and air flow would therefore be expected to generalize for compressor-inlet air densities greater than that corresponding to a 30,000-foot altitude and a flight Mach number of 0.67. Satisfactory generalization of the corrected pressure, temperature, and air flow would not necessarily result in a constant value of combustion efficiency because combustion efficiency is dependent on the actual pressure, temperature, and air flow. The corrected fuel flow and corrected specific fuel consumption would obviously vary with the combustion efficiency. Corrected jet thrust would also be expected to vary with flight Mach number because it is sensitive, under critical flow conditions in the jet nozzle, not only to the internal flow conditions but it is also a function of the excess pressure over ambient pressure existing at the nozzle outlet. However, when the product of this excess pressure and the jet area is properly introduced into the jet-thrust term, as described in reference 1, a generalization of the corrected engine

thrust in terms of a thrust parameter $\frac{F_j + p_0 A_s}{8}$ would be expected.

The corrected engine performance data (table II) obtained at a simulated altitude of 30,000 feet and flight Mach numbers from 0.27 to 1.25 are compared to show the effect of flight Mach number on the

2115
corrected values of engine performance parameters (figs. 23 to 27). The corrected jet-thrust parameter presented in figure 23 generalized over the range of engine speeds for which the jet nozzle was choked. The corrected air flow (fig. 24) generalized for Mach numbers from 0.67 to 1.25 for the entire range of engine speeds investigated, but decreased slightly at the lower Mach numbers. The corrected fuel flow (fig. 25) increased as flight Mach number decreased at the low engine speeds but generalized at the higher engine speeds. This generalization indicates that at high engine speeds the combustor pressure and temperature were sufficiently high and that combustion efficiency was unaffected. The nearly constant value of combustion efficiency at high engine speed is illustrated by the data of figure 26. At the lower engine speeds, there is an indication of increasing combustion efficiency with increasing flight Mach number but because of data scatter, curves could not be drawn for each flight Mach number. The corrected tail-pipe indicated temperature (fig. 27) showed a slightly greater sensitivity to flight Mach number than either the corrected jet-thrust parameter or the corrected fuel flow as indicated by the separation of the flight Mach number curves from the generalized curve at higher corrected engine speeds. The effect of flight Mach number on the generalization of engine performance data may be summarized as follows: Over the range of inlet pressures investigated (628 to 1569 lb/sq ft corresponding to flight Mach numbers of 0.27 to 1.25 at 30,000-ft altitude), the corrected jet-thrust parameter generalized for corrected engine speeds for which the jet nozzle was choked. The corrected fuel flow and corrected indicated tail-pipe temperature generalized for corrected engine speeds slightly above that for which the jet nozzle was choked. The corrected air flow was sensitive to inlet-air density at 30,000 feet for Mach numbers below 0.67. At higher altitudes where it was shown that engine components become more sensitive to changes in engine inlet-air density, the corrected performance parameters would be expected to show a greater sensitivity to varying flight Mach number than was evident at the 30,000-foot-altitude conditions.

SECONDARY ALTITUDE EFFECTS

The high-altitude corrected performance data (figs. 16 to 22) have shown the actual corrected engine performance to be poorer than the corrected performance predicted from sea-level data. Also, the data for varying flight Mach number (figs. 23 to 27) showed that the corrected performance parameters did not generalize over the complete operating range. This lack of generalization was evident to some extent even when the jet nozzle was choked. These departures are attributed to two fundamental effects. The first is the well-known fact that combustion efficiency decreases with decreasing pressure and temperature. Although variations in the combustion efficiency may thus explain the changes in performance parameters involving fuel flow, it does not account for

variations in corrected thrust, air flow, and exhaust-gas temperatures. Because these performance variations indicate internal losses and are associated with high-altitude operation, they may be attributed to an effect of Reynolds number as discussed in references 1 to 5. The second fundamental factor then is the effect of low Reynolds number on energy losses induced by increasing boundary-layer build up and some flow separation from the walls of the flow channels within the engine. These energy losses are then reflected in decreased component efficiencies.

The flow characteristics that are dependent on the Reynolds number for a given flow system have been expressed as a Reynolds number index. (See reference 6.)

$$\text{Re index} = \frac{P}{\mu \sqrt{T}} \quad (1)$$

When this expression is put in terms of pressure, temperature, and viscosity ratios, the Reynolds number index may be expressed, as in reference 7, by

$$\text{Re index} \equiv \frac{\delta}{\rho \sqrt{\theta}} \quad (2)$$

The variation of Reynolds number index with altitude and flight Mach number is tabulated in table III.

The Reynolds number index may, for all practical purposes, be expressed as

$$\text{Re index} \approx \frac{\delta}{\theta} \quad (3)$$

because the viscosity of gases over a reasonable temperature range is nearly proportional to the square root of the absolute temperature. From this expression, it can be seen that to obtain the lowest possible Reynolds number the engine-inlet pressure should be low and the inlet temperature high. The second phase of the investigation was therefore conducted with the inlet-air temperature held constant at 520° R while the inlet pressure was reduced progressively until the limit of the test facilities was reached. These data, obtained on engine serial number A-074460 for 90 and 100 percent of rated engine speed and for constant flight Mach numbers of 0.37, 0.62, and 0.91, are tabulated in table IV and plotted in figures 28 to 32. The dashed curves on these figures represent values obtained from faired curves through data obtained in the first phase of the investigation on engine serial number A-071878.

These data are plotted as the ratio of the corrected altitude performance to the corrected performance predicted from static sea-level performance of the engine. The magnitude of this ratio thus indicates the departure of the altitude performance from the predicted performance for various values of Reynolds number index. All the data for a given engine, and for a given engine speed over a range of flight Mach numbers correlate to a single curve.

The air flow (fig. 28) and jet-thrust parameter (fig. 29) fall below the predicted values at low values of Reynolds number index. The air flow for the engine used in the first phase of the investigation has the same trend as the second engine but the effects of low Reynolds number are greater on the performance of the first engine. The fuel flow (fig. 30) increases above the predicted values as the Reynolds number index was reduced and again the trend is the same for both engines with the first engine being affected more at the low values of Reynolds number index. This increase in fuel flow at low Reynolds numbers resulted from the decreased combustion efficiency that accompanied the decreasing engine-inlet pressure. When the fuel flow was corrected to a unity combustion efficiency (burned fuel) to isolate the Reynolds number effects, the burned fuel flow (fig. 31) was less than that predicted from static sea-level calibration. Again the effect of Reynolds number was greater on the first engine. The decrease in burned fuel flow was not as great, however, as the decrease in air flow (fig. 28). The ratio of burned fuel to air flow therefore increased as required to obtain the increased tail-pipe temperatures of figure 32. The effect of the low Reynolds number was similar for both engines but, in general, was somewhat greater on the first engine.

The correlation of the data of figures 28 to 32 with Reynolds number index show these parameters to be independent of flight Mach number and that departures from predicted performance are significant only below a Reynolds number index of 0.5 at the two engine speeds investigated. At the lower engine speed (corrected engine speed 90 percent of rated), the departures of the actual performance from the predicted performance were generally greater than that for rated engine speed. The departure of actual engine performance at high altitude from that predicted by low-altitude performance may be accounted for by Reynolds number and combustion-efficiency effects.

Combustion efficiency was separated from the fuel-consumption data of figure 30 to isolate the Reynolds number effect in figure 31. No attempt has yet been made to correlate this combustion-efficiency data. A correlation of the combustion efficiency with flight conditions is required, however, if reasonably accurate predictions of flight fuel consumption are to be made possible.

Combustion efficiency has been correlated with the parameter $P_b t_b / V_b$ as discussed in reference 8. An attempt to derive this parameter in terms of engine-inlet pressure and temperature and of engine speed by use of the conservation-of-energy and continuity equations led to a somewhat complex expression. A more useful parameter can be obtained by a combination of engine operating conditions as follows:

Because total and static pressures at a given station vary in the same manner, the equation may be written as

$$\frac{P_b t_b}{V_b} = K \frac{P_b^2}{W_a}$$

Because total and static pressures at a given station vary in the same manner, this expression may be written as

$$K \frac{P_b^2}{W_a} \approx K' \frac{P_b^2}{W_a}$$

Then

$$K' \frac{P_b^2}{W_a} = K' P_2 \sqrt{T_2} \left(\frac{P_2}{W_a \sqrt{T_2}} \right) \left(\frac{P_b}{P_2} \right)^2$$

$$= K' \delta \sqrt{\theta} \left(\frac{\delta}{W_a \sqrt{\theta}} \right) \left(\frac{P_b}{P_2} \right)^2$$

For both engines used in this investigation, the product of $\left(\frac{\delta}{W_a \sqrt{\theta}} \right) \left(\frac{P_b}{P_2} \right)^2$ was found empirically to be approximately proportional to the corrected engine speed to the second power.

Therefore

$$\frac{P_b t_b}{V_b} \propto \delta \sqrt{\theta} \left(\frac{N}{\sqrt{\theta}} \right)^2$$

The correlation of $\delta N \sqrt{\theta} \left(\frac{N}{\sqrt{\theta}} \right)^2$ with $\frac{P_b t_b}{V_b}$ is shown in figure 33. The correlation of η_b and $\delta N \sqrt{\theta} \left(\frac{N}{\sqrt{\theta}} \right)^2$ is shown in figure 34. The engine fuel-air ratio is known to affect combustion efficiency in some combustors (reference 8). This fuel-air-ratio effect is unaccounted for

in this parameter and the few points for which the fuel-air ratio was below 0.007 did not correlate and therefore are not plotted on the figure.

It is to be noted that the performance of both engines of the same model type are not in agreement. This difference in measured performance is attributable to several factors: difference in accumulated running time on each engine, tolerances in manufacturing specifications for the fuel nozzles and other parts, possible trends of different fuel-flow measuring instruments on each engine at low fuel flows, and the improved technique in the running of the second phase of the investigation. It is believed that the main contributing factors are the longer accumulated running time on the first engine (about 30 percent) and possibly poorer spray quality from the fuel nozzles, which would explain the poorer combustion efficiency depicted in figure 33.

In order to illustrate the magnitude of departures of actual from predicted performance, consider a flight condition of 60,000-foot altitude at a Mach number of 0.62 and an actual engine speed of 10,600 rpm (90 percent of rated speed), which is a corrected engine speed of 11,750 rpm. The engine speed ratio is 1.00 and, by interpolation from

table III, the Reynolds number index $\frac{\delta}{\phi \sqrt{\theta}}$ is 0.12 and the engine operating parameter $\delta \sqrt{\theta} \left(\frac{N}{\sqrt{\theta}} \right)^2$ is 1.15×10^7 . With these values the actual corrected performance as compared with the predicted corrected performance of the second engine were taken from figures 28 to 32 to be as follows: air-flow loss, 5 percent; jet-thrust parameter loss, 4 percent; fuel-flow increase, 7 percent; burned fuel-flow decrease, 4 percent; and tail-pipe-indicated-temperature increase, 1.5 percent. The engine combustion efficiency decreased 15 percent as seen in figure 33 for the second engine. Computed from these values the jet-thrust loss was 6.5 percent, the net-thrust loss was 7 percent, and the increase in specific fuel consumption was 15.5 percent. These trends would be greater for the first engine or at a lower Reynolds number for either engine.

SUMMARY OF RESULTS

The performance of a centrifugal-flow-compressor-type turbojet engine was investigated over a range of simulated-flight conditions from sea level to 65,000 feet and flight Mach numbers from 0.27 to 1.25. The results of this investigation may be summarized as follows:

1. Engine performance data could be generalized by conventional methods for altitudes up to 30,000 feet at a flight Mach number of 0.67.

At an altitude of 30,000 feet, performance data could also be generalized for varying flight Mach number over the range of engine speeds at which critical flow existed in the jet nozzle. At higher altitude conditions, the engine performance was correlated by plotting performance parameters against a Reynolds number index based on engine inlet-air pressure, temperature, and viscosity. For the corrected engine speeds investigated (90 and 100 percent of rated speed), this correlation included the effect of flight Mach number.

2112

2. An empirical correlation parameter, based on engine-inlet pressure and temperature and on engine speed, correlated combustion efficiency for all data obtained except at fuel-air ratios below 0.007.

3. At an altitude of 60,000 feet, a Mach number of 0.62, and an actual engine speed of 10,600 rpm (90 percent of rated), the engine performance as compared to the predicted performance was found to be as follows: air-flow loss, 5 percent; jet-thrust loss, 6.5 percent; tail-pipe-indicated-temperature increase, 1.5 percent; net-thrust loss, 7 percent; specific-fuel-consumption increase, 15.5 percent; and engine-combustion-efficiency decrease, 15 percent. At the lower engine speed investigated, the departure of engine performance from predicted performance was generally greater than for the higher speed and the first engine used in the investigation indicated a greater Reynolds number effect on performance than the second engine.

Lewis Flight Propulsion Laboratory,
National Advisory Committee for Aeronautics,
Cleveland, Ohio.

APPENDIX

SYMBOLS AND METHODS OF CALCULATIONS

Symbols

A	area, sq ft
F	thrust, lb
g	acceleration due to gravity, 32.2 ft/sec ²
H	enthalpy, Btu/lb
J	mechanical equivalent of heat, 778 ft-lb/Btu
K,K'	proportionality constants
M	Mach number
N	engine speed, rpm
P	absolute total pressure, lb/sq ft
p	absolute static pressure, lb/sq ft
R	gas constant, 53.3 ft-lb/(lb)(°R)
Re	Reynolds number
T	total temperature, °R
t	static temperature, °R
V	velocity, ft/sec
V _b	burner reference velocity, ft/sec
W _a	air flow, lb/sec
W _f	fuel flow, lb/hr
W _g	gas flow, lb/sec
β	thermocouple impact recovery factor
γ	ratio of specific heats

2113

- δ ratio of compressor-inlet absolute total pressure to absolute static pressure of NACA standard atmosphere at sea level
- η_b combustion efficiency
- θ ratio of compressor-inlet absolute total temperature to absolute static temperature of NACA standard atmosphere at sea level
- μ absolute viscosity of air at compressor inlet (values obtained from reference 10), ft^2/sec
- φ ratio of absolute viscosity of air at compressor inlet to viscosity of NACA standard atmosphere at sea level

Subscripts:

- alt altitude
- b burner inlet
- i indicated
- j jet
- n net
- SL sea level
- s seal

Station notation (fig. 2):

- 0 free stream
- 1 cowl inlet
- 2 compressor inlet
- 3 compressor outlet
- 4 turbine inlet
- 5 diffuser outlet
- 6 tail pipe (upstream of jet nozzle)

- 7 jet-nozzle inlet
 8 jet-nozzle outlet (throat)

2113

Methods of Calculations

Air flow. - Engine air flow was calculated by subtracting the fuel flow from the computed gas flow through the engine. The gas flow was computed from measurements of temperature in the tail pipe at station 6 and total and static pressure at the jet-nozzle inlet at station 7:

$$W_a = W_g - \frac{W_f}{3600}$$

where

$$W_g = \frac{P_7 A_7}{R t_7} \sqrt{2gJ\Delta H_7}$$

and ΔH_7 is the enthalpy difference between total- and static-pressure conditions, as determined from reference 9.

The static temperature was calculated from the indicated temperature by the following relation:

$$t_7 = T_{6,i} - \beta \left(\frac{V_7^2}{2gR \frac{\gamma}{\gamma-1}} \right)$$

$$t_7 = \frac{T_{6,i}}{1 + \beta \left(\frac{T_7}{t_7} - 1 \right)}$$

where the temperature ratio was determined from the jet-nozzle-inlet total to static pressure ratio by means of reference 9. The gas velocity at station 6 was assumed to be equal to the velocity at station 7. The thermocouple impact recovery factor β was evaluated at 0.80 from thermocouple calibrations.

Simulated flight speed. - The simulated flight speed at which the engine was operated was determined from the following relation:

$$v_0 = \sqrt{2gR \frac{\gamma}{\gamma-1} t_0 \left[\left(\frac{P_2}{P_0} \right)^{\frac{\gamma-1}{\gamma}} - 1 \right]}$$

where γ was assumed to be 1.40.

Flight Mach number. - The flight Mach number was calculated from the compressor-inlet total to ambient static pressure ratio, assuming 100-percent ram recovery, by the following relation:

$$M_0 = \sqrt{\frac{2}{\gamma-1} \left[\left(\frac{P_2}{P_0} \right)^{\frac{\gamma-1}{\gamma}} - 1 \right]}$$

where γ was assumed to be 1.40.

Jet thrust. - The jet thrust was determined from the altitude-chamber thrust indicator by multiplying the diaphragm pressure by a constant and adding a correction factor to account for the pressure differential across the tail-pipe seal. The relation used was:

$$F_j = F_i + A_s (P_2 - p_0)$$

Net thrust. - Net thrust was calculated from jet thrust by subtracting the engine inlet-air momentum, according to the relation

$$F_n = F_j - \frac{W_a V_0}{g}$$

Burner reference velocity. - The burner reference velocity used in the combustion-efficiency correlation parameter is

$$V_b = \frac{W_a R t_b}{A_b P_b}$$

where A_b is the maximum cross-sectional area of the burner flow passages.

REFERENCES

1. Barson, Zelmar, and Wilsted, H. D.: Altitude-Chamber Performance of British Rolls-Royce Nene II Engine. I - Standard 18.75-Inch-Diameter Jet Nozzle. NACA RM E9I23, 1949.
2. Vincent, K. R., and Gale, B. M.: Altitude Performance of J35-A-17 Turbojet Engine in an Altitude Chamber. NACA RM E50I15, 1950.
3. Meyer, Carl L., and Bloomer, Harry E.: Altitude-Wind-Tunnel Investigation of Performance and Windmilling Drag Characteristics of Westinghouse X24C-4B Axial-Flow Turbojet Engine. NACA RM E8J25a, 1948.
4. Conrad, E. William, and Sobolewski, Adam E.: Altitude-Wind-Tunnel Investigation of J47 Turbojet-Engine Performance. NACA RM E9G09, 1949.
5. Sanders, Newell D.: Performance Parameters for Jet-Propulsion Engines. NACA TN 1106, 1946.
6. Gabriel, David S., Carman, L. Robert, and Trautwein, Elmer E.: The Effect of Inlet Pressure and Temperature on the Efficiency of a Single-Stage Impulse Turbine Having 11.0-Inch Pitch-Line Diameter Wheel. NACA ACR E5E19, 1945.
7. Sanders, Newell D., and Behun, Michael: Generalization of Turbojet-Engine Performance in Terms of Pumping Characteristics. NACA TN 1927, 1949.
8. Childs, J. Howard: Preliminary Correlation of Efficiency of Aircraft Gas-Turbine Combustors for Different Operating Conditions. NACA RM E50F15, 1950.
9. Amorosi, A.: Gas Turbine Gas Charts. Res. Memo. 6-44 (NavShips 250-330-6), Bur. Ships, Navy Dept., Dec. 1944.
10. Keenan, Joseph H., and Kaye, Joseph: Gas Tables. John Wiley & Sons, Inc., 1948.

TABLE I - PERFORMANCE AND OPERATIONAL DATA

Point	Altitude (ft)	Flight Mach number M_0	Engine speed N (rpm)	Jet thrust F_j (lb)	Air flow W_a (lb/sec)	Fuel flow W_f (lb/hr)	Compressor- inlet total temperature T_2 (°R)	Compressor- outlet indicated temperature T_3 (°R)	Tail-pipe indicated gas tem- perature $T_{6,1}$ (°C)	Compressor- inlet total pressure, P_2 (in. Hg abs.)
1	0	0.63	4028	381	58.61	750	555	599	871	38.83
2		.64	4986	696	44.70	995	580	625	955	39.11
3		.63	5938	868	48.87	1190	553	644	1006	39.83
4		.64	5952	982	50.92	1215	580	654	1025	39.11
5		.63	6972	1355	57.68	1500	559	688	1082	39.11
6		.63	7941	1857	64.60	1915	589	725	1140	39.11
7		.64	7955	1794	67.33	1860	554	722	1121	38.83
8		.63	8944	1585	70.99	2500	564	789	1223	38.21
9	10,000	0.64	5,968	661	36.43	800	524	612	963	26.75
10		.64	8,005	1357	49.08	1350	524	692	1078	26.65
11		.64	9,972	2817	65.50	2500	519	782	1278	26.80
12		.64	10,574	3448	70.75	3100	518	816	1379	26.80
13		.64	11,151	4079	74.84	3700	524	856	1505	26.80
14		.64	11,597	4883	79.85	4600	517	892	1638	26.81
15	20,000	0.65	5,961	474	25.89	750	484	573	898	17.80
16		.65	7,994	1017	36.61	1050	475	640	992	17.80
17		.65	9,966	2035	45.79	1800	480	752	1262	17.80
18		.65	10,540	2586	49.95	2250	481	775	1374	17.85
19		.66	11,117	3066	53.33	2800	484	812	1494	17.90
20		.65	11,641	3587	56.15	3350	482	845	1632	17.79
21	30,000	0.28	7,968	590	19.07	850	417	584	1114	8.92
22		.26	8,958	788	23.55	950	413	627	1150	8.97
23		.26	9,983	1146	27.48	1150	414	683	1276	8.97
24		.28	10,554	1442	29.35	1375	415	714	1380	9.02
25		.28	11,095	1652	30.39	1650	415	747	1512	8.92
26		.28	11,655	1922	31.92	2000	416	789	1664	9.02
27		.47	6,063	296	14.36	700	428	524	1009	9.82
28		.44	7,913	555	21.80	850	423	584	1034	9.87
29		.47	9,980	1245	28.46	1260	425	689	1238	9.82
30		.48	10,546	1531	31.80	1500	425	722	1346	9.87
31		.48	11,061	1832	33.41	1800	422	754	1482	9.92
32		.48	11,689	2152	34.58	2150	428	798	1655	9.88
33		.68	7,913	630	23.27	710	467	630	970	11.60
34		.67	7,913	751	25.73	-----	446	612	950	11.70
35		.68	8,991	1106	30.47	-----	445	659	1041	11.70
36		.68	10,002	1575	34.38	-----	445	713	1217	11.55
37		.69	10,543	1824	32.84	1510	463	756	1349	11.60
38		.67	10,577	1927	36.80	-----	444	748	1348	11.56
39		.67	11,078	2207	38.12	-----	449	778	1470	11.50
40		.66	11,647	2591	40.09	-----	446	816	1639	11.60
41		.69	11,663	2635	39.99	-----	444	816	1635	11.65
42		.71	11,705	2579	39.07	2360	460	826	1653	11.80
43		.83	7,283	550	19.19	600	543	685	960	13.30
44		.83	7,732	736	24.32	785	485	839	915	13.32
45		.84	7,988	884	27.15	750	463	628	905	13.37
46		.84	9,708	1300	28.62	1000	555	807	1209	13.40
47		.83	9,994	1561	31.79	1220	521	787	1245	13.30
48		.83	10,319	1854	34.32	1440	498	781	1308	13.35
49		.84	10,588	2279	37.99	1740	465	762	1556	13.37
50		.83	11,380	2574	40.01	2200	494	841	1562	13.40
51		.83	11,714	3027	43.16	2665	467	833	1685	13.32
52		.95	7,969	905	29.71	760	480	644	829	15.17
53		.95	8,988	1352	34.52	1028	485	698	1011	15.07
54		.96	9,969	1986	39.51	1484	491	755	1208	15.17
55		.95	10,527	2532	43.33	1920	473	768	1348	15.17
56		.96	11,168	3109	47.90	2490	467	800	1487	15.27
57		.96	11,686	3353	48.14	2645	486	853	1627	15.27
58		1.09	7,913	1277	36.24	785	461	625	798	17.88
59		1.08	7,944	1084	32.53	650	510	673	838	17.81
60		1.09	9,025	1751	39.51	1000	498	711	996	17.71
61		1.09	10,059	2530	46.11	1680	498	763	1210	17.71
62		1.09	10,537	3284	50.61	2260	464	759	1340	17.80
63		1.08	10,574	2926	49.13	2050	502	798	1333	17.71
64		1.08	11,137	3495	53.10	2600	496	826	1464	17.81
65		1.09	11,655	4318	58.35	3455	463	825	1635	17.80
66		1.09	11,672	3970	54.67	3150	499	863	1618	17.76
67		1.25	8,011	1329	38.35	640	547	716	811	22.12
68		1.26	8,921	2953	52.80	1744	548	813	1208	22.23
69		1.26	10,574	3473	56.10	2175	548	842	1326	22.15
70	40,000	0.68	8,969	680	19.14	682	423	639	1043	7.37
71		.68	10,042	1068	22.23	1148	420	691	1214	7.39
72		.68	10,569	1285	23.40	1524	421	723	1334	7.39
73		.67	11,103	1472	24.40	1498	422	756	1479	7.39
74		.68	11,666	1706	25.34	1750	421	796	1641	7.34
75	50,000	6.67	9,014	457	11.00	674	424	643	1077	4.59
76		.68	9,932	646	12.62	780	424	691	1234	4.64
77		.67	10,481	759	13.61	906	426	724	1360	4.59
78		.67	11,081	892	14.22	1088	426	762	1503	4.59
79		.67	11,711	1065	14.73	1300	427	804	1691	4.59

OBTAINED AT SIMULATED-ALTITUDE CONDITIONS

Compressor-outlet pressure, P_3 (in. Hg abs.)	Combustor-outlet total pressure, P_4 (in. Hg abs.)	Tail-pipe total pressure, P_7 (in. Hg abs.)	Exhaust static pressure P_0 (in. Hg abs.)	Fuel-pump-discharge pressure (lb/sq in. gage)	Fuel manifold pressure (lb/sq in. gage)	Oil-pump-discharge pressure (lb/sq in. gage)	Oil-pump temperature (°F)	Point
42.69	40.15	31.86	29.83	140	60	5	120	1
46.56	45.04	32.88	29.81	200	74	7	116	2
55.93	51.85	33.89	29.83	160	75	10	120	3
55.93	51.69	34.07	29.81	200	85	9	119	4
66.28	61.21	35.83	29.91	200	99	12	120	5
79.15	72.97	37.92	29.91	240	122	15	122	6
79.49	73.48	38.14	29.83	190	100	15	130	7
94.92	87.36	40.31	29.31	280	156	18	129	8
39.76	36.74	23.41	20.35	145	60	8	110	9
57.55	53.44	26.80	20.30	175	80	10	100	10
87.98	81.35	34.44	20.30	205	120	20	100	11
99.03	92.25	37.78	20.30	250	156	22	110	12
108.90	101.68	41.22	20.30	300	200	22	115	13
121.10	113.70	45.68	20.30	340	264	22	125	14
27.30	23.24	15.75	13.40	140	55	5	90	15
41.65	38.49	18.63	13.40	150	65	11	60	16
61.30	57.21	23.75	13.40	180	90	18	70	17
70.56	65.89	26.65	13.40	200	110	19	70	18
77.99	73.25	28.91	13.40	220	155	21	90	19
85.07	80.06	32.11	13.40	260	165	23	100	20
23.34	21.73	10.89	8.45	150	54	15	50	21
29.47	27.41	12.33	8.55	150	57	20	55	22
36.52	34.12	14.23	8.55	160	66	22	60	23
40.55	38.02	15.53	8.55	160	75	25	70	24
44.20	41.46	16.73	8.45	175	80	25	80	25
48.43	45.54	18.31	8.55	190	95	27	100	26
16.60	15.82	9.69	8.45	140	50	8	55	27
25.40	25.57	11.55	8.65	145	54	18	50	28
38.94	36.41	11.91	8.45	160	67	22	60	29
43.85	41.04	16.52	8.55	190	75	22	50	30
47.84	44.95	18.04	8.60	180	85	24	50	31
52.30	49.23	19.64	8.45	190	100	25	70	32
26.73	24.64	11.67	8.60	140	53	6	86	33
28.35	26.07	12.29	8.65	800	55	10	75	34
36.28	33.28	14.22	8.60	500	60	20	70	35
44.35	41.11	16.71	8.45	180	72	20	70	36
47.45	44.22	17.52	8.40	165	79	15	98	37
49.56	46.13	18.62	8.55	180	83	22	75	38
54.31	50.62	20.20	8.55	200	95	24	80	39
59.62	55.93	22.42	8.65	205	115	25	85	40
62.32	56.10	22.43	8.50	---	---	---	--	41
58.66	55.18	22.13	8.45	200	112	20	100	42
23.83	21.12	10.89	8.50	130	45	5	145	43
27.63	25.52	11.90	8.47	140	50	7	110	44
30.59	28.14	12.62	8.47	160	55	9	70	45
38.04	34.99	14.57	8.40	150	60	10	140	46
43.04	39.70	16.17	8.50	160	65	10	155	47
48.34	44.87	17.87	8.60	170	75	18	120	48
54.18	50.62	19.93	8.47	180	84	18	90	49
59.36	55.65	22.12	8.50	200	105	20	120	50
65.77	61.98	24.67	8.47	225	125	25	90	51
32.82	30.26	13.27	8.47	140	54	7	81	52
41.87	38.57	15.79	8.47	150	64	12	84	53
52.30	48.33	19.31	8.37	165	79	15	86	54
60.57	56.56	22.39	8.47	180	92	17	90	55
69.38	65.06	25.74	8.47	210	120	20	90	56
72.67	68.24	27.10	8.47	215	136	22	98	57
38.93	35.74	14.87	8.43	143	58	11	65	58
35.76	32.90	14.05	8.50	150	56	9	20	59
47.56	43.83	17.75	8.40	150	68	12	85	60
60.62	56.34	22.37	8.40	180	88	15	90	61
72.17	67.24	26.48	8.45	200	113	20	84	62
67.82	62.57	24.98	8.50	200	103	16	100	63
75.46	70.70	28.21	8.60	210	125	20	110	64
87.95	82.66	32.89	8.50	260	175	25	86	65
81.97	77.04	30.77	8.40	260	155	25	115	66
41.22	37.51	15.57	8.52	150	55	10	130	67
68.07	62.69	25.12	8.43	185	95	15	135	68
76.77	71.04	28.35	8.43	200	110	18	140	69
23.40	21.63	9.05	5.42	850	50	14	55	70
29.53	27.37	10.91	5.42	270	58	15	60	71
32.62	30.33	12.11	5.44	150	62	16	70	72
35.74	33.37	13.23	5.49	160	69	17	80	73
39.16	36.63	14.61	5.39	180	78	19	85	74
13.68	12.69	5.22	5.39	825	38	5	75	75
17.09	15.69	6.27	5.39	825	46	9	85	76
19.18	17.77	7.03	5.39	825	50	18	90	77
21.08	19.67	7.69	5.39	825	53	11	95	78
23.26	21.59	8.58	5.39	880	57	10	105	79



TABLE II - PERFORMANCE DATA ADJUSTED TO STANDARD ALTITUDE AND
(Adjusted for variations in)

Point	Altitude (ft)	Flight Mach number M_0	Engine speed (rpm)		Jet thrust (lb)			Net thrust (lb)	
			Altitude N	Corrected $N/\sqrt{\theta}$	Altitude F_j	Corrected F_j/θ	Parameter $F_1 + P_0 A_s$ θ	Altitude F_n	Corrected F_n/θ
1	0	0.67	4061	3891	424	314	3493	-501	-371
2		.67	4989	4780	652	483	3603	-416	-308
3		.67	5999	5747	944	699	3868	-225	-167
4		.67	5980	5729	932	690	3816	-282	-209
5		.67	7011	6717	1339	992	4121	-38	-28
6		.67	7985	7650	1861	1393	4512	539	261
7		.67	8029	7692	1920	1422	4560	308	228
8		.67	8951	8575	2673	1980	5143	930	689
9	10,000	0.67	5,976	5,933	698	746	3809	-154	-166
10		.67	8,016	7,957	1443	1554	4823	297	380
11		.67	10,045	9,972	2984	3192	6280	1452	1564
12		.67	10,655	10,578	3629	3908	6895	1986	2160
13		.67	11,176	11,095	4287	4617	7709	2552	2748
14		.67	11,799	11,713	5118	5512	8602	3279	3531
15	20,000	0.67	5,981	6,170	489	805	3873	-81	-131
16		.67	8,065	8,351	1073	1730	4806	260	419
17		.67	9,937	10,251	2144	3456	8546	1111	1790
18		.67	10,608	10,943	2712	4372	7460	1599	2577
19		.67	11,154	11,506	3198	5155	8243	2009	3238
20		.67	11,703	12,072	3711	5982	8068	2454	3956
21	30,000	0.67	7,989	8,882	817	1979	5,923	453	1453
22		.27	9,004	10,036	819	2628	6,588	619	1985
23		.27	10,024	11,172	1191	3823	7,793	957	3072
24		.27	10,583	11,796	1490	4763	8,731	1241	3984
25		.27	11,126	12,401	1727	5542	9,490	1466	4706
26		.27	11,675	13,011	1986	6375	10,323	1715	5605
27		.45	6,036	6,640	508	902	4,486	98	291
28		.45	7,983	8,760	574	1682	6,332	261	765
29		.45	10,020	11,023	1295	3793	7,591	888	2544
30		.45	10,588	11,648	1684	4641	8,260	1126	3300
31		.45	11,164	12,282	1886	5525	9,094	1409	4128
32		.45	11,894	12,865	2224	6517	10,080	1725	5055
33		.67	7,753	8,337	646	1613	4664	138	345
34		.67	7,934	8,532	769	1919	4997	224	560
35		.67	8,044	9,726	1127	2812	5875	484	1209
36		.67	10,038	10,795	1626	4058	7105	890	2221
37		.67	10,374	11,156	1885	4649	7665	1149	2867
38		.67	11,627	11,428	1999	4990	8073	1213	3026
39		.67	11,070	11,904	2291	5718	8815	1468	3664
40		.67	11,677	12,557	2686	6703	8809	1830	4568
41		.67	11,719	12,602	2694	6723	9761	1846	4607
42		.67	11,554	12,425	2579	6435	9418	1742	4588
43		.82	6,753	7,119	569	1237	3898	5	11
44		.82	7,590	8,001	760	1653	4301	113	245
45		.82	8,019	8,453	910	1978	4616	207	449
46		.82	8,898	9,380	1335	2902	5513	624	1140
47		.82	9,461	9,974	1616	3512	6173	737	1603
48		.82	9,988	10,529	1911	4155	6806	988	2147
49		.82	10,604	11,178	2346	5100	7738	1559	2955
50		.82	11,058	11,657	2644	5747	8390	1575	3424
51		.82	11,708	12,342	3128	6799	9447	2000	4348
52		.95	8,024	8,282	954	1785	4111	34	64
53		.95	9,002	9,292	1435	2686	5027	354	663
54		.95	9,824	10,244	2095	3921	6220	858	1606
55		.95	10,679	11,023	2668	4994	7320	1337	2503
56		.95	11,400	11,767	3254	6092	8402	1802	3374
57		.95	11,893	12,070	3509	6569	8879	2020	3782
58		1.09	8,311	8,391	1332	2137	4101	122	197
59		1.09	7,933	8,008	1135	1821	3809	-11	-18
60		1.09	9,121	9,208	1844	2958	4934	460	738
61		1.09	10,146	10,243	2664	4274	6250	1049	1683
62		1.09	11,031	11,137	3441	4943	7497	1738	2789
63		1.09	10,643	10,745	3081	5871	6942	1354	2172
64		1.09	11,277	11,385	3659	5520	7882	1814	2911
65		1.09	12,216	12,335	4498	7217	9195	2549	4090
66		1.09	11,784	11,897	4169	6688	8658	2268	3622
67		1.25	7,964	7,800	1388	1798	3402	-172	-223
68		1.25	9,854	9,651	3067	3974	5553	928	1202
69		1.25	10,502	10,285	3615	4685	6268	1337	1733
70	40,000	0.67	9,019	9,929	687	2745	5,031	286	1183
71		.67	10,134	11,157	1075	4299	7,380	624	2496
72		.67	10,652	11,727	1297	5186	8,269	822	3285
73		.67	11,178	12,307	1493	5968	9,054	996	3984
74		.67	11,758	12,945	1733	6930	10,013	1217	4867
75	50,000	0.67	9,053	9,967	461	2974	6058	237	1830
76		.67	9,975	10,982	640	4128	7207	388	2490
77		.67	10,502	11,562	766	4940	8024	489	3150
78		.67	11,103	12,224	900	5805	8891	610	3934
79		.67	11,720	12,903	1065	6867	9953	764	4927

NACA

CORRECTED TO NACA STANDARD SEA-LEVEL ATMOSPHERIC CONDITIONS
simulated operating conditions)

Altitude Wa	Air flow (lb/sec)		Fuel flow (lb/hr)		Engine combustion efficiency η_b	Net-thrust specific fuel consumption (lb/(hr)(lb thrust))		Tail-pipe indicated gas temperature (°R)		Point
	Corrected W_a/\sqrt{g}	5	Altitude Wf	Corrected W_f/\sqrt{g}		Altitude Wf/Fn	Corrected $W_f/F_n\sqrt{g}$	Altitude Tg,1	Corrected $T_{g,1}/\theta$	
39.82	30.79	575	408	77.37	----	----	----	886	813	1
45.95	35.53	864	615	84.94	----	----	----	963	884	2
50.32	38.91	1055	747	88.92	----	----	----	1026	942	3
52.25	40.40	1099	780	93.50	----	----	----	1034	949	4
59.25	45.81	1388	985	97.65	----	----	----	1093	1005	5
66.35	51.30	1840	1306	95.18	5.431	5.203	1153	1058	6	
69.39	55.65	1784	1266	99.25	5.796	5.553	1142	1048	7	
74.99	57.98	2511	1782	91.65	2.699	2.586	1224	1124	8	
37.79	40.99	824	861	85.10	----	----	967	953	9	
51.10	55.43	1318	1409	75.44	4.435	4.403	1078	1063	10	
67.42	73.13	2575	2751	97.62	1.771	1.756	1296	1277	11	
72.79	78.96	3214	3436	97.42	1.610	1.598	1400	1380	12	
77.41	83.97	3832	4097	99.56	1.501	1.490	1511	1489	13	
82.03	88.98	4809	5141	98.91	1.466	1.455	1666	1642	14	
26.61	42.05	746	1240	68.27	----	----	904	968	15	
37.70	58.91	1079	1794	86.43	4.150	4.281	1017	1063	16	
47.89	74.83	1857	3087	96.20	1.671	1.724	1254	1335	17	
51.61	80.64	2348	3905	98.09	1.469	1.515	1391	1481	18	
55.12	86.12	2912	4842	96.37	1.449	1.495	1503	1600	19	
58.28	91.06	3513	5842	97.82	1.432	1.477	1649	1755	20	
19.33	57.38	889	3179	75.82	1.963	2.188	1115	1365	21	
24.55	70.12	992	3550	88.60	1.604	1.788	1161	1443	22	
28.44	81.90	1200	4293	100.70	1.253	1.597	1286	1598	23	
30.25	87.09	1425	5097	101.73	1.148	1.279	1387	1724	24	
31.68	91.21	1730	6187	100.96	1.180	1.315	1520	1889	25	
32.93	94.83	2070	7405	101.02	1.207	1.345	1669	2074	26	
14.92	39.75	728	2347	57.55	7.351	8.065	1010	1222	27	
22.41	59.69	895	2886	74.64	3.429	3.772	1047	1267	28	
30.51	81.27	1315	4240	92.77	1.514	1.666	1248	1510	29	
32.77	87.87	1558	5022	96.18	1.383	1.521	1357	1642	30	
34.13	90.90	1867	6017	98.08	1.324	1.457	1505	1821	31	
35.75	95.15	2223	7167	100.02	1.288	1.417	1657	2005	32	
24.55	56.97	719	1930	78.88	5.202	5.594	931	1077	33	
26.50	61.03	----	----	----	----	----	955	1104	34	
31.04	72.03	----	----	----	----	----	1053	1218	35	
35.56	82.52	----	----	----	----	----	1226	1418	36	
34.49	80.05	1536	4121	94.87	1.336	1.437	1306	1510	37	
38.02	88.23	----	----	----	----	----	1361	1574	38	
39.77	92.29	----	----	----	----	----	1467	1597	39	
41.33	95.91	----	----	----	----	----	1647	1906	40	
40.96	95.05	----	----	----	----	----	1651	1909	41	
40.21	95.32	2367	6353	100.20	1.356	1.458	1611	1863	42	
22.31	46.01	576	1321	66.77	113.8	120.0	825	917	43	
25.62	52.84	795	1823	63.78	7.058	7.440	880	978	44	
27.84	57.41	775	1776	76.28	3.752	3.955	911	1013	45	
32.07	66.13	941	2157	91.61	1.795	1.892	1016	1129	46	
34.75	71.66	1195	2739	92.46	1.620	1.708	1118	1239	47	
36.56	75.39	1437	3293	95.08	1.454	1.533	1226	1362	48	
39.04	80.51	1794	4111	96.09	1.320	1.391	1360	1512	49	
42.29	87.20	2196	5032	98.00	1.393	1.469	1475	1639	50	
44.62	92.01	2752	6307	97.85	1.375	1.450	1653	1837	51	
31.09	56.38	806	1558	72.38	23.58	24.34	881	939	52	
36.56	66.29	1092	2110	110.91	3.083	3.182	1014	1081	53	
41.82	75.84	1536	2967	94.61	1.789	1.847	1198	1277	54	
45.01	81.63	2052	3964	97.42	1.534	1.583	1386	1477	55	
49.11	89.07	2660	5140	98.08	1.475	1.523	1549	1651	56	
50.35	91.32	2979	5757	97.95	1.475	1.522	1628	1735	57	
36.99	57.19	860	1385	99.62	7.004	7.071	669	886	58	
34.11	64.20	680	1101	77.87	----	----	836	852	59	
41.17	65.42	1064	1727	94.24	2.314	2.336	1017	1037	60	
48.04	76.35	1756	2844	97.00	1.673	1.689	1236	1267	61	
50.65	80.49	2479	4016	96.74	1.425	1.439	1468	1497	62	
51.40	81.68	2173	3519	98.22	1.605	1.620	1350	1376	63	
54.90	87.25	2757	4465	98.74	1.518	1.535	1501	1550	64	
57.99	92.16	5775	6111	100.28	1.480	1.494	1796	1831	65	
56.86	90.36	5339	5408	98.48	1.479	1.493	1650	1682	66	
40.26	53.27	664	843	74.92	----	----	802	769	67	
55.21	73.05	1798	2283	97.52	1.939	1.899	1191	1143	68	
58.80	77.80	2249	2854	98.99	1.681	1.646	1307	1254	69	
19.33	70.19	907	3994	64.80	3.066	3.375	1054	1278	70	
22.31	81.01	1174	5168	75.32	1.680	2.070	1236	1498	71	
23.51	85.38	1351	5948	79.88	1.644	1.810	1355	1642	72	
24.54	89.12	1525	6713	86.36	1.530	1.684	1499	1817	73	
25.63	95.10	1798	7916	89.84	1.477	1.526	1667	2021	74	
11.07	64.85	685	4863	52.01	2.887	3.178	1086	1317	75	
12.57	73.59	785	5570	64.61	2.031	2.236	1245	1509	76	
13.73	80.43	918	6515	69.13	1.878	2.068	1355	1643	77	
14.35	84.03	1112	7896	70.60	1.823	2.007	1509	1829	78	
14.88	87.15	1315	9333	73.88	1.720	1.894	1694	2053	79	

NACA

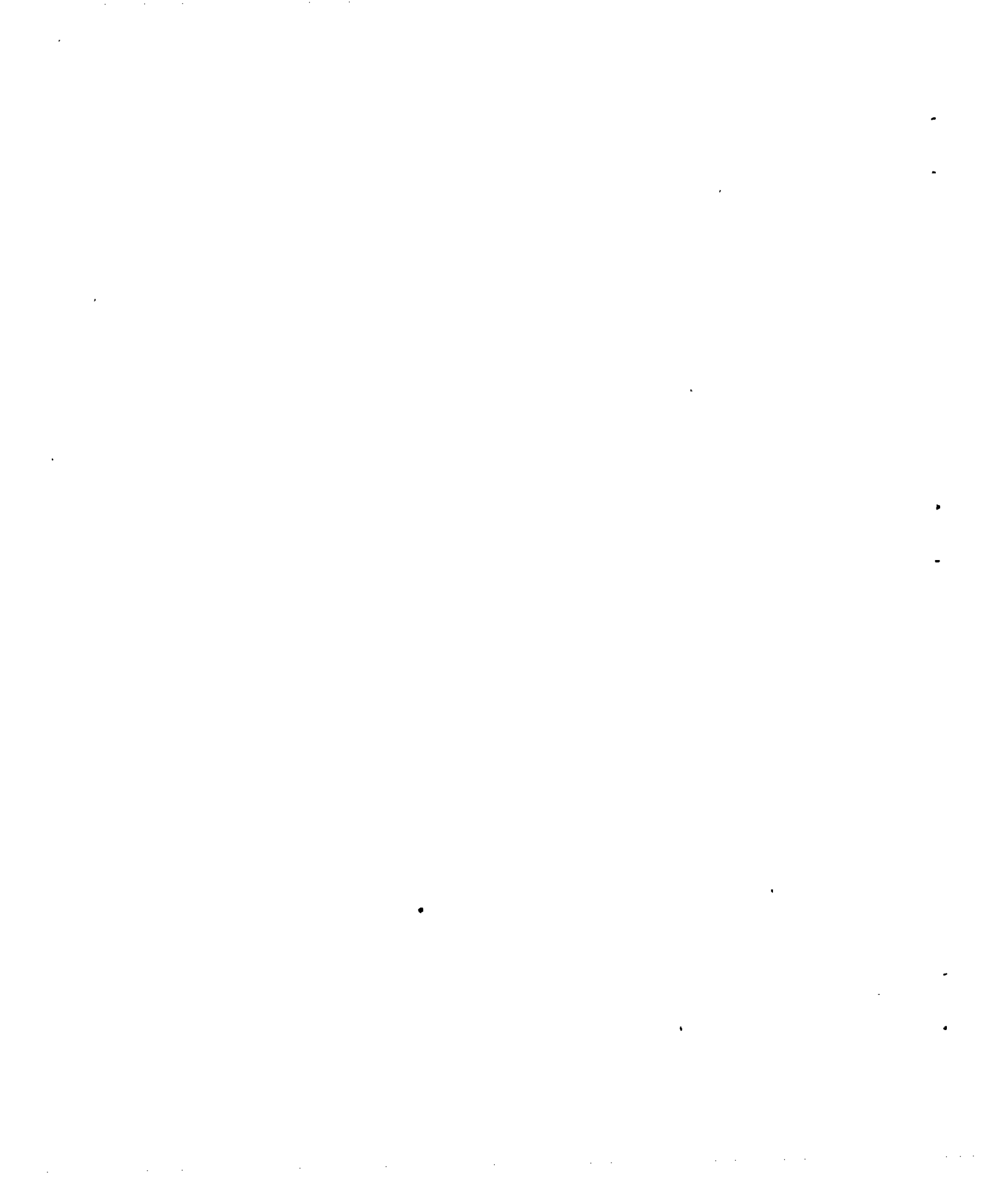


TABLE III - REYNOLDS NUMBER INDEX VARIATION
WITH FLIGHT MACH NUMBER AND ALTITUDE

Altitude (ft)	Flight Mach number M_0	δ	θ	φ	Reynolds number index $5/\Psi\theta$	Altitude (ft)	Flight Mach number M_0	δ	θ	φ	Reynolds number index $5/\Psi\theta$	
0	0	1.000	1.000	1.000	1.000	30,000	0.6	0.3787	0.8509	0.8862	0.4633	
	.1	1.007	1.002	1.002	1.004		.7	.4118	.8715	.9029	.4286	
	.2	1.028	1.008	1.006	1.018		.8	.4522	.8954	.9207	.5190	
	.3	1.064	1.018	1.013	1.041		.9	.5019	.9222	.9416	.5551	
	.4	1.117	1.032	1.023	1.075		1.0	.5619	.9524	.9655	.5964	
	.5	1.186	1.050	1.036	1.117		35,000	0	0.2352	0.7595	0.8149	0.3319
	.6	1.276	1.072	1.051	1.173		.1	.2368	.7611	.8164	.3325	
	.7	1.387	1.098	1.069	1.238		.2	.2418	.7655	.8196	.3372	
	.8	1.524	1.128	1.090	1.316		.3	.2502	.7732	.8257	.3446	
	.9	1.691	1.162	1.117	1.404		.4	.2627	.7838	.8337	.3559	
5000	1.0	1.893	1.200	1.141	1.516		.5	.2789	.7975	.8443	.3699	
	0	0.8318	0.9657	0.9753	0.8679		.6	.3001	.8141	.8576	.3878	
	.1	.8374	.9676	.9764	.8718		.7	.3262	.8339	.8727	.4093	
	.2	.8554	.9734	.9809	.8839		.3	.3583	.8566	.8910	.4345	
	.3	.8852	.9830	.9875	.9041		.4	.3977	.8825	.9111	.4647	
	.4	.9291	.9965	.9973	.9333		.5	.4452	.9112	.9334	.4987	
	.5	.9868	1.014	1.010	.9703		0	0.1353	0.7572	0.8130	0.2619	
	.6	1.061	1.035	1.025	1.018		.1	.1866	.7588	.8141	.2651	
	.7	1.154	1.060	1.044	1.073		.2	.1905	.7632	.8175	.2667	
	.8	1.268	1.089	1.064	1.141		.3	.1972	.7709	.8239	.2726	
10,000	.9	1.407	1.122	1.086	1.223		.4	.2070	.7815	.8321	.2814	
	1.0	1.576	1.159	1.117	1.309		.5	.2198	.7950	.8430	.2924	
	0	0.6881	0.9312	0.9491	0.7513		.6	.2364	.8118	.8562	.3065	
	.1	.6923	0.9331	.9504	.7541		.7	.2570	.8314	.8714	.3255	
	.2	.7075	.9587	.9549	.7647		.8	.2824	.8539	.8889	.3438	
	.3	.7320	.9480	.9621	.7814		.9	.3134	.8798	.9090	.3676	
	.4	.7684	.9609	.9714	.8069		1.0	.3506	.9085	.9310	.3951	
	.5	.8157	.9776	.9836	.8398		40,000	0	0.1459	0.7572	0.8130	0.2052
	.6	.8776	.9983	.9989	.8794		.1	.1468	.7588	.8141	.2071	
	.7	.9542	1.022	1.015	.9291		.2	.1500	.7632	.8175	.2100	
	.8	1.048	1.050	1.037	.9859		.3	.1552	.7709	.8239	.2145	
	.9	1.163	1.082	1.058	1.057		.4	.1630	.7815	.8321	.2216	
15,000	1.0	1.302	1.117	1.083	1.137		.5	.1730	.7950	.8430	.2302	
	0	0.5643	0.8968	0.9223	0.6461		.6	.1862	.8118	.8562	.2414	
	.1	.5681	.8987	.9233	.6490		.7	.2024	.8314	.8714	.2548	
	.2	.5799	.9040	.9281	.6572		.8	.2224	.8539	.8889	.2708	
	.3	.6002	.9131	.9347	.6720		.9	.2467	.8798	.9090	.2894	
	.4	.6300	.9256	.9448	.6931		1.0	.2762	.9085	.9310	.3112	
	.5	.6692	.9416	.9570	.7206		45,000	0	0.1149	0.7572	0.8130	0.1624
	.6	.7198	.9615	.9719	.7553		.1	.1157	.7588	.8141	.1631	
	.7	.7826	.9848	.9891	.7973		.2	.1181	.7632	.8175	.1654	
	.8	.8601	1.012	1.008	.8482		.3	.1223	.7709	.8239	.1691	
	.9	.9542	1.042	1.031	.9082		.4	.1284	.7815	.8321	.1746	
20,000	1.0	1.068	1.076	1.055	.9762		.5	.1362	.7950	.8430	.1812	
	0	0.4596	0.8626	0.8960	0.5523		.6	.1466	.8118	.8562	.1900	
	.1	.4629	.8644	.8966	.5553		.7	.1594	.8314	.8714	.2006	
	.2	.4726	.8696	.9016	.5622		.8	.1751	.8539	.8889	.2132	
	.3	.4891	.9780	.9072	.5764		.9	.1943	.8798	.9090	.2279	
	.4	.5132	.8902	.9172	.5930		1.0	.2175	.9085	.9310	.2451	
	.5	.5454	.9058	.9289	.6170		50,000	0	0.1149	0.7572	0.8130	0.1624
	.6	.5865	.9247	.9440	.6461		.1	.1157	.7588	.8141	.1631	
	.7	.6375	.9470	.9610	.6817		.2	.1181	.7632	.8175	.1654	
	.8	.7004	.9728	.9798	.7248		.3	.1223	.7709	.8239	.1691	
	.9	.7769	1.002	1.002	.7746		.4	.1284	.7815	.8321	.1746	
25,000	1.0	.8700	1.035	1.026	.8341		.5	.1362	.7950	.8430	.1812	
	0	0.3713	0.8281	0.8682	0.4696		.6	.1466	.8118	.8562	.1900	
	.1	.3737	.8299	.8700	.4715		.7	.1594	.8314	.8714	.1980	
	.2	.3814	.8347	.8740	.4776		.3	.0930	.7632	.8175	.1302	
	.3	.3948	.8430	.8804	.4884		.4	.0963	.7709	.8239	.1331	
	.4	.4145	.8545	.8891	.5043		.5	.1011	.7815	.8321	.1374	
	.5	.4399	.8696	.9016	.5233		.6	.1073	.7950	.8430	.1428	
	.6	.4751	.8877	.9151	.5487		.7	.1155	.8118	.8562	.1497	
	.7	.5147	.9092	.9316	.5794		.8	.1256	.8314	.8714	.1580	
	.8	.5657	.9339	.9515	.6152		.9	.1379	.8539	.8889	.1679	
30,000	.9	.6276	.9620	.9724	.6581		1.0	.1530	.8798	.9090	.1795	
	1.0	.7023	.9934	.9950	.7082		60,000	0	0.0905	0.7572	0.8130	0.1279
	0	0.2968	0.7638	0.8144	0.3959		.1	.0911	.7588	.8141	.1285	
	.1	.2989	.7954	.8430	.3975		.2	.0733	.7632	.8175	.1026	
	.2	.3052	.9002	.8469	.4029		.3	.0758	.7709	.8239	.1048	
35,000	.3	.3158	.8081	.8525	.4121		.4	.0796	.7815	.8321	.1082	
	.4	.3315	.8193	.8621	.4248		.5	.0845	.7950	.8430	.1124	
	.5	.3519	.8335	.8727	.4416		.6	.0909	.8118	.8562	.1178	
	.6						.7	.0988	.8314	.8714	.1244	
	.7						.8	.1086	.8539	.8889	.1322	
40,000	.8						.9	.1205	.8798	.9090	.1413	
	.9						1.0	.1349	.9085	.9310	.1520	
	0											

NACA

TABLE IV - ALTITUDE

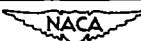
Point	Average corrected engine speed (rpm) $\frac{N}{\sqrt{\theta}}$	Average flight Mach number M_0	Altitude (ft)	Inlet total temperature T_1 ($^{\circ}$ R)	Inlet total pressure P_1 $\left(\frac{lb}{sq\ ft}\right)$	Corrected jet thrust $F_j/6$ (lb)	Corrected jet thrust parameter $\frac{F_j + p_0 A_8}{6}$	Corrected air flow $\frac{W_a \sqrt{\theta}}{6}$ $\left(\frac{lb}{sec}\right)$	Corrected fuel flow $\frac{W_f}{6 \sqrt{\theta}}$ $\left(\frac{lb}{hr}\right)$	Corrected tail-pipe temperature $T_{6,1}$ ($^{\circ}$ R)
1	11,750	0.37	10,000	510	1600	5002	8790	87.35	5194	1700
2			20,000	526	1066	4899	8687	86.04	5326	1696
3			30,000	530	688.0	4841	8629	84.57	5366	1709
4			40,000	529	427.2	4852	8640	84.63	5485	1703
5			50,000	524	262.9	4683	8471	80.86	5618	1728
6	11,750	0.62	10,000	524	1885	5594	8799	86.28	5253	1709
7			20,000	529	1266	5506	8711	85.77	5255	1695
8			30,000	518	826.7	5426	8631	85.53	5226	1693
9			40,000	517	507.5	5342	8547	83.85	5283	1700
10			50,000	526	315.1	5241	8446	83.02	5379	1695
11			60,000	523	197.2	5111	8316	81.64	5713	1710
12	11,750	0.91	20,000	520	1646	6334	8785	85.28	5140	1707
13			30,000	528	1077	6319	8770	85.14	5236	1690
14			40,000	529	665	6325	8776	85.07	5276	1685
15			50,000	522	412	6196	8647	83.12	5313	1687
16			60,000	532	245	5988	8439	81.48	5572	1719
17			65,000	535	192	5922	8373	80.63	5622	1730
18	10,600	0.37	10,000	527	1601	3524	7312	76.06	3581	1445
19			20,000	525	1073	3435	7223	76.15	3534	1441
20			30,000	519	705.6	3359	7147	75.15	3485	1441
21			40,000	524	430.6	3302	7090	74.32	3717	1468
22			50,000	528	262.3	3333	7121	70.44	3940	1501
23			60,000	536	163.4	3111	6899	66.59	4680	1576
24	10,600	0.62	10,000	522	1899	3891	7096	77.70	3350	1374
25			20,000	521	1265	3891	7096	77.81	3373	1384
26			30,000	522	826.0	3857	7062	78.28	3395	1374
27			40,000	525	509.1	3773	6978	78.02	3475	1382
28			50,000	524	314.3	3696	6901	73.53	3544	1407
29			60,000	528	190.1	3615	6820	70.79	4146	1448
30	10,600	0.91	20,000	518	1646	4641	7092	77.87	3304	1356
31			30,000	518	1077	4592	7043	77.61	3282	1353
32			40,000	518	664.1	4601	7052	76.70	3343	1352
33			50,000	532	412.4	4488	6939	75.63	3431	1366
34			60,000	522	245.4	4404	6855	73.25	3816	1397
35			65,000	525	203.7	4302	6753	72.13	3921	1411

NACA

2113

CORRECTION-FACTOR DATA

Reynolds number index $\frac{5}{\Phi \sqrt{\theta}}$	$F_j / 5$ $(F_j)_{SL}$	$\frac{F_j + POA_8}{5}$ $(F_j + POA_8)_{SL}$	$\frac{W_a \sqrt{\theta}}{5}$ $(W_a)_{SL}$	$\frac{W_f}{5 \sqrt{\theta}}$ $(W_f)_{SL}$	$\frac{T_{6,i}}{\theta}$ $(T_{6,i})_{SL}$	Combustion efficiency η_b	$\frac{W_f \eta_b}{5 \sqrt{\theta}}$ $(W_f \eta_b)_{SL}$	$\left(\frac{W_f \eta_b}{W_a \sqrt{\theta}} \right)_{alt}$ $\left(\frac{W_f \eta_b}{W_a} \right)_{SL}$	Point
0.7561	1.0004	1.0011	1.012	0.9856	1.000	1.021	1.0006	0.9887	1
.5038	.9798	.9894	.9981	1.011	.9976	.990	.9949	.9968	2
.3251	.9682	.9828	.9811	1.018	1.0053	.980	.9923	1.011	3
.2019	.9704	.9840	.9818	1.041	1.0018	.958	.9915	1.010	4
.1242	.9366	.9648	.9381	1.066	1.0165	.925	.9806	1.045	5
0.8908	1.0079	1.0045	1.001	1.014	1.0095	1.016	1.0032	1.002	6
.5983	.9921	.9944	.9950	1.014	1.0012	1.002	.9898	.9948	7
.3907	.9777	.9853	.9922	1.009	1.000	.995	.9774	.9851	8
.2398	.9625	.9757	.9727	1.020	1.004	.975	.9682	.9954	9
.1489	.9443	.9642	.9631	1.038	1.0012	.956	.9665	1.004	10
.0932	.9209	.9493	.9470	1.103	1.010	.890	.9558	1.009	11
0.7779	0.9990	1.0006	0.9974	0.9923	1.010	1.024	0.9987	1.001	12
.5090	.9966	.9989	.9957	1.011	1.000	.991	.9846	.9889	13
.3143	.9976	.9995	.9950	1.019	.9970	.979	.9801	.9850	14
.1947	.9773	.9846	.9722	1.026	.9982	.950	.9577	.9851	15
.1158	.9445	.9612	.9530	1.076	1.0172	.922	.9748	1.023	16
.0907	.9341	.9536	.9430	1.085	1.024	.883	.9419	.9988	17
0.7566	1.009	1.0058	1.001	1.023	1.000	0.987	1.0028	1.008	18
.5071	.9891	.9935	1.002	1.010	.9972	1.001	.9938	.9918	19
.3335	.9680	.9831	.9888	.9957	.9972	.979	.9584	.9693	20
.2035	.9515	.9752	.9779	1.062	1.0159	.950	.9919	1.014	21
.1240	.9605	.9795	.9268	1.126	1.0388	.901	.9972	1.076	22
.0772	.8965	.9490	.8762	1.337	1.091	.778	1.0228	1.167	23
0.8974	0.9977	1.0008	0.9787	1.000	1.001	0.998	0.9949	1.0166	24
.5978	.9977	1.0008	1.000	1.007	1.008	1.002	1.0060	1.006	25
.3904	.9889	.9961	1.006	1.013	1.001	.989	.9994	.9944	26
.2406	.9674	.9842	.9771	1.037	1.007	.958	.9908	1.015	27
.1485	.9477	.9733	.9451	1.058	1.025	.936	.9872	1.045	28
.0898	.9269	.9619	.9099	1.238	1.055	.804	.9920	1.090	29
0.7779	0.9981	0.9989	1.001	1.010	1.004	0.990	1.0034	1.002	30
.5090	.9875	.9920	.9976	1.004	1.001	.988	.9948	.9972	31
.3138	.9895	.9932	.9859	1.022	1.001	.962	.9865	1.001	32
.1947	.9652	.9773	.9721	1.049	1.011	.938	.9871	1.015	33
.1158	.9471	.9655	.9415	1.167	1.034	.857	1.0031	1.065	34
.0964	.9252	.9511	.9271	1.199	1.044	.806	.9693	1.046	35



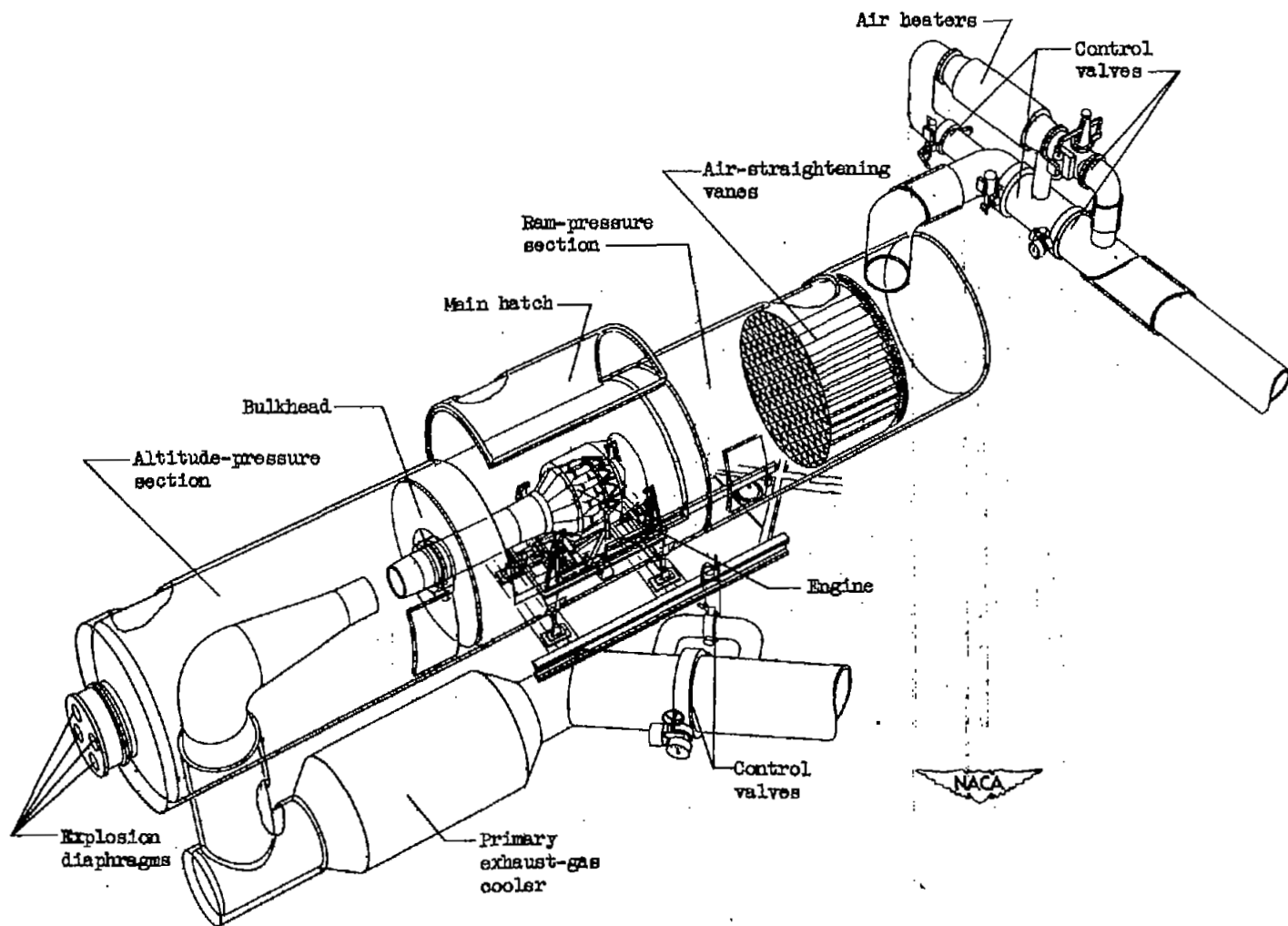


Figure 1. - Sketch of altitude chamber showing engine installed in test section.

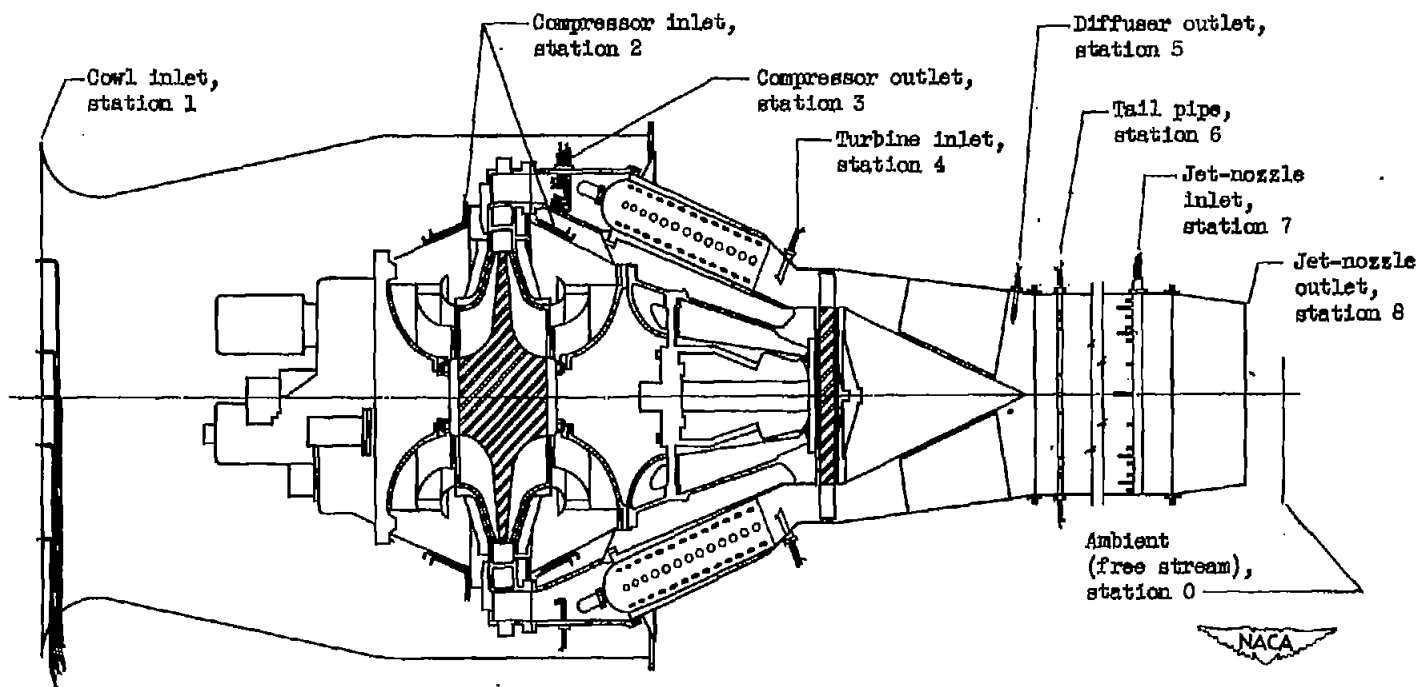
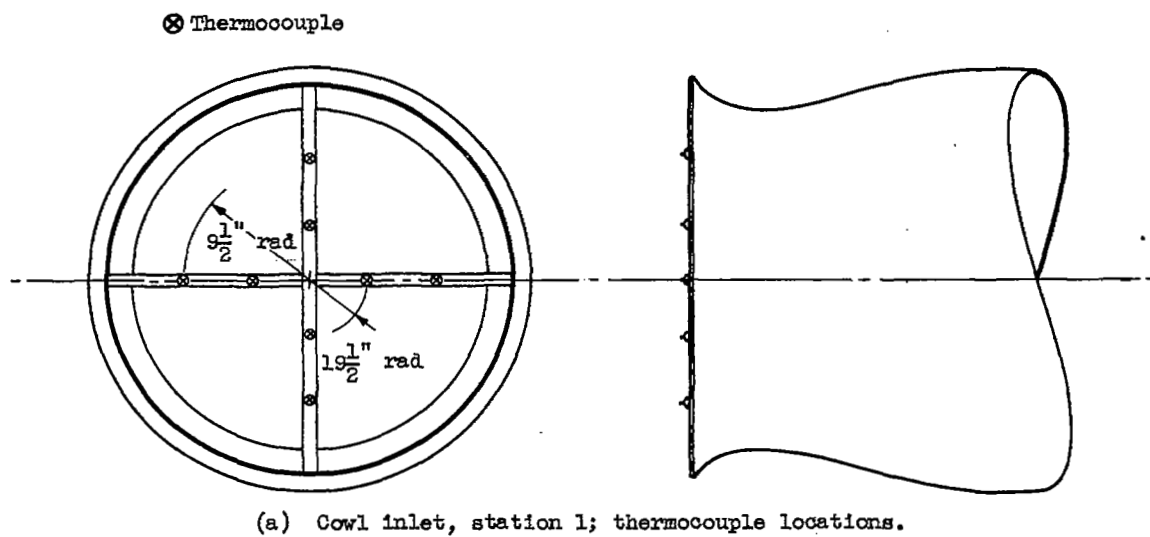
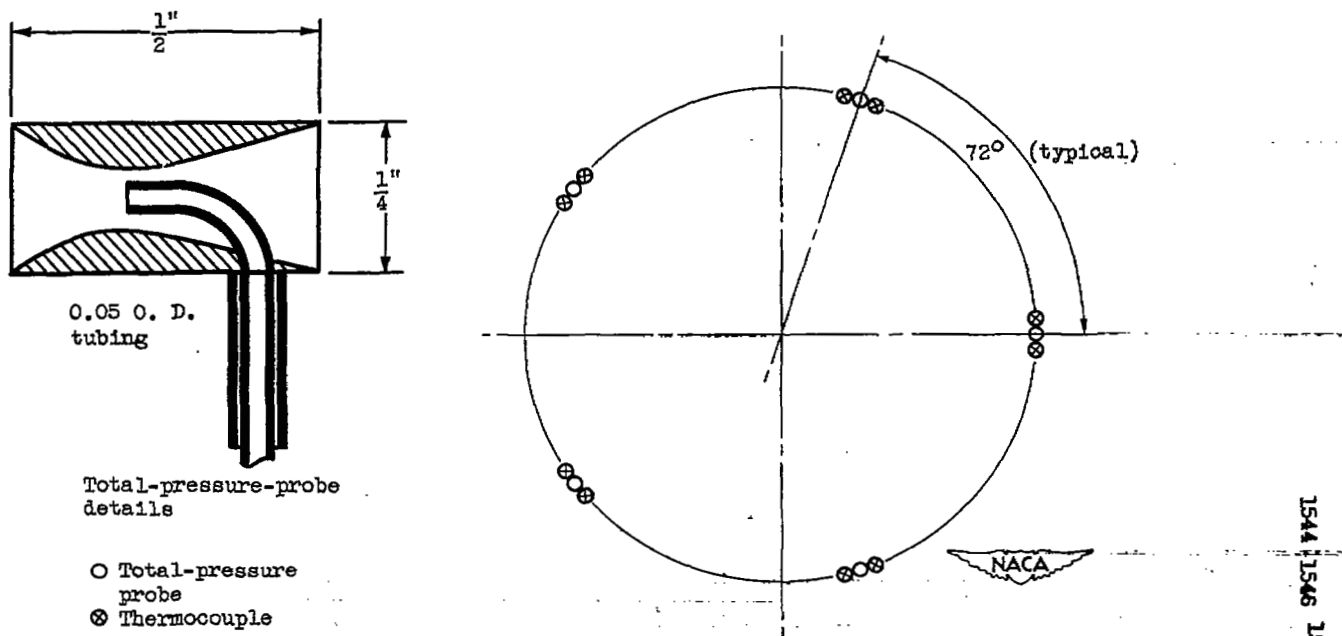


Figure 2. - Instrumentation stations.



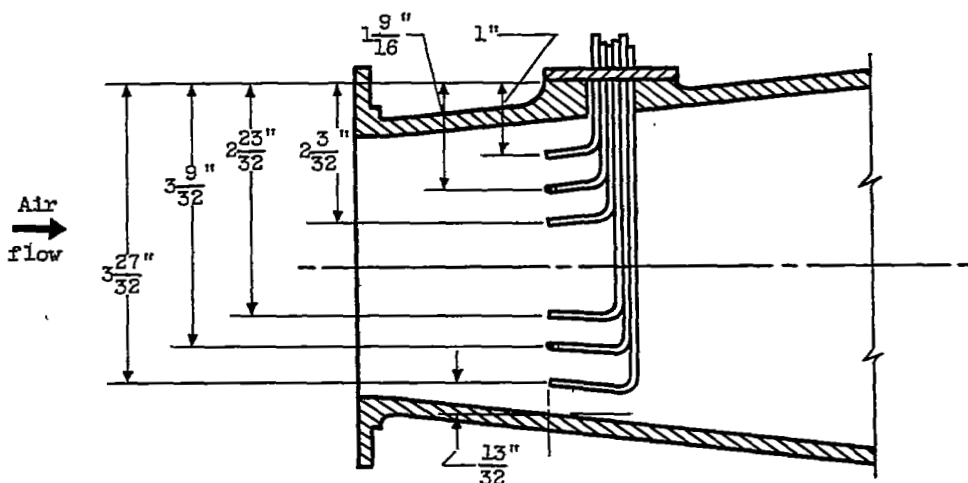
(a) Cowl inlet, station 1; thermocouple locations.



(b) Compressor inlet, station 2; instrumentation on fore and aft screens identical.

Figure 3. - Details of instrumentation.

2113

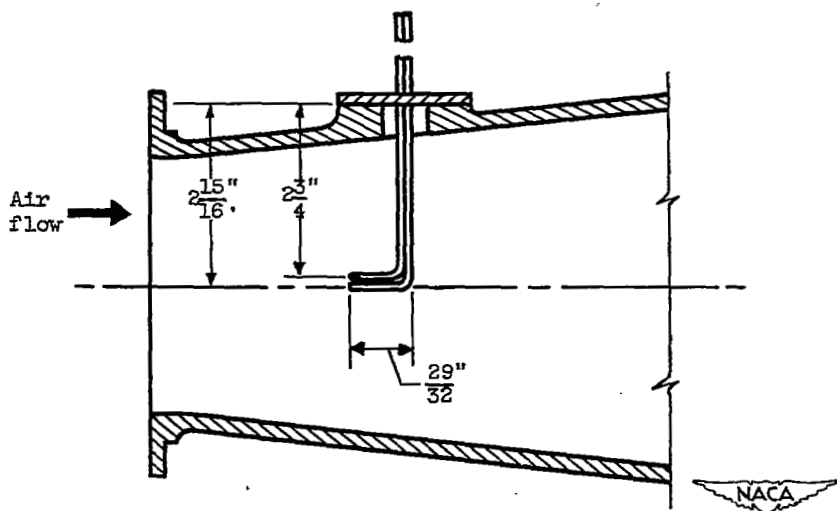


(c) Compressor outlet, station 3; typical installation (adapters 4, 9, and 13).

Thermocouple



Total pressure

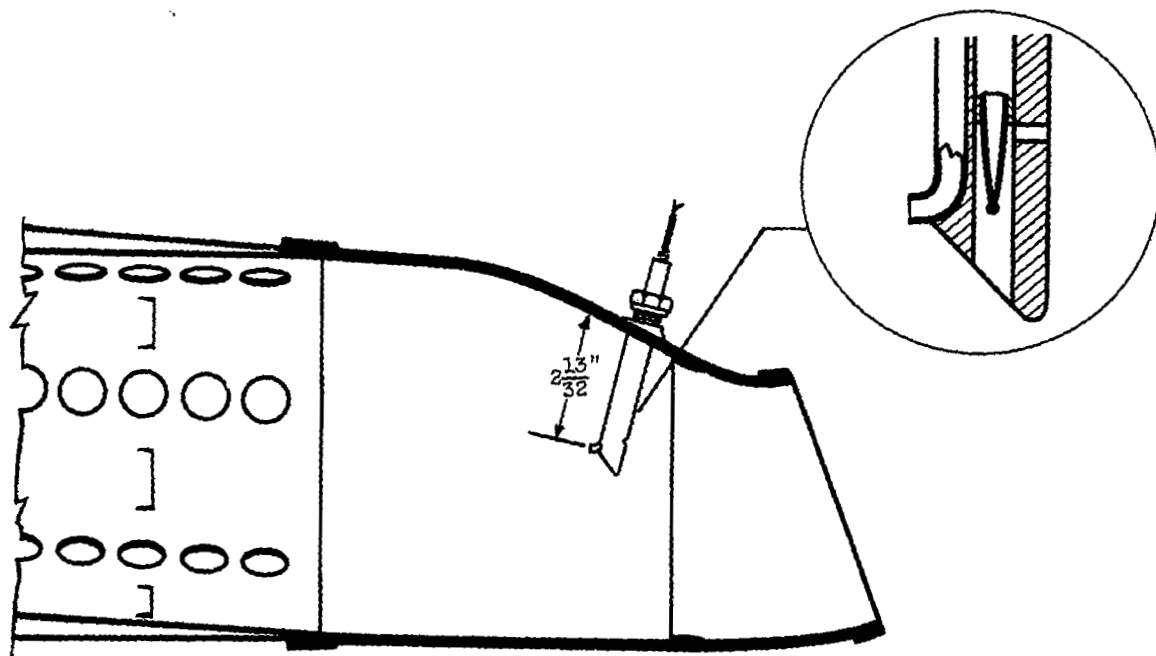


(d) Compressor outlet, station 3; typical installation (adapters 1, 2, 3, and 12).

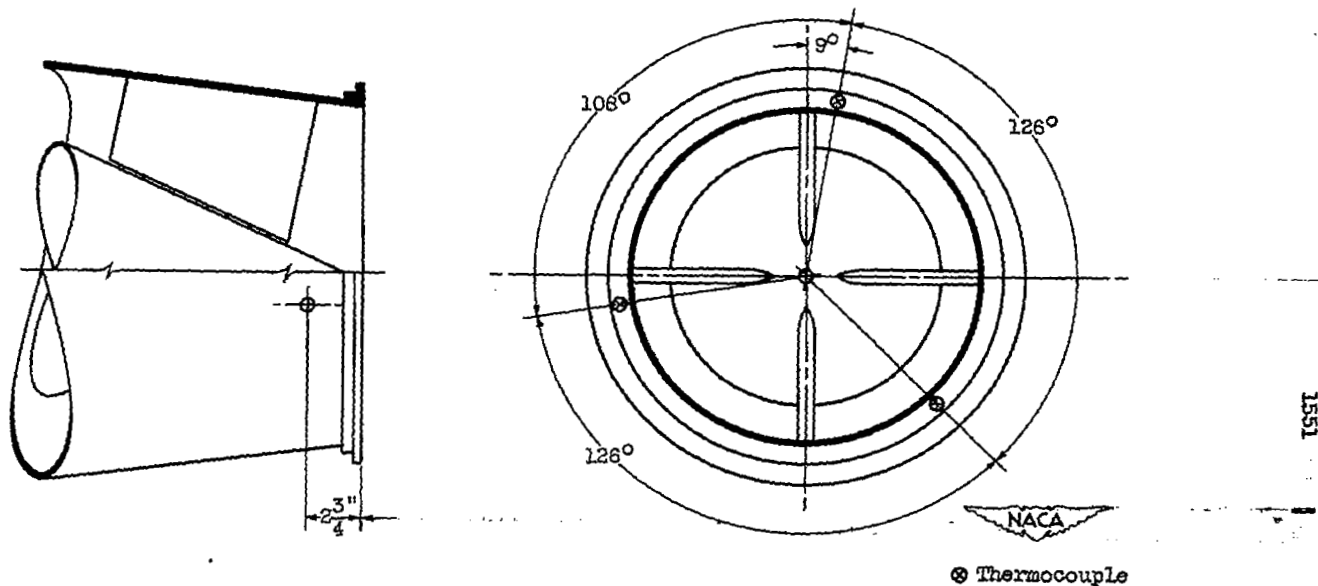
Figure 3. - Continued. - Details of instrumentation.

2240

1354

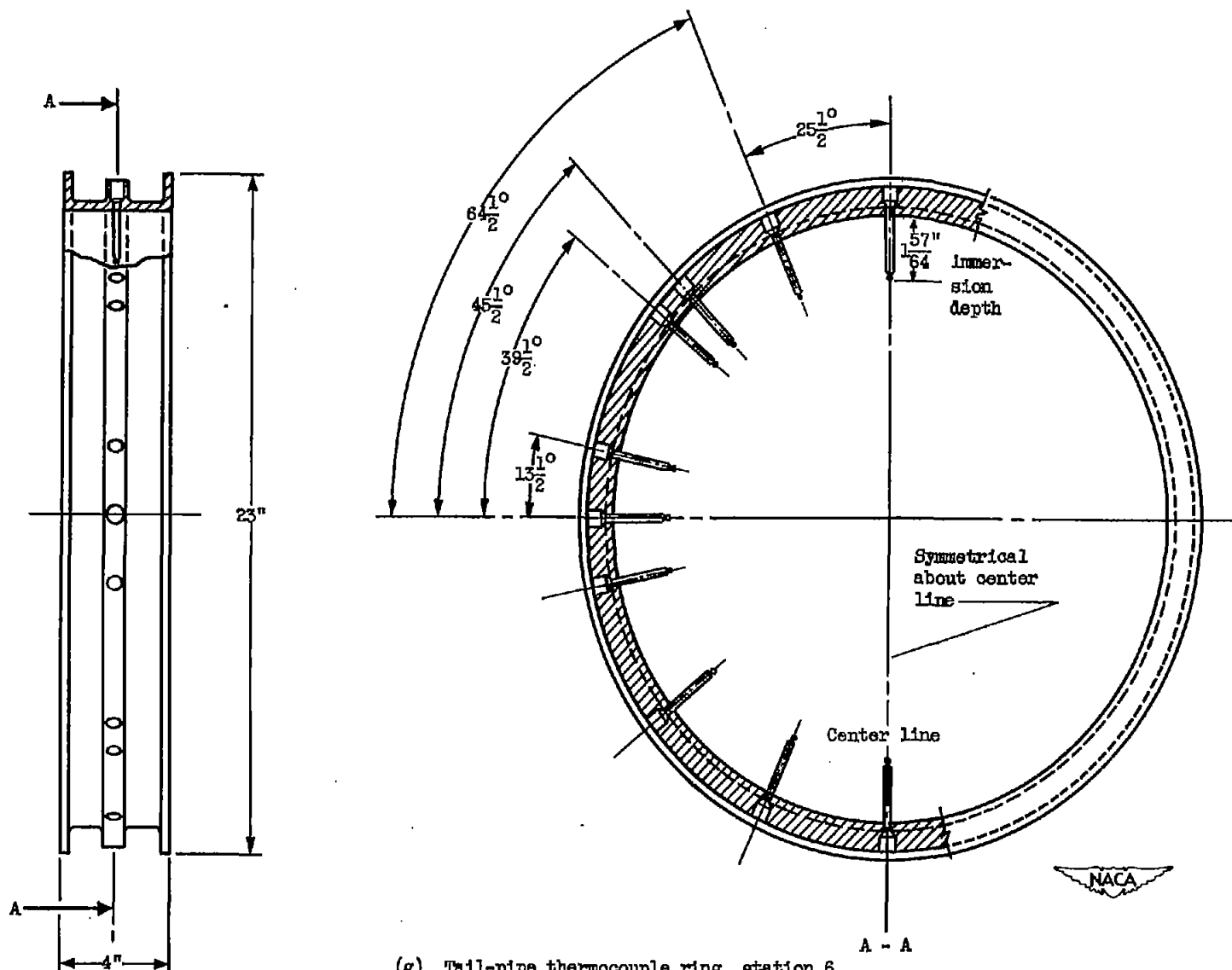


(e) Turbine inlet, station 4; one total-pressure and thermocouple probe in each combustor; typical installation.



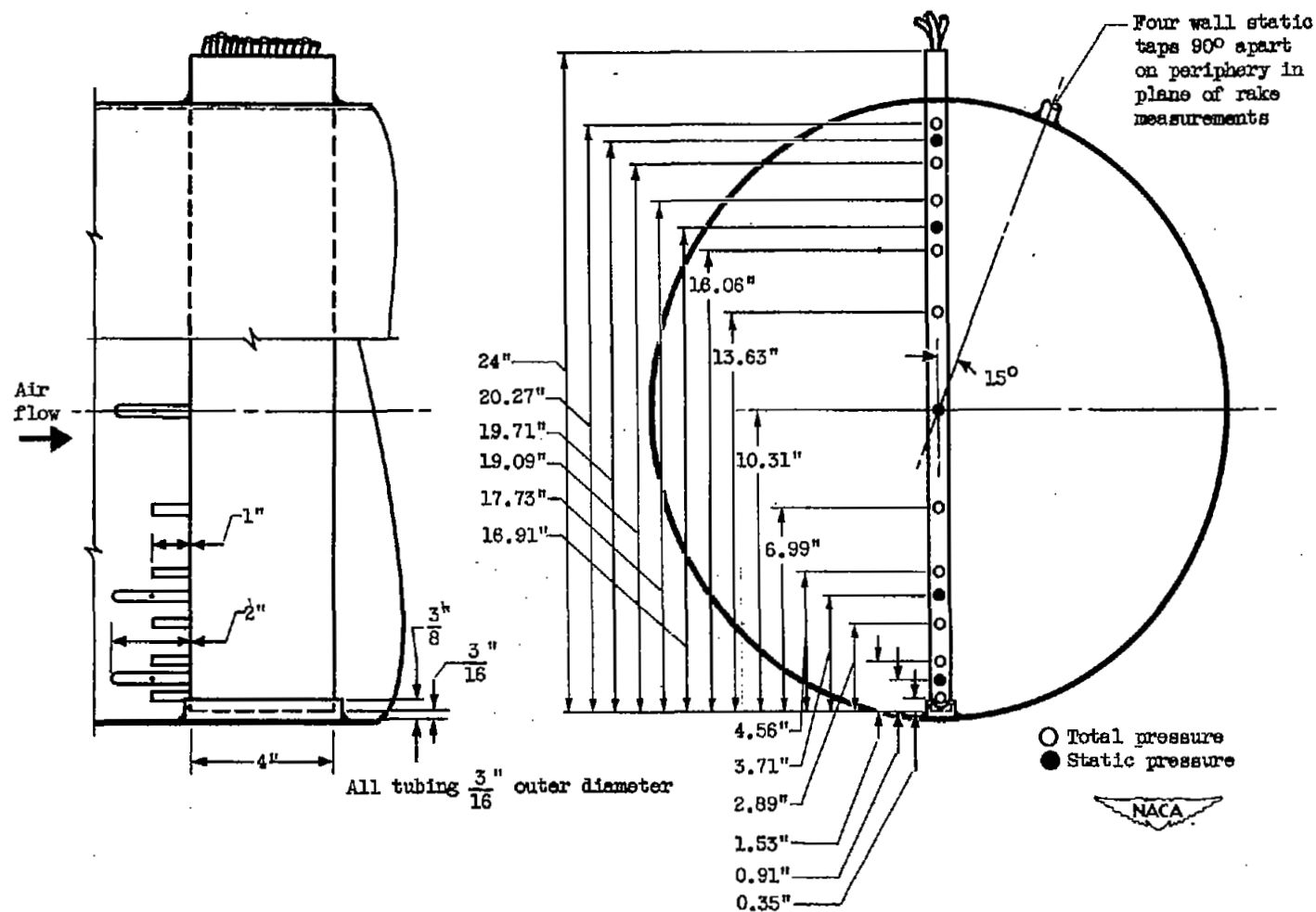
(f) Diffuser-outlet thermocouples; station 5.

Figure 3. - Continued. - Details of instrumentation.



(g) Tail-pipe thermocouple ring, station 6.

Figure 3. - Continued. Details of instrumentation.



(h) Tail-pipe rake (jet-nozzle inlet), station 7.

Figure 3. - Concluded. Details of instrumentation.

2113

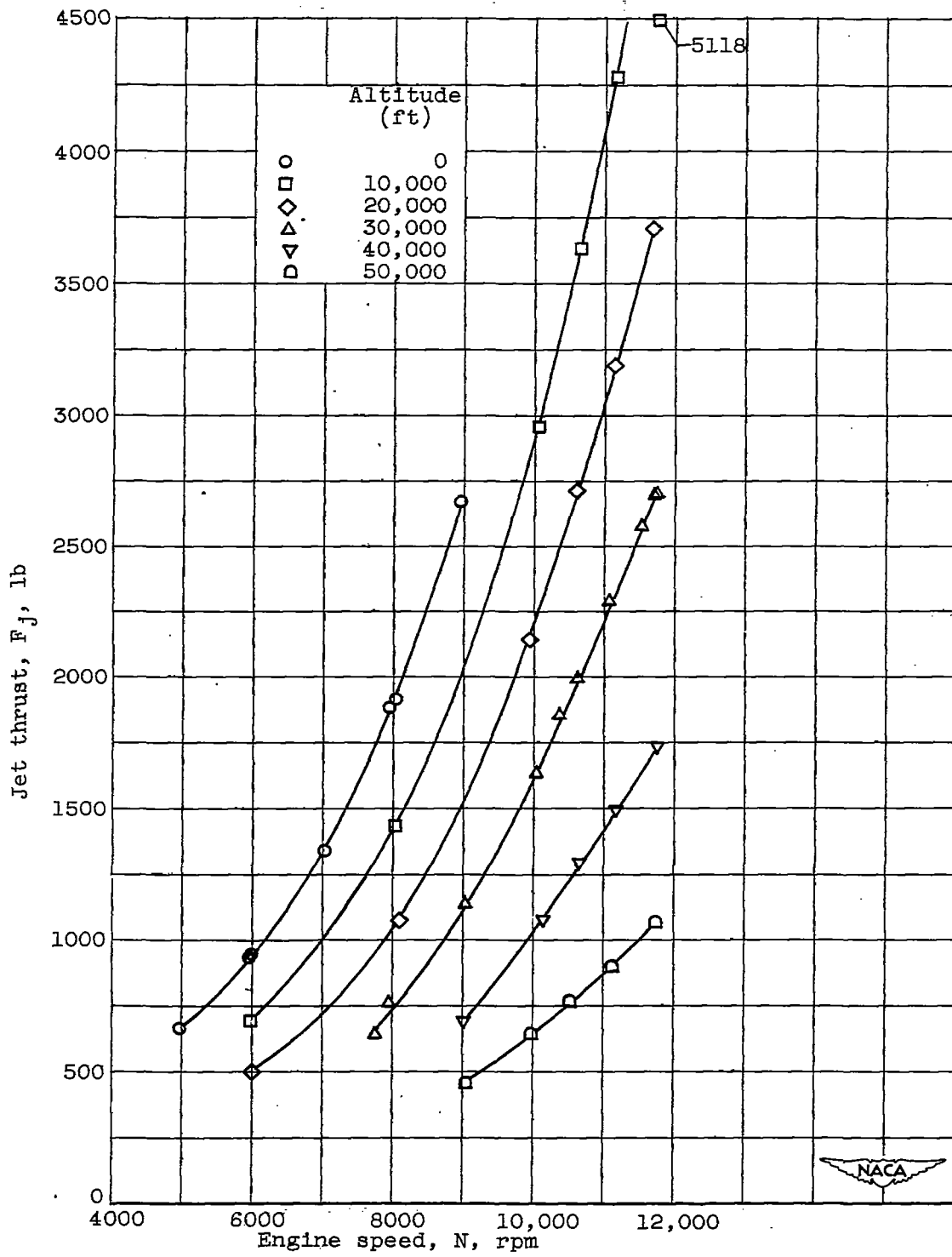


Figure 4. - Effect of altitude on jet thrust. Flight Mach number 0.67.

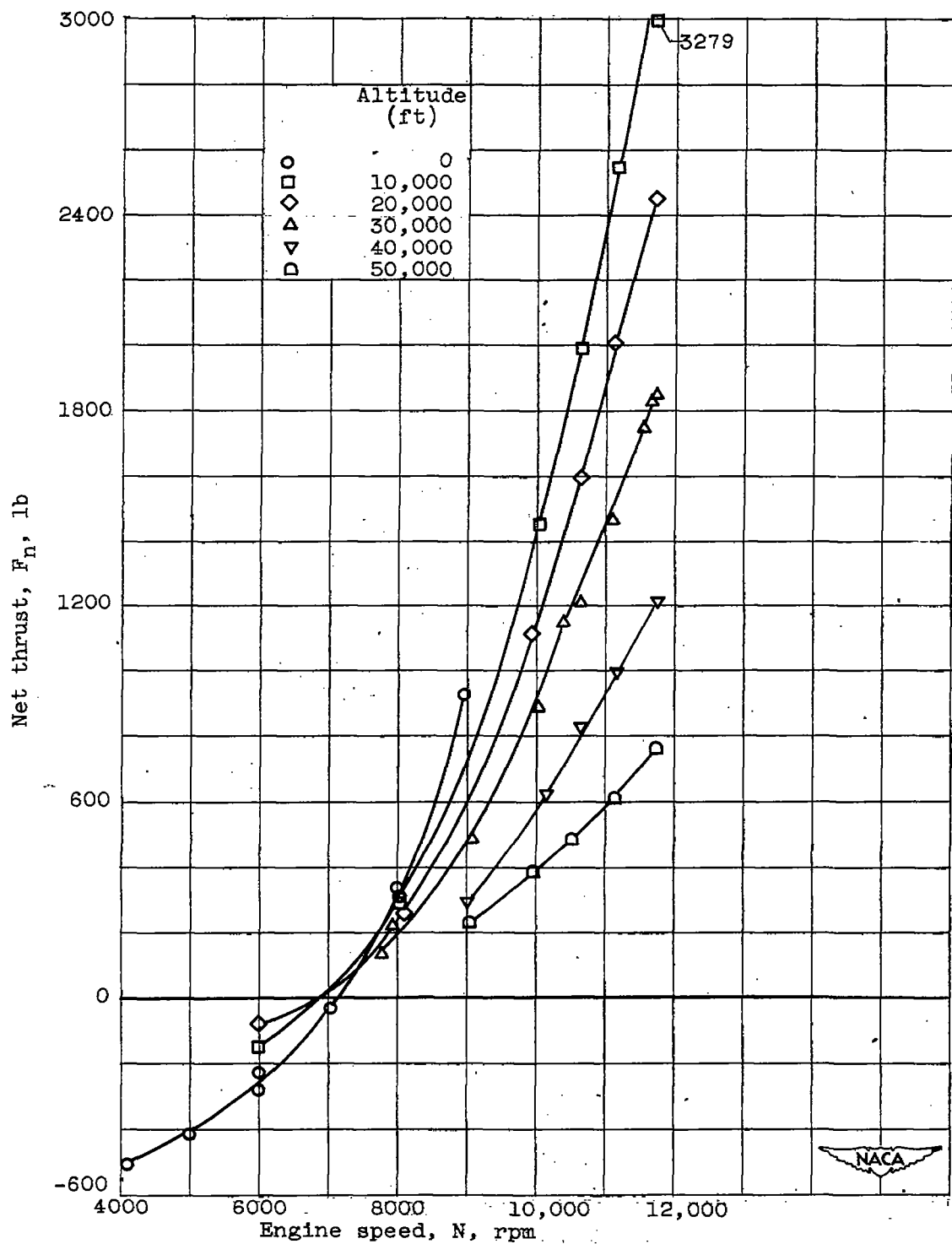


Figure 5. - Effect of altitude on net thrust. Flight Mach number, 0.67.

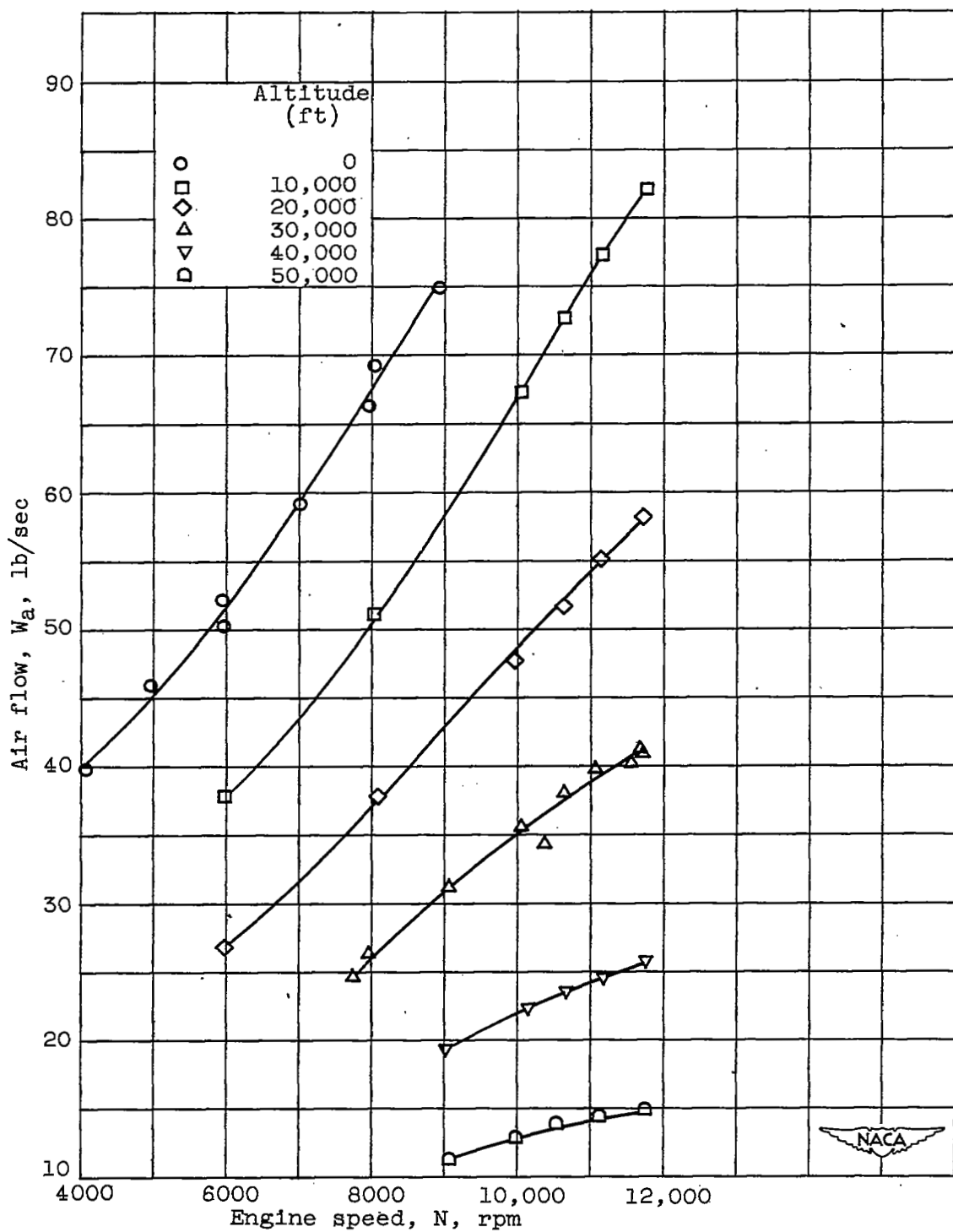


Figure 6. - Effect of altitude on air flow. Flight Mach number, 0.67.

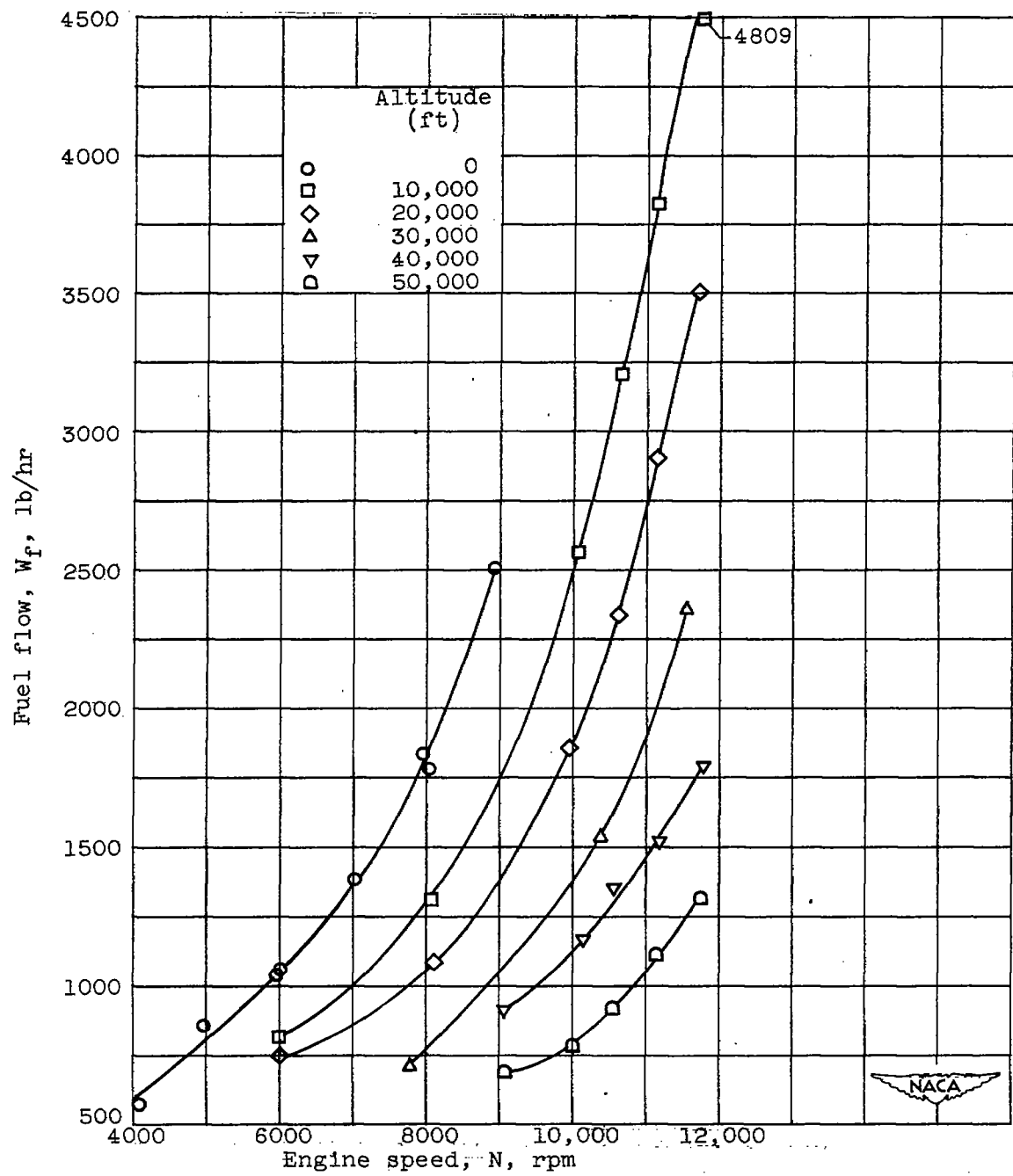


Figure 7. - Effect of altitude on fuel flow. Flight Mach number, 0.67.

2113

2113

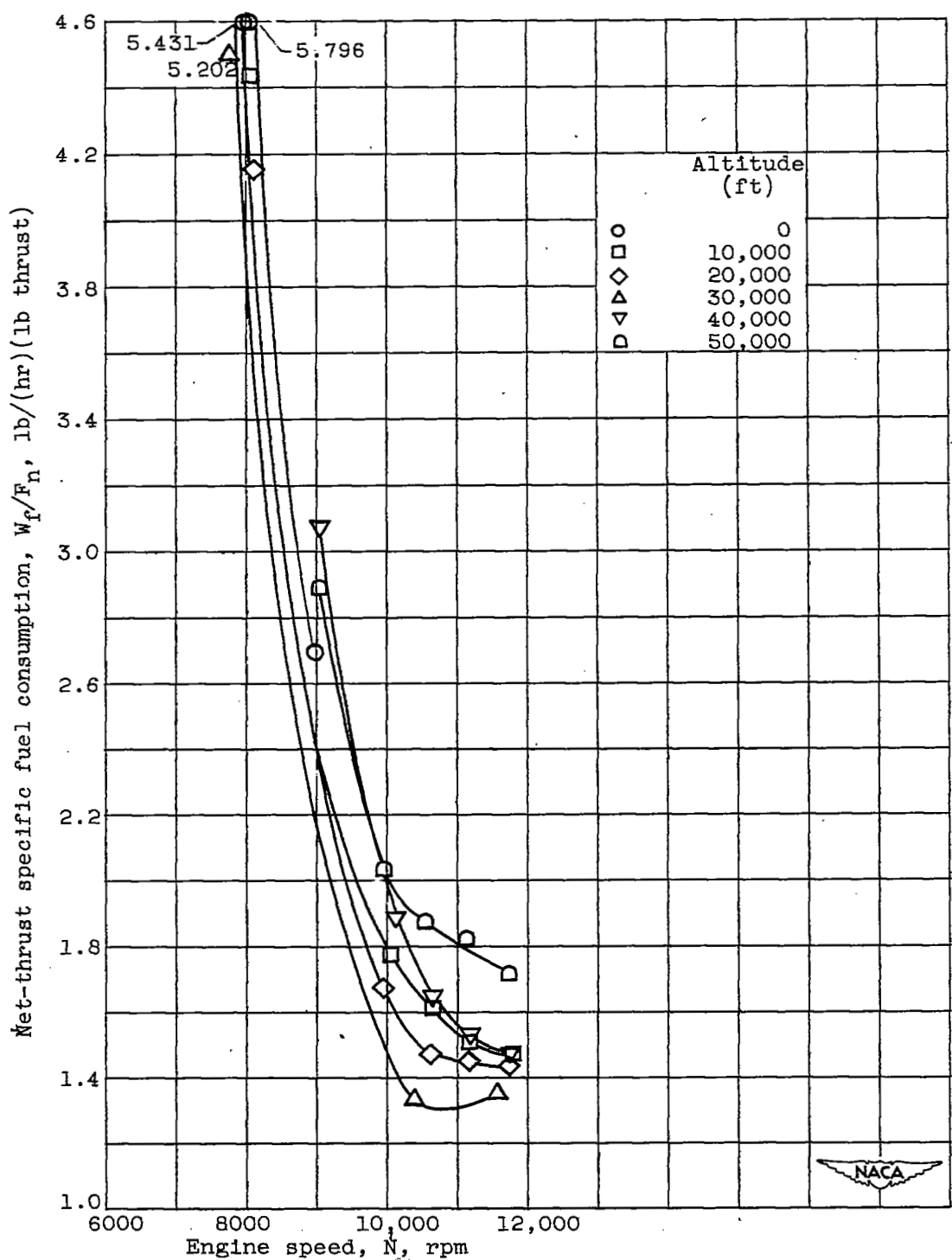


Figure 8. - Effect of altitude on net-thrust specific fuel consumption. Flight Mach number, 0.67.

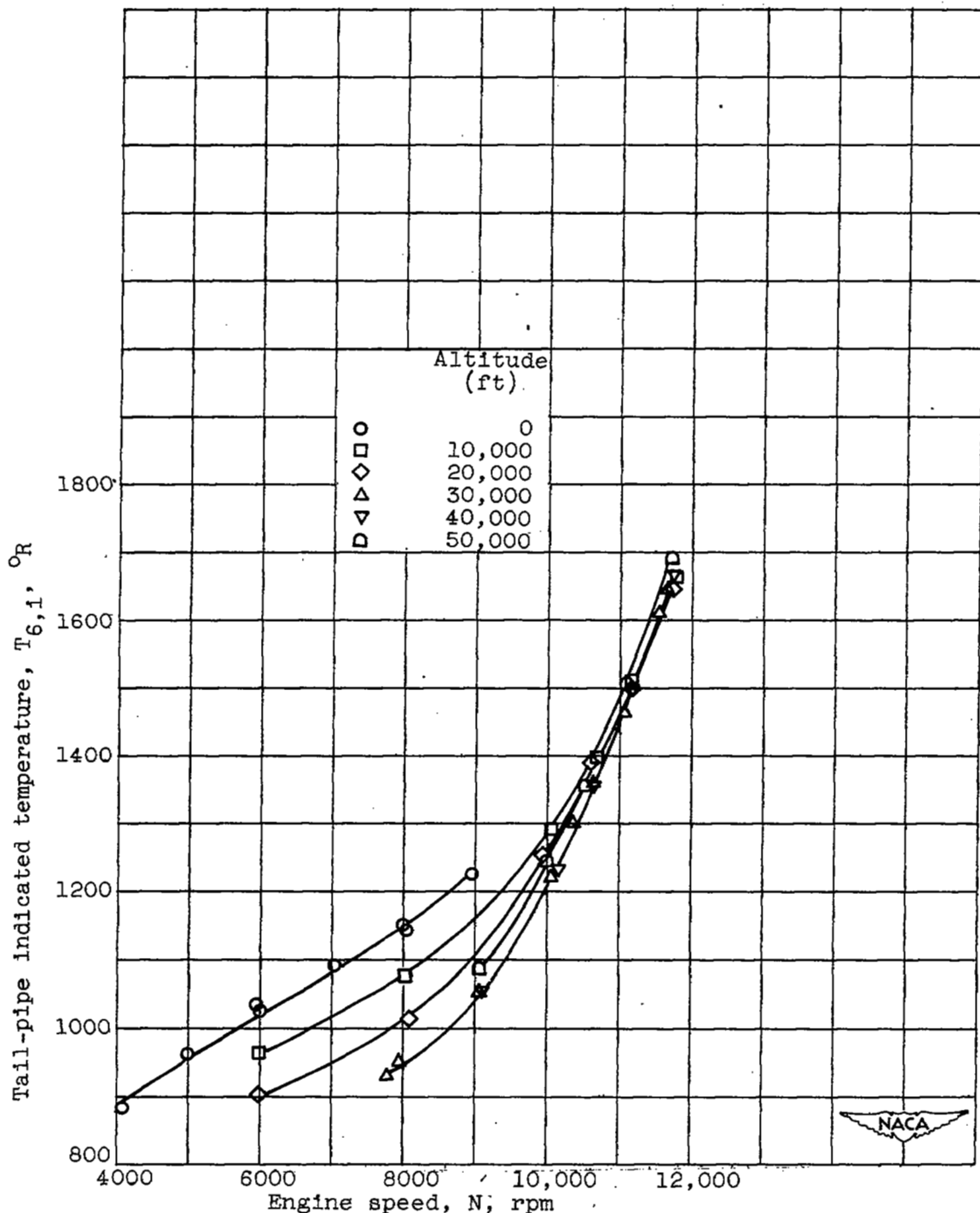


Figure 9: - Effect of altitude on tail-pipe temperature. Flight Mach number, 0.67.

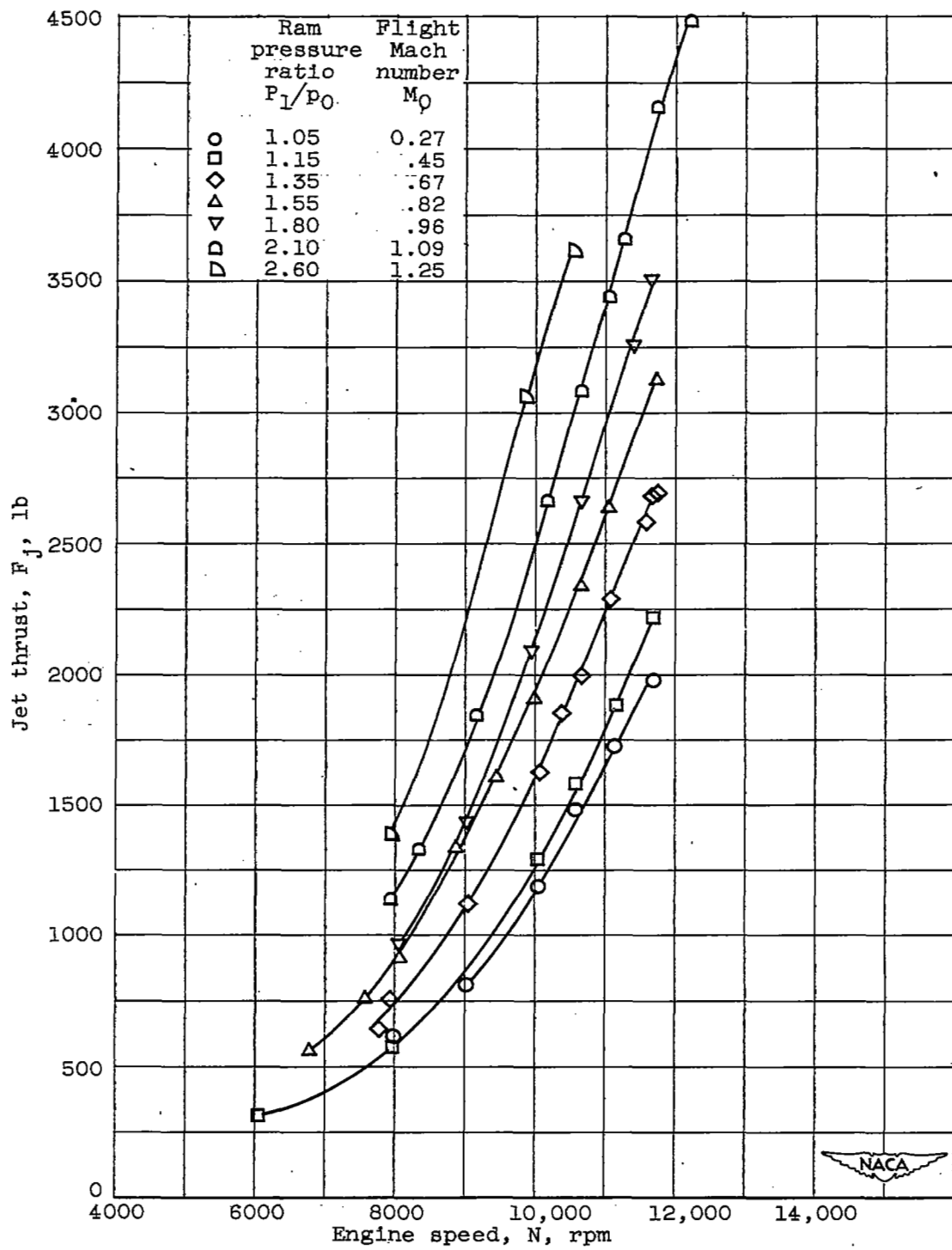


Figure 10. - Effect of flight Mach number on jet thrust. Altitude, 30,000 feet.



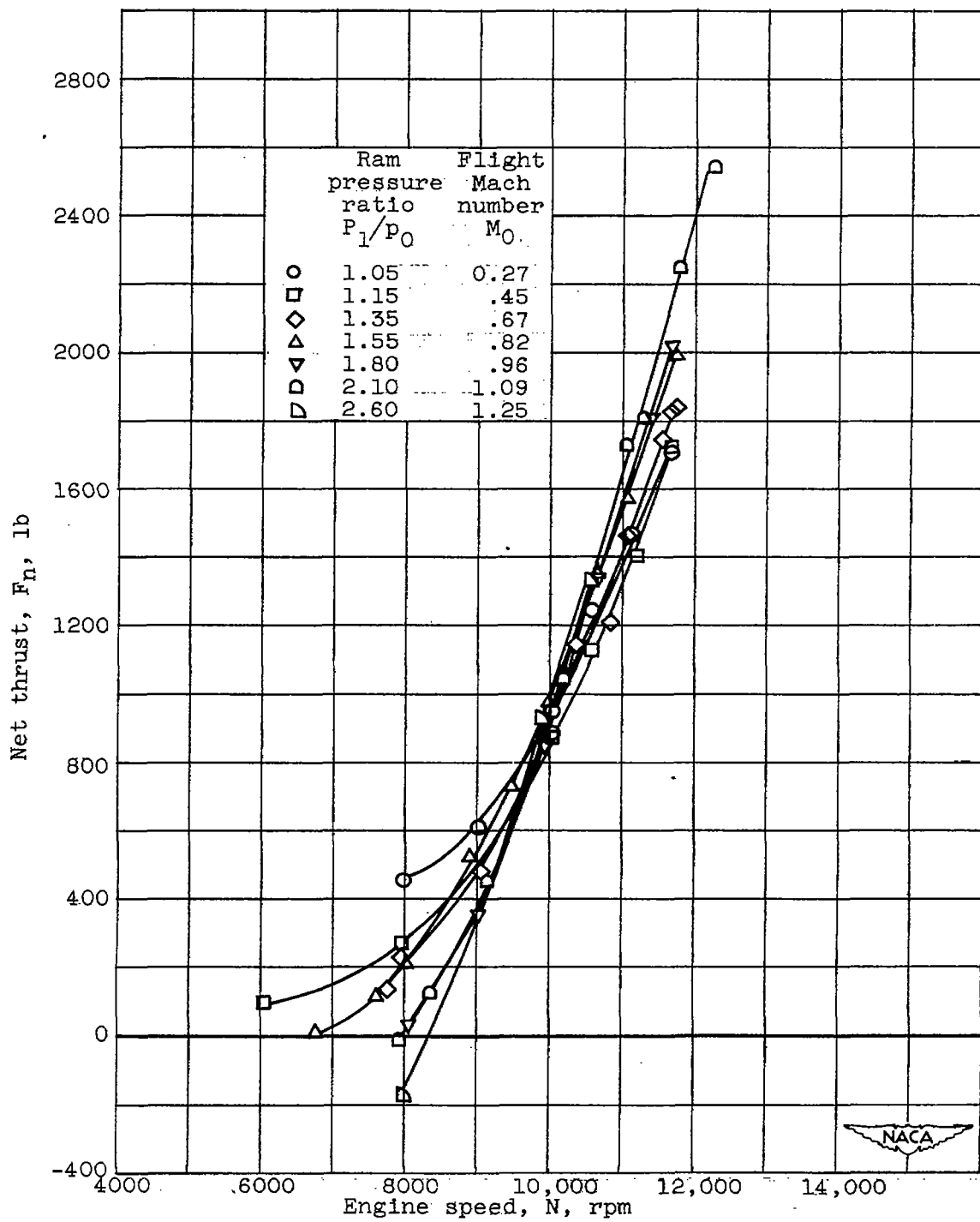


Figure 11. - Effect of flight Mach number on net thrust. Altitude, 30,000 feet.

2115

2113

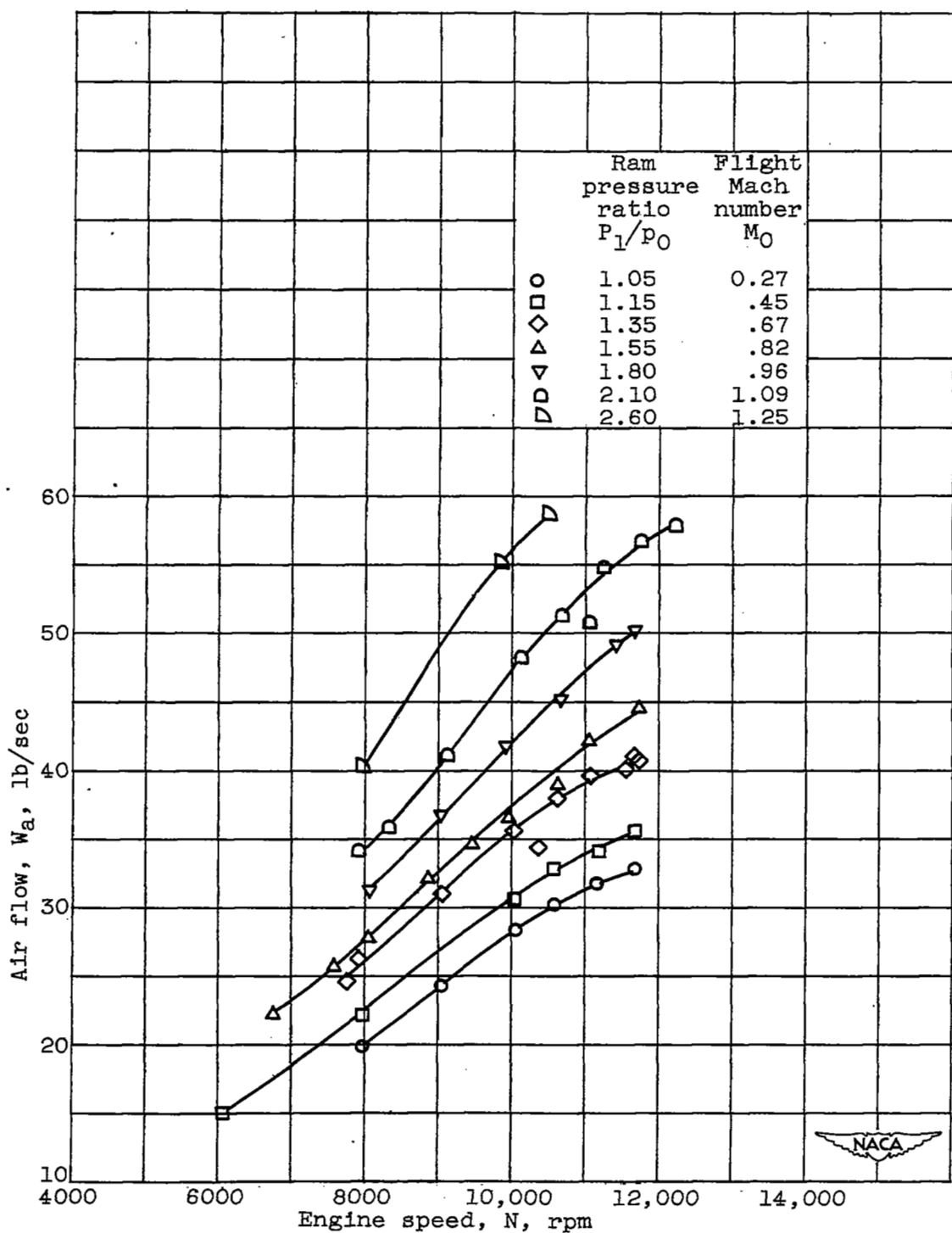


Figure 12. - Effect of flight Mach number on air flow.
Altitude, 30,000 feet.

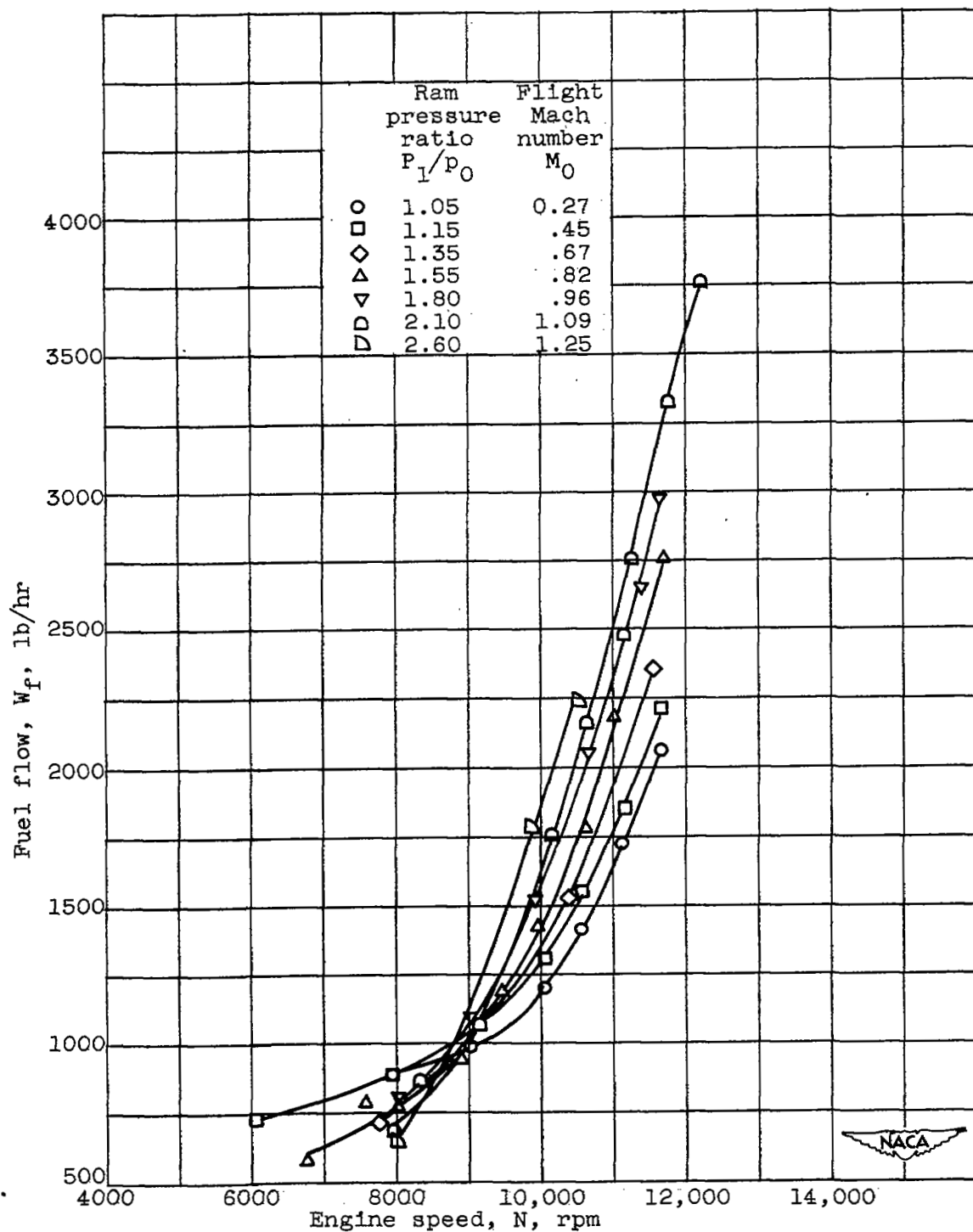


Figure 13. - Effect of flight Mach number on fuel flow.
Altitude, 30,000 feet.

212

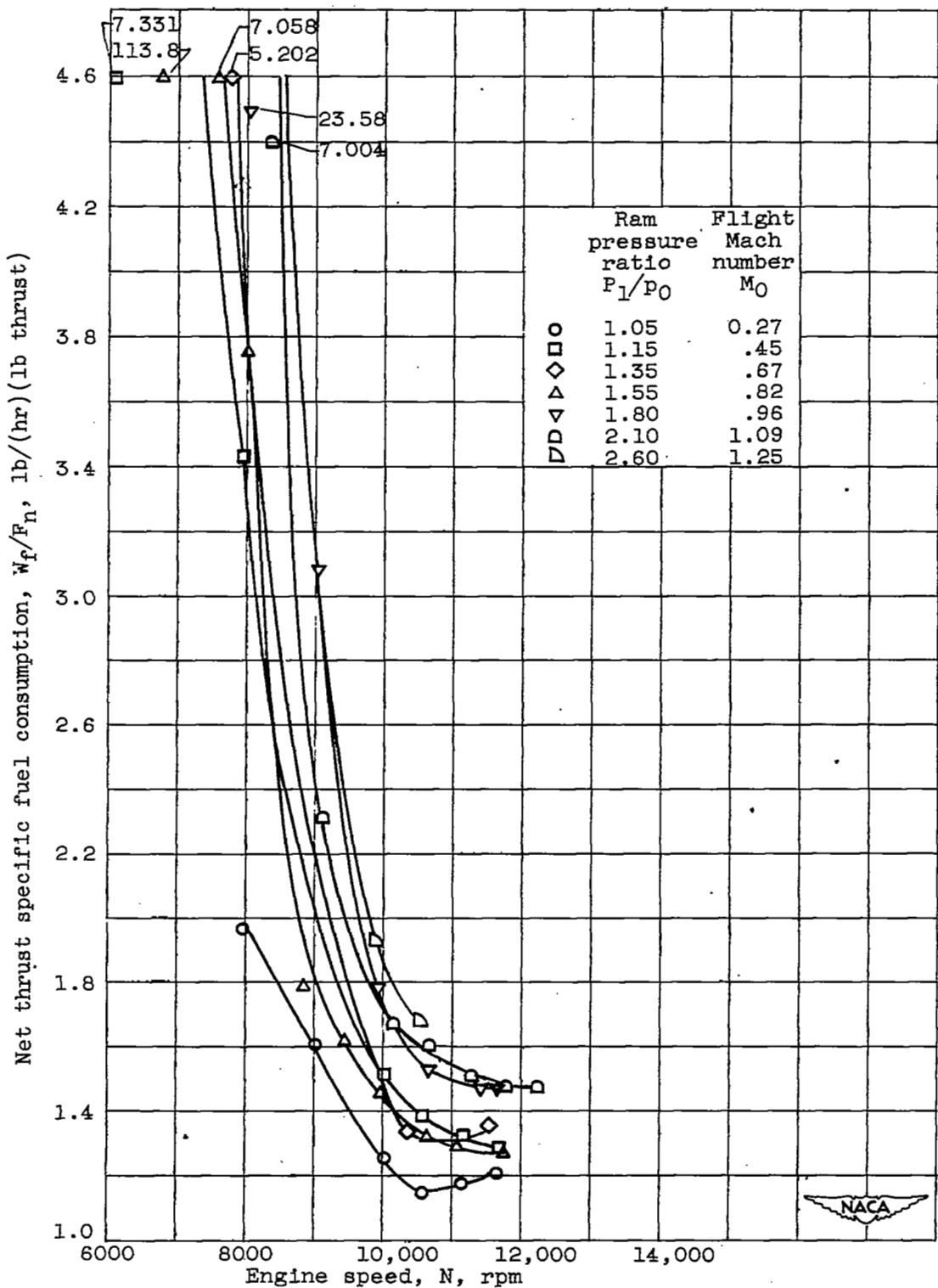


Figure 14. - Effect of flight Mach number on net-thrust specific fuel consumption. Altitude, 30,000 feet.

2113

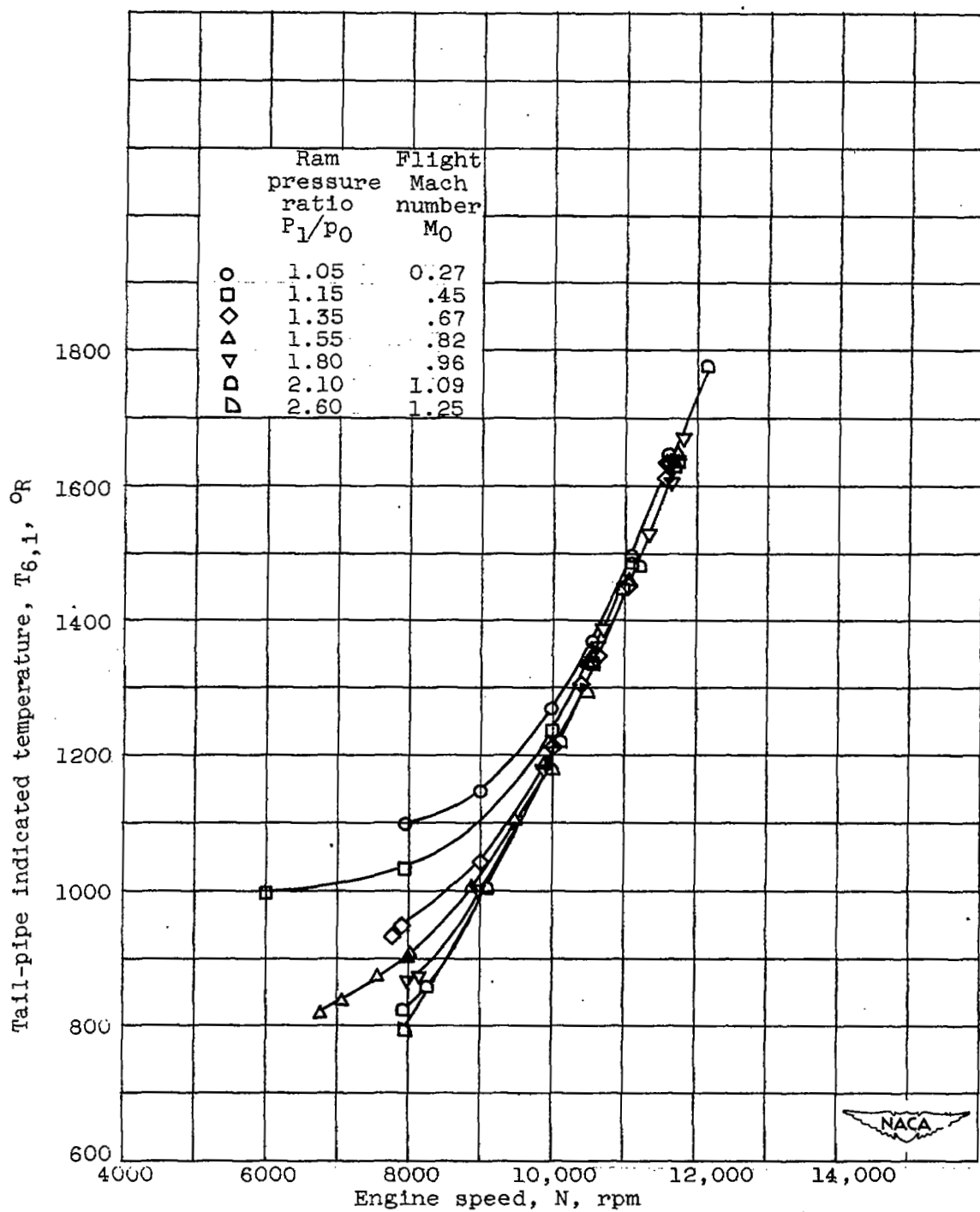


Figure 15. - Effect of flight Mach number on tail-pipe temperature.
Altitude, 30,000 feet.

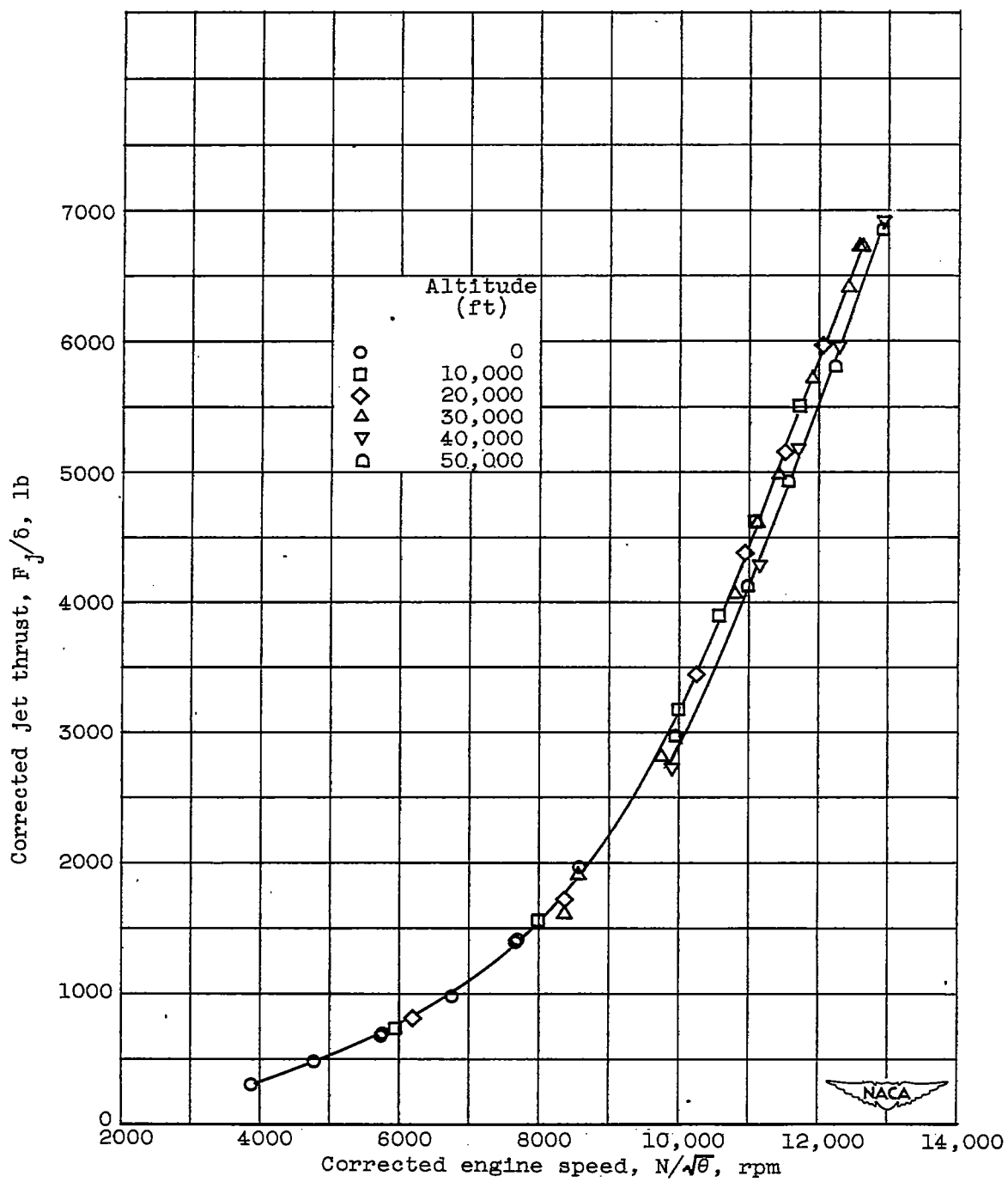


Figure 16. - Effect of altitude on corrected jet thrust. Flight Mach number, 0.67.

2113

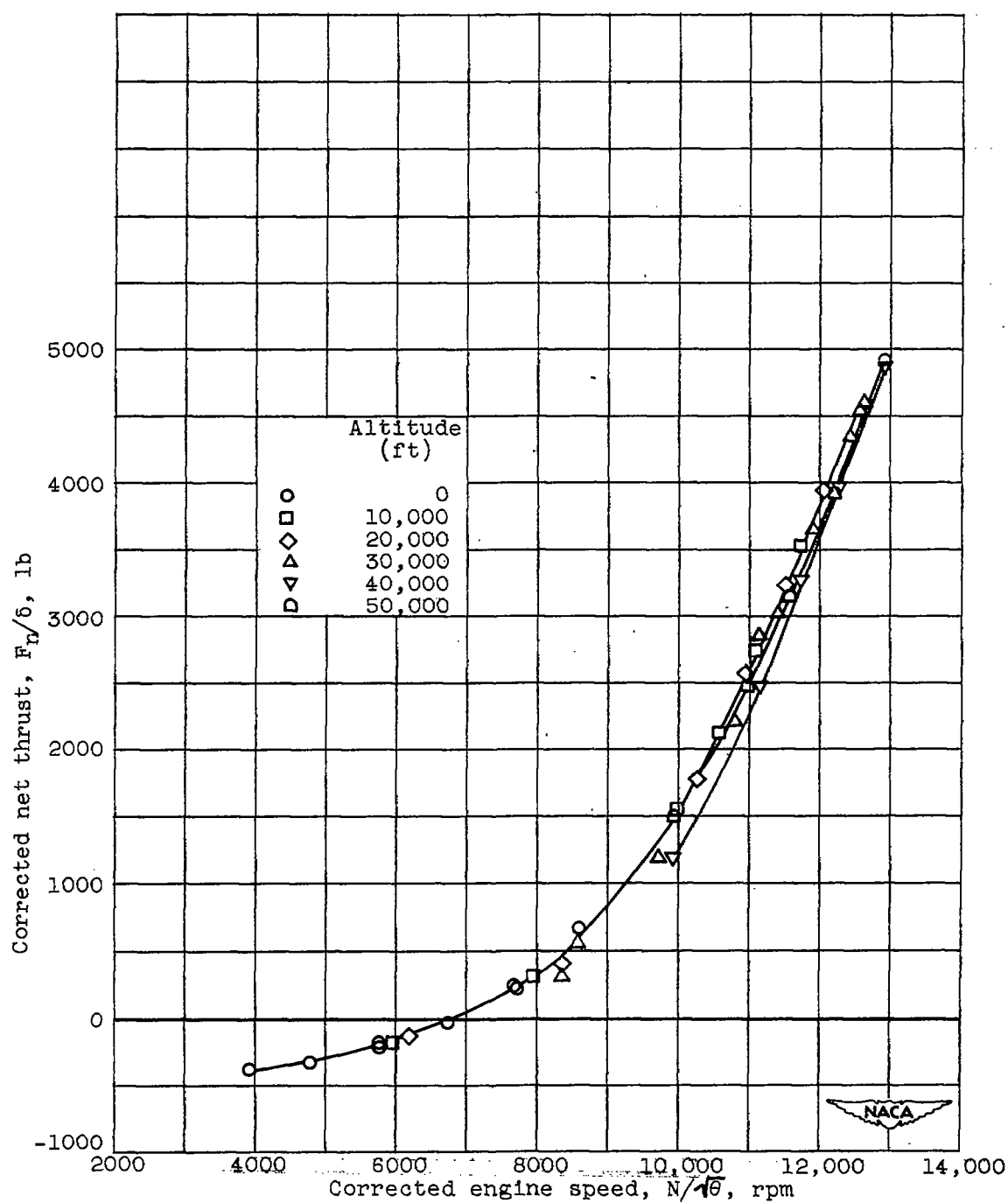


Figure 17. - Effect of altitude on corrected net thrust. Flight Mach number, 0.67.

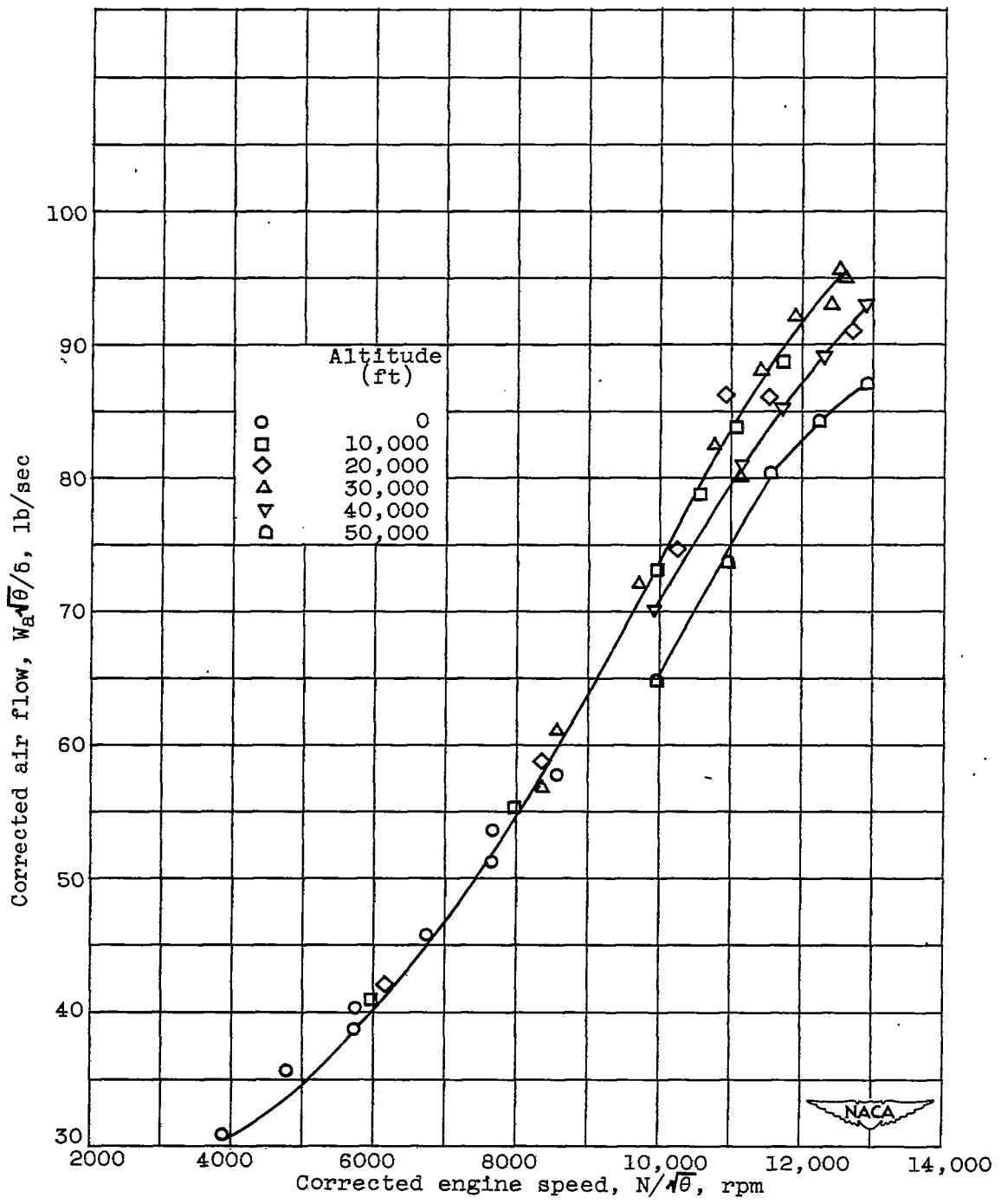


Figure 18. - Effect of altitude on corrected air flow. Flight Mach number, 0.67.

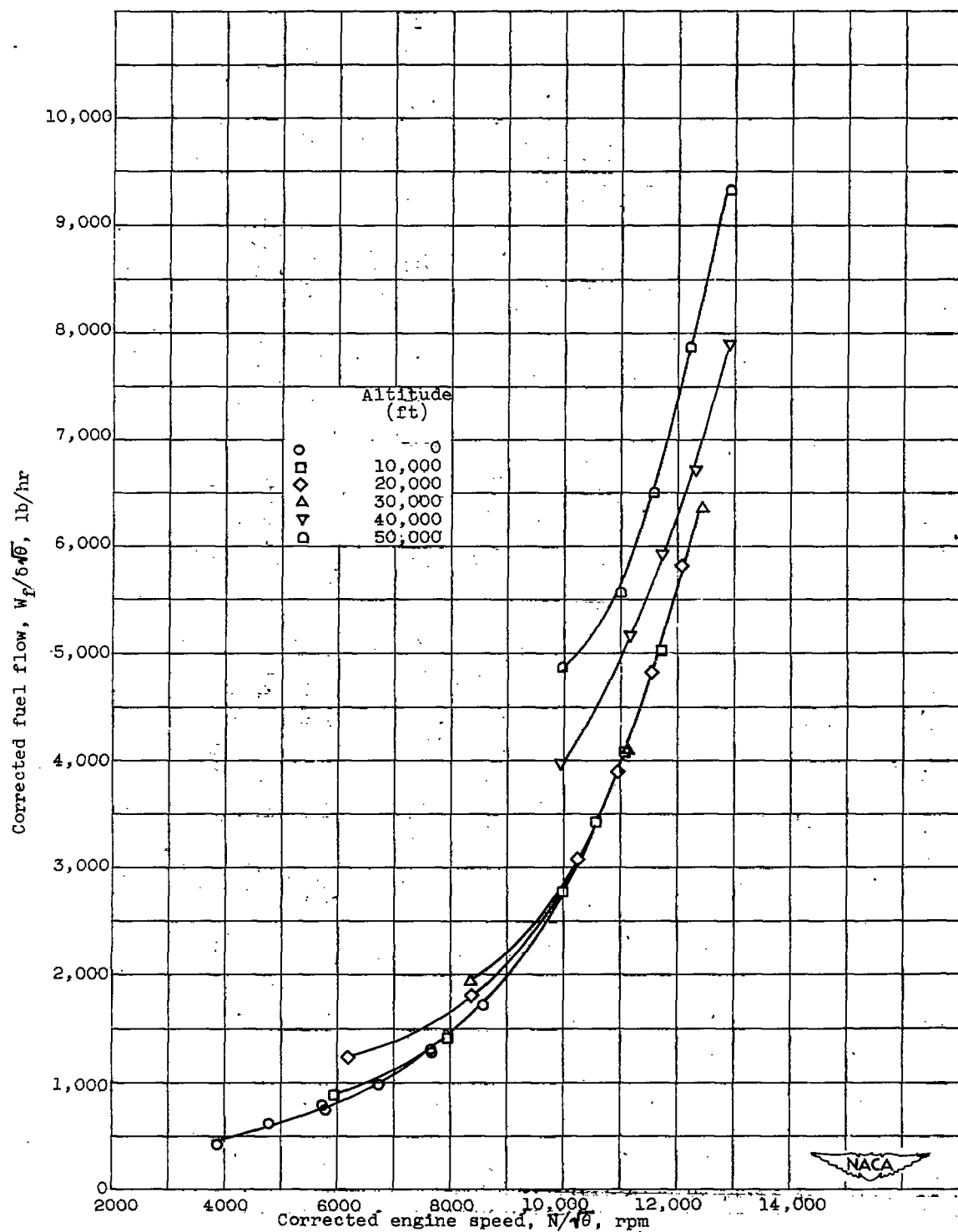


Figure 19. - Effect of altitude on corrected fuel flow. Flight Mach number, 0.67.

2113

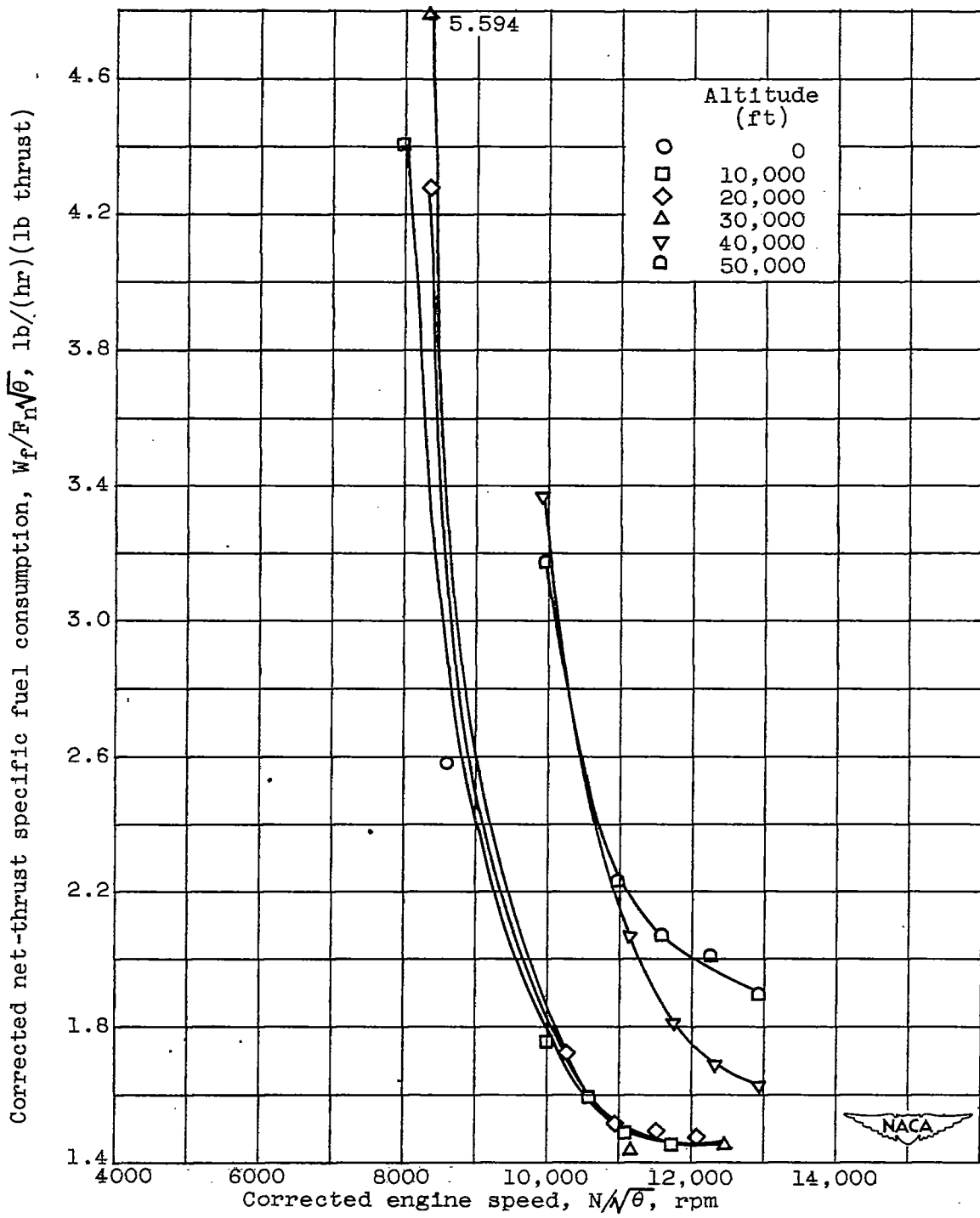


Figure 20. - Effect of altitude on corrected net-thrust specific fuel consumption. Flight Mach number, 0.67.

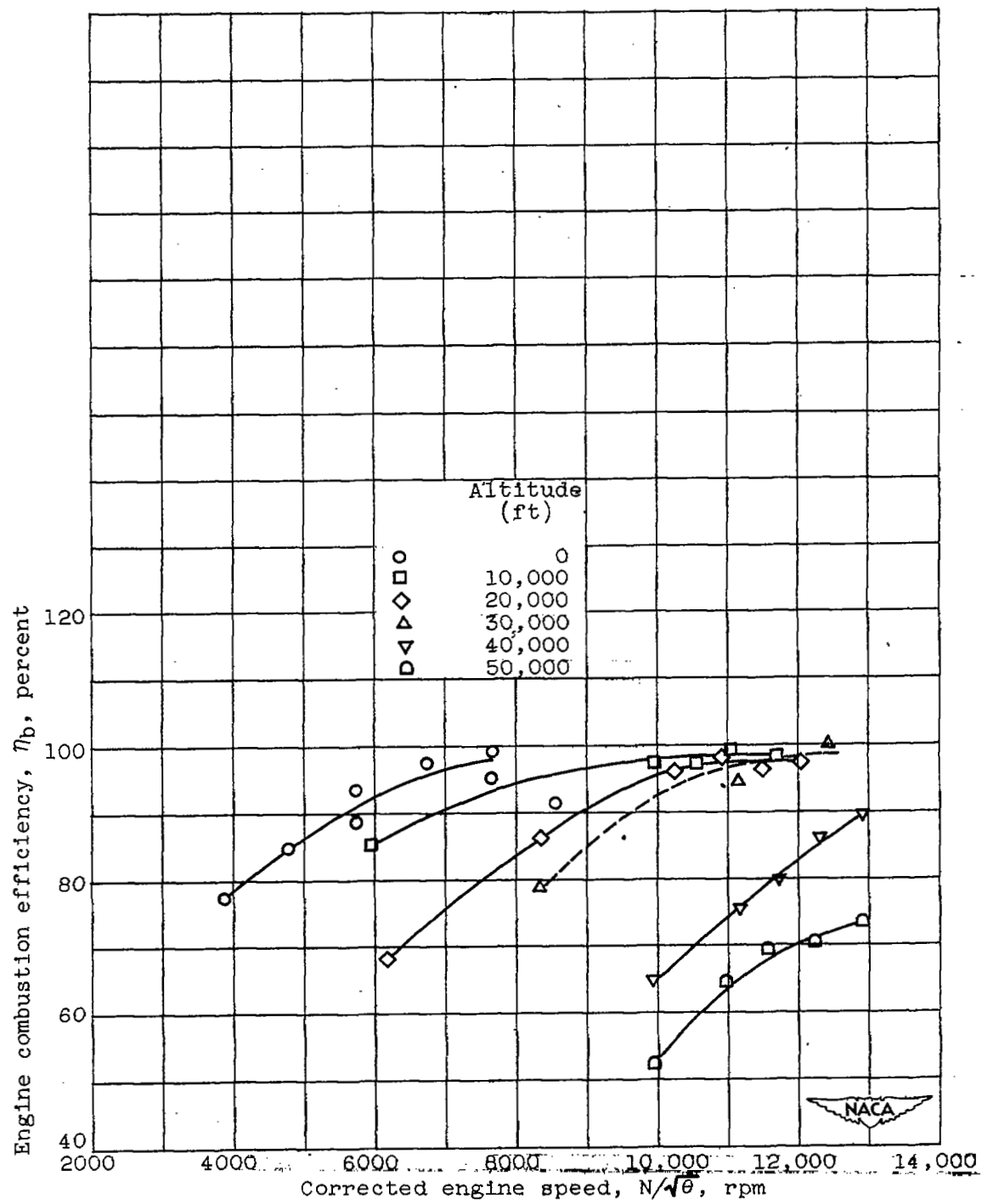


Figure 21. --Effect of altitude on engine combustion efficiency.
Flight Mach number, 0.67.

2113

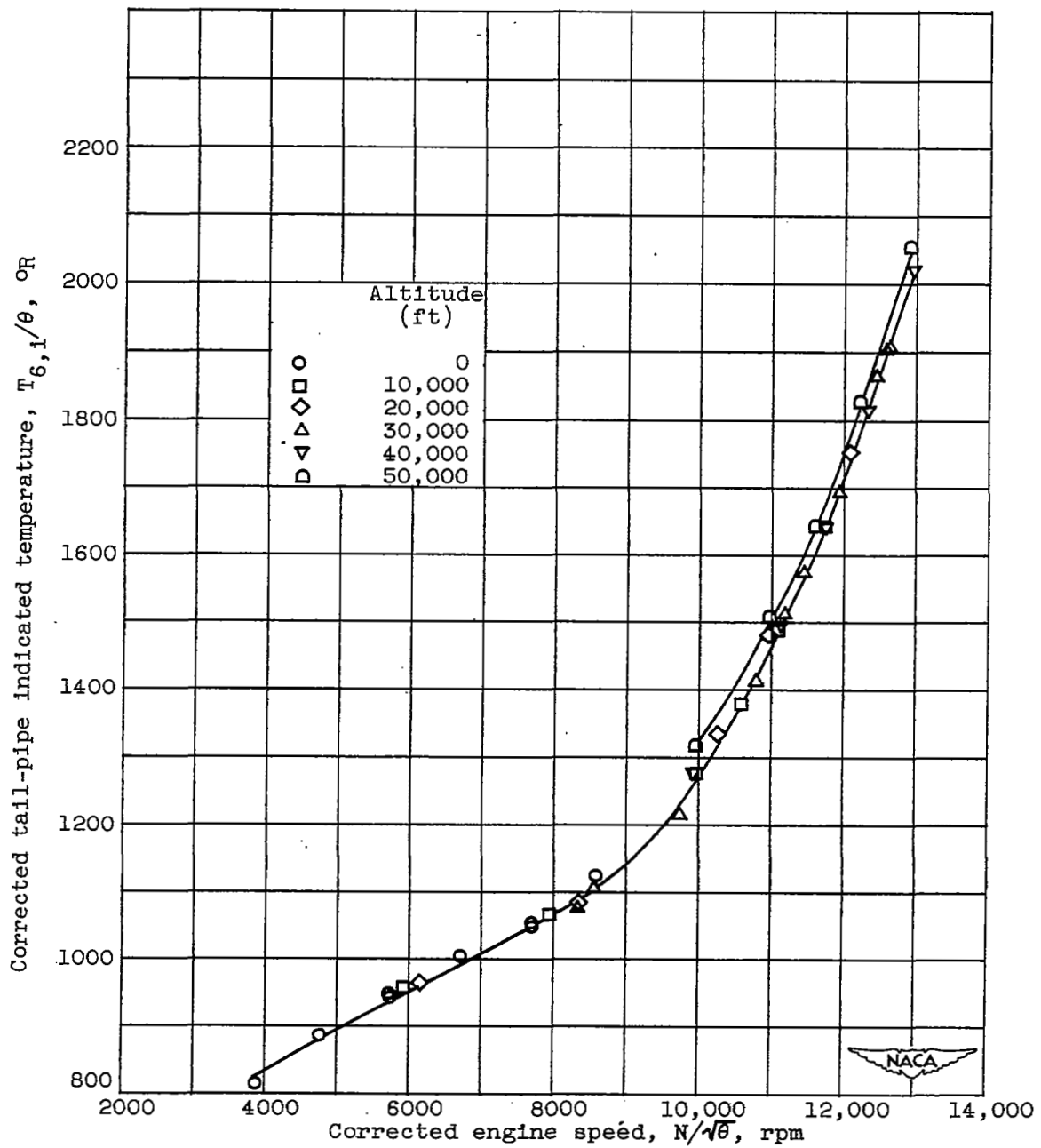


Figure 22. - Effect of altitude on corrected tail-pipe indicated temperature. Flight Mach number, 0.67.

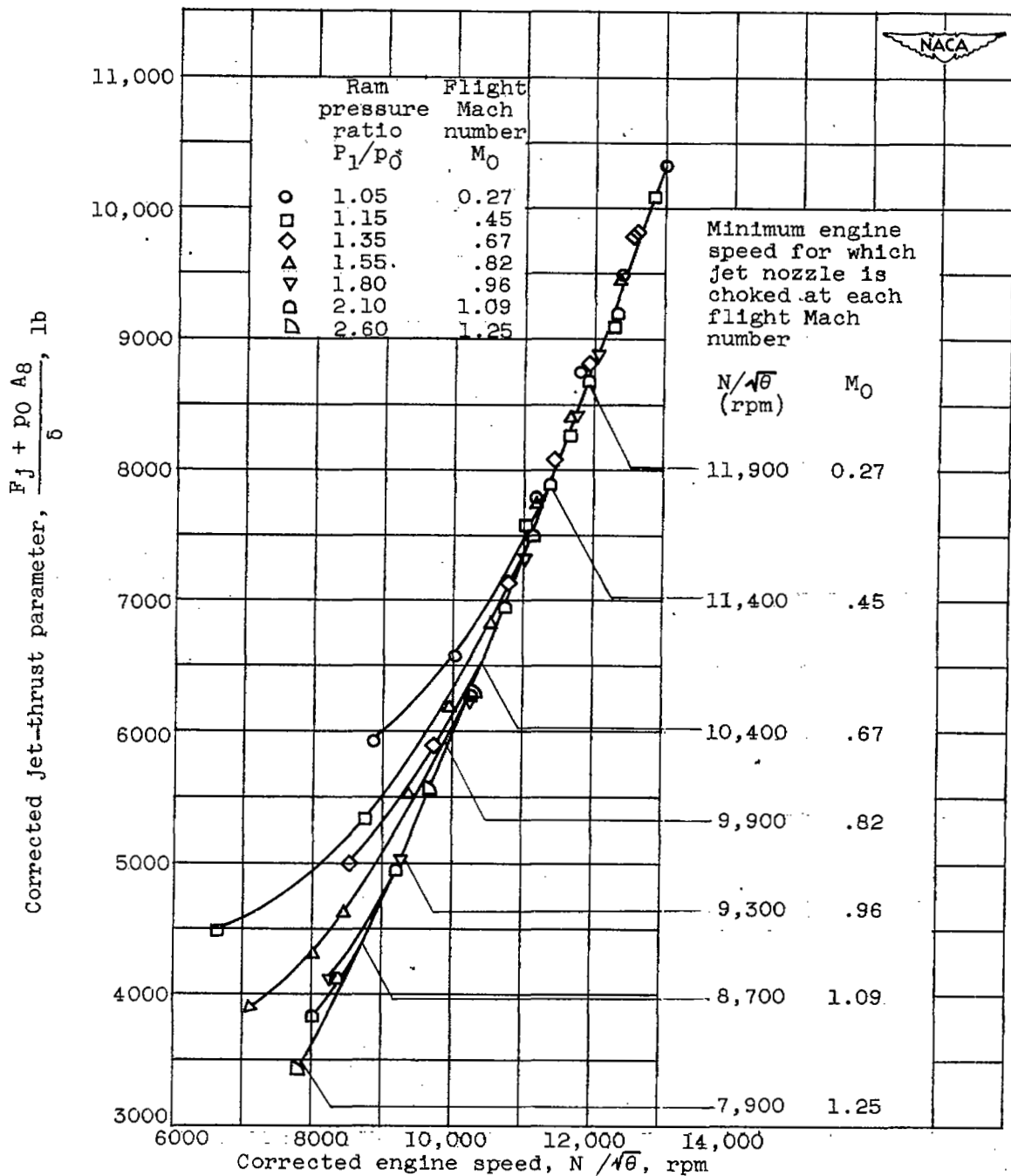


Figure 23. - Effect of flight Mach number on corrected jet-thrust parameter. Altitude, 30,000 feet.

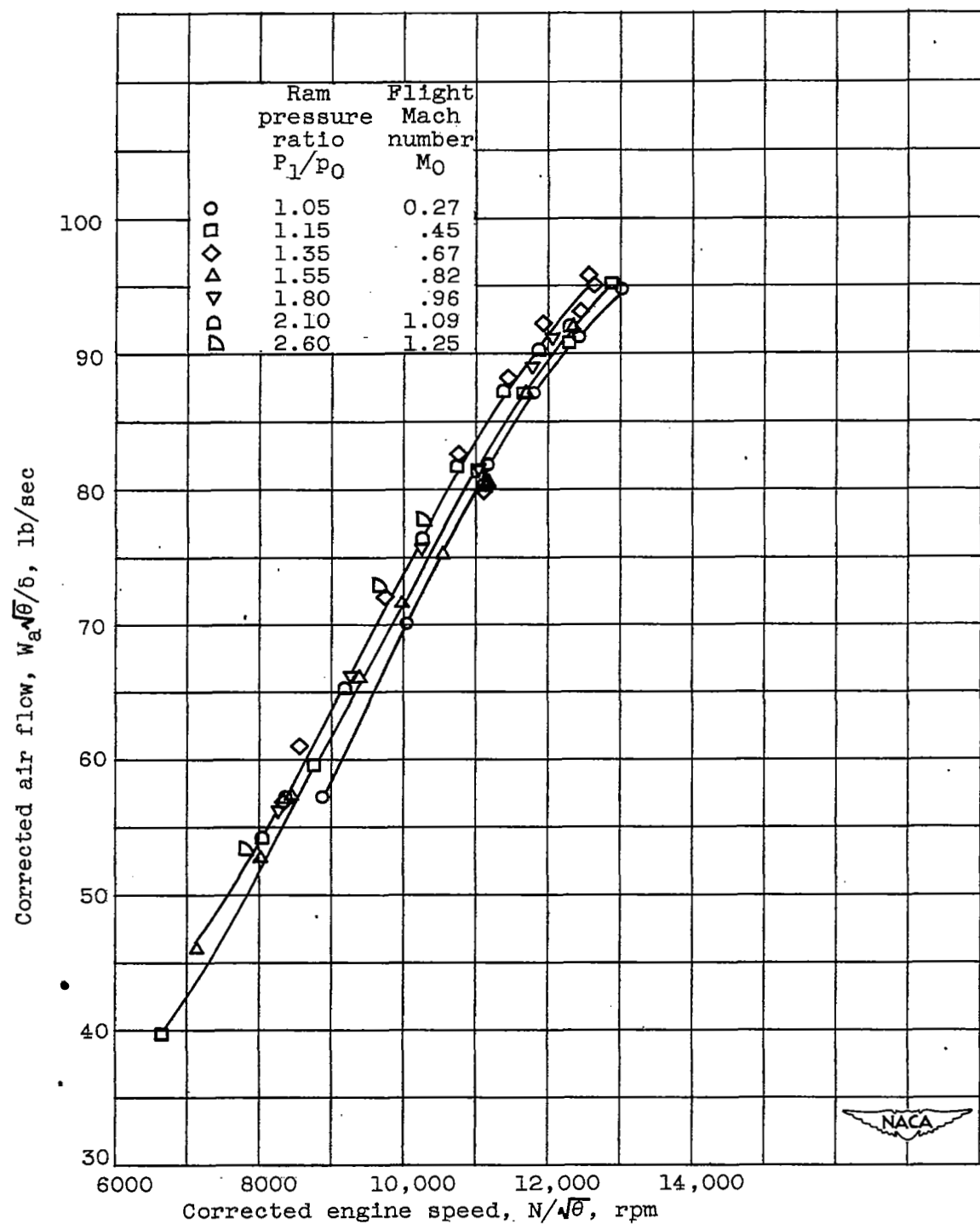


Figure 24. - Effect of flight Mach number on corrected air flow.
Altitude, 30,000 feet.

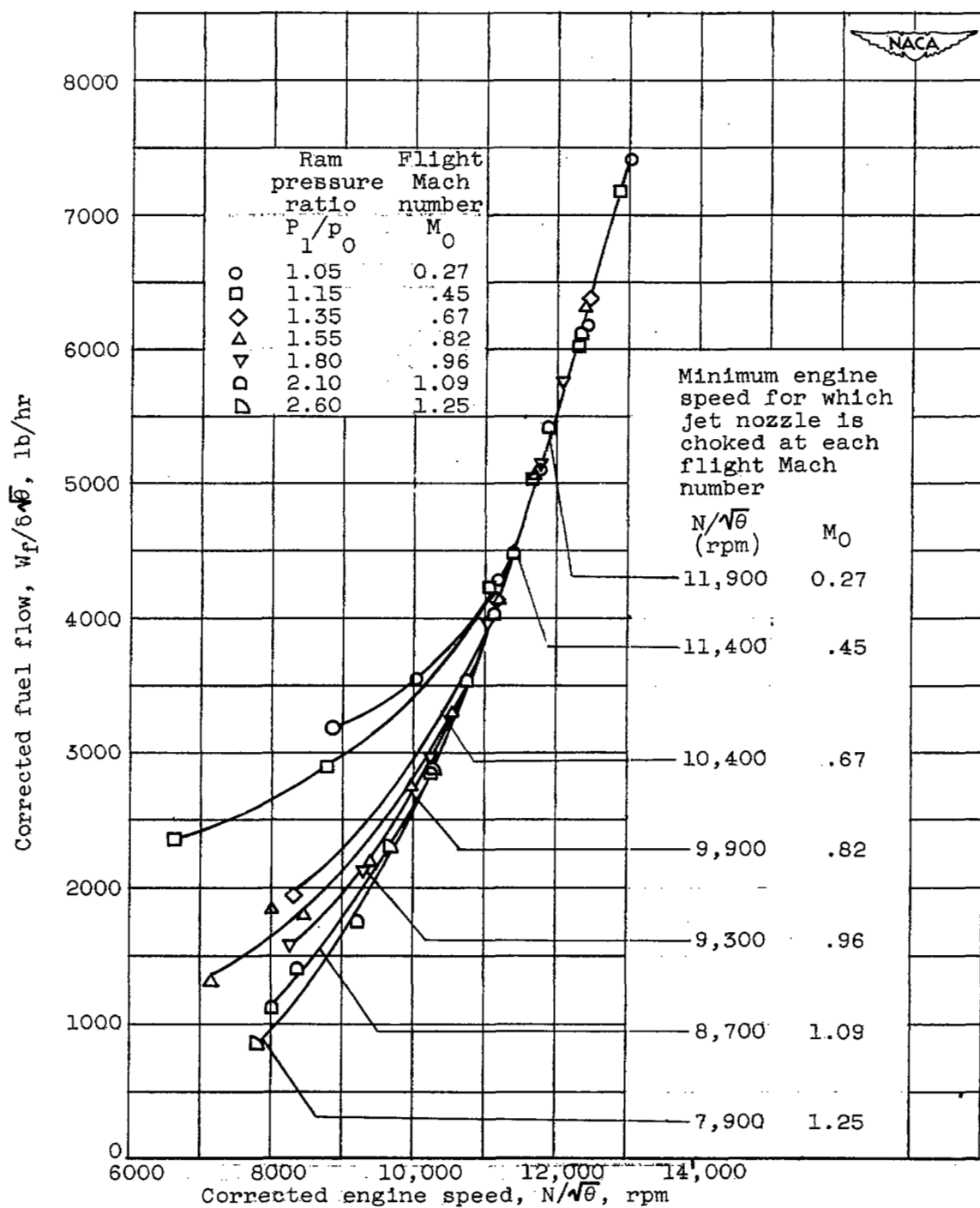


Figure 25. - Effect of flight Mach number on corrected fuel flow.
Altitude, 30,000 feet.

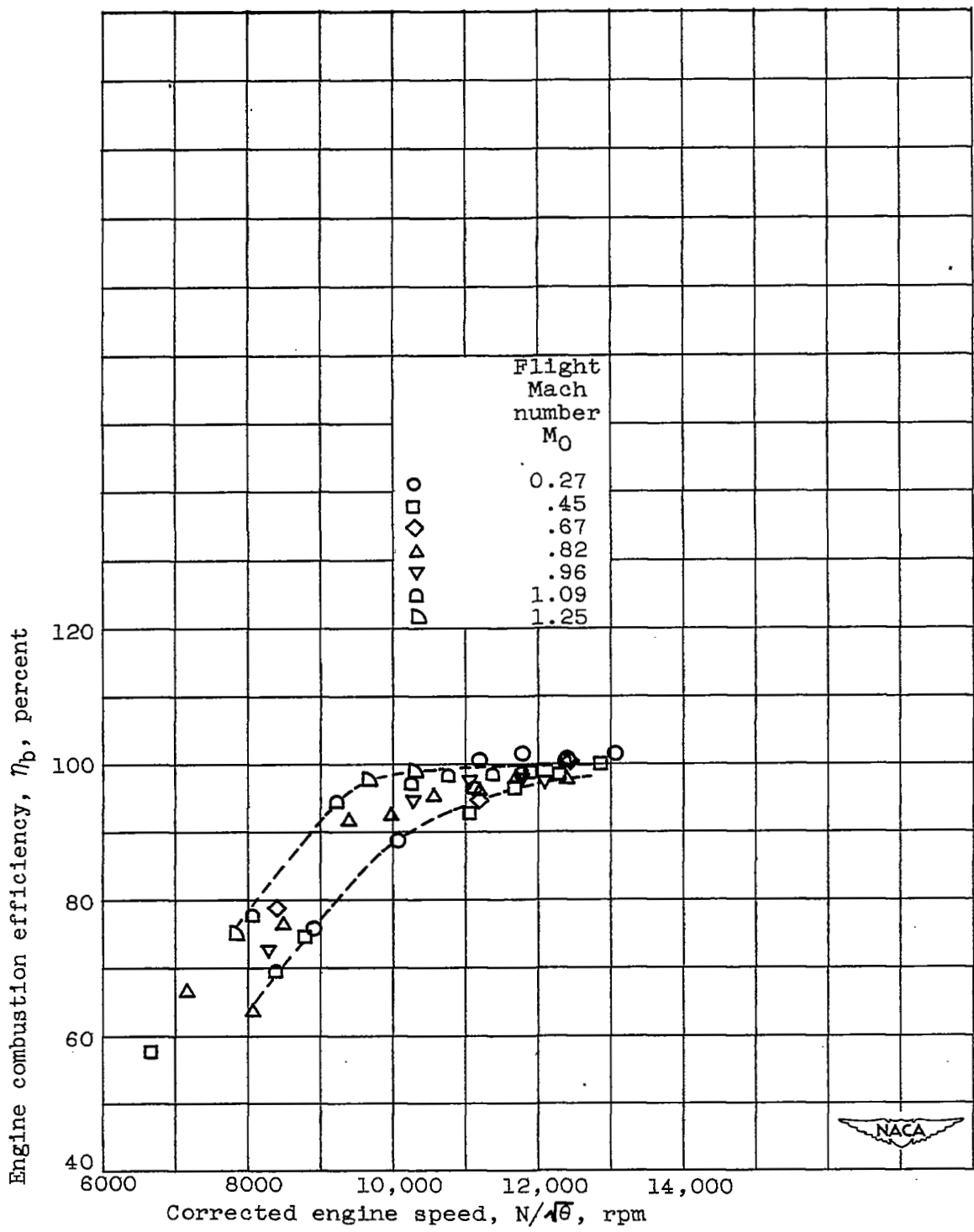


Figure 26. - Effect of flight Mach number on engine combustion efficiency. Altitude, 30,000 feet.

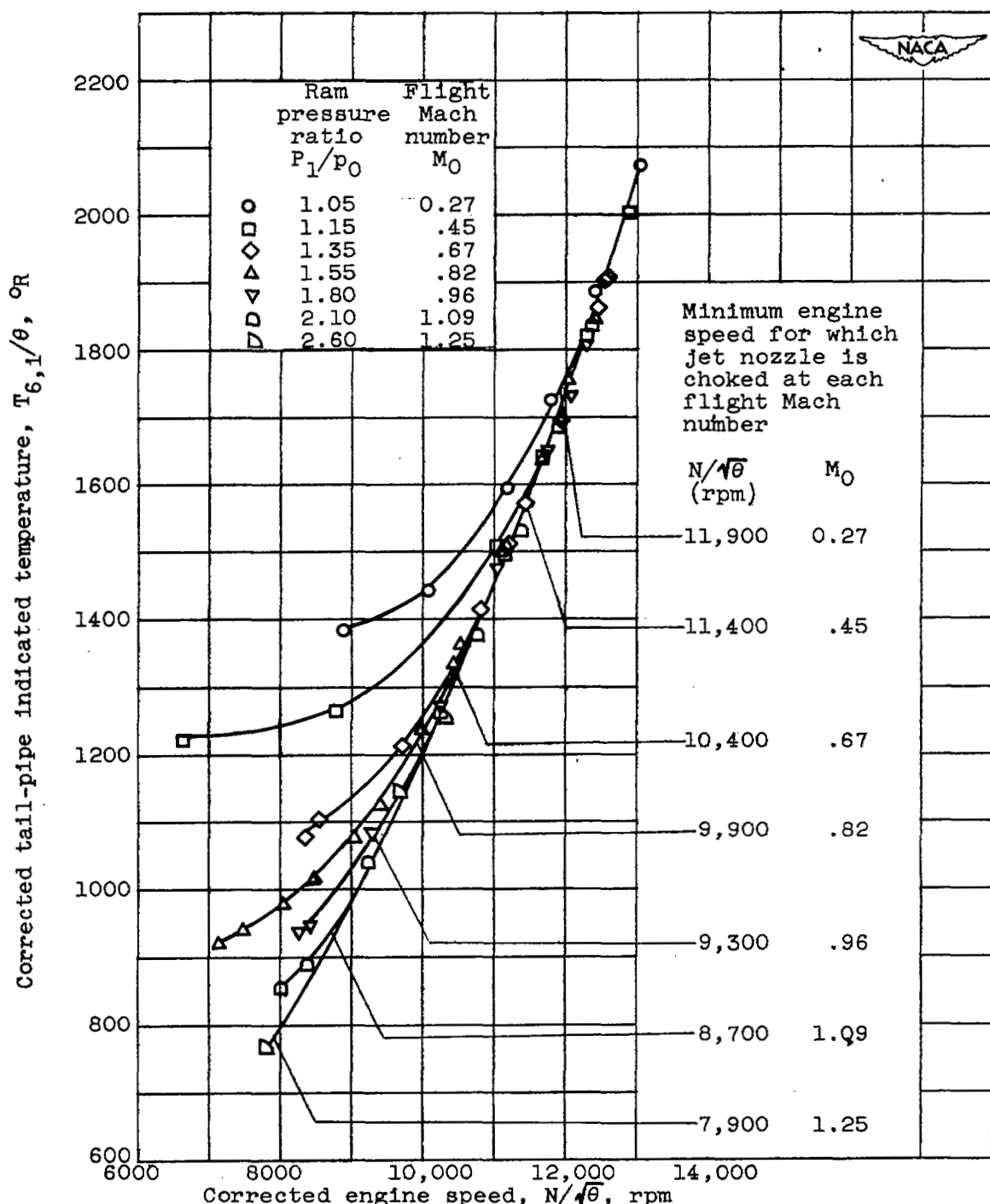


Figure 27. - Effect of flight Mach number on corrected tail-pipe indicated temperature. Altitude, 30,000 feet.

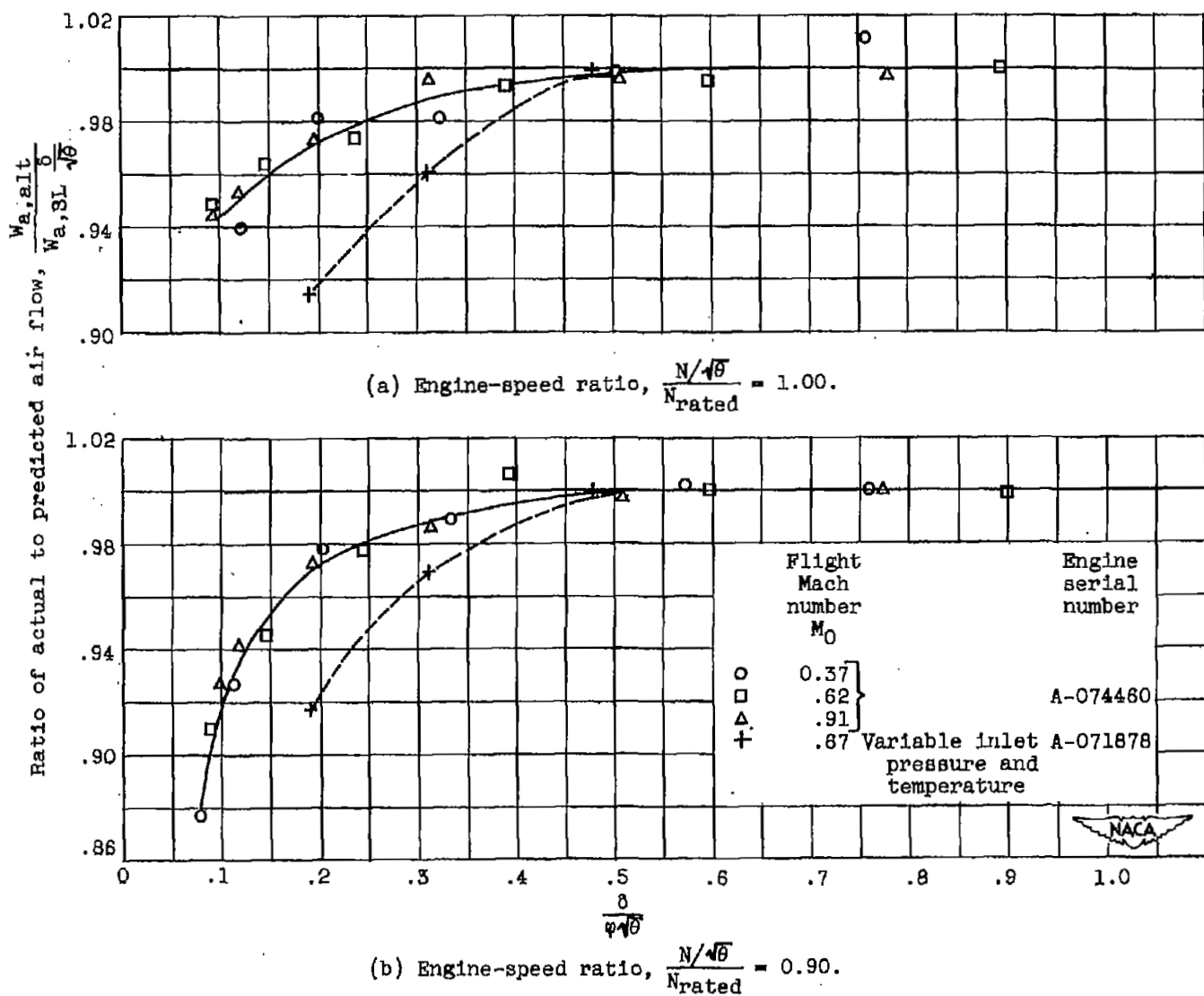


Figure 28. - Ratio of actual to predicted air flow.

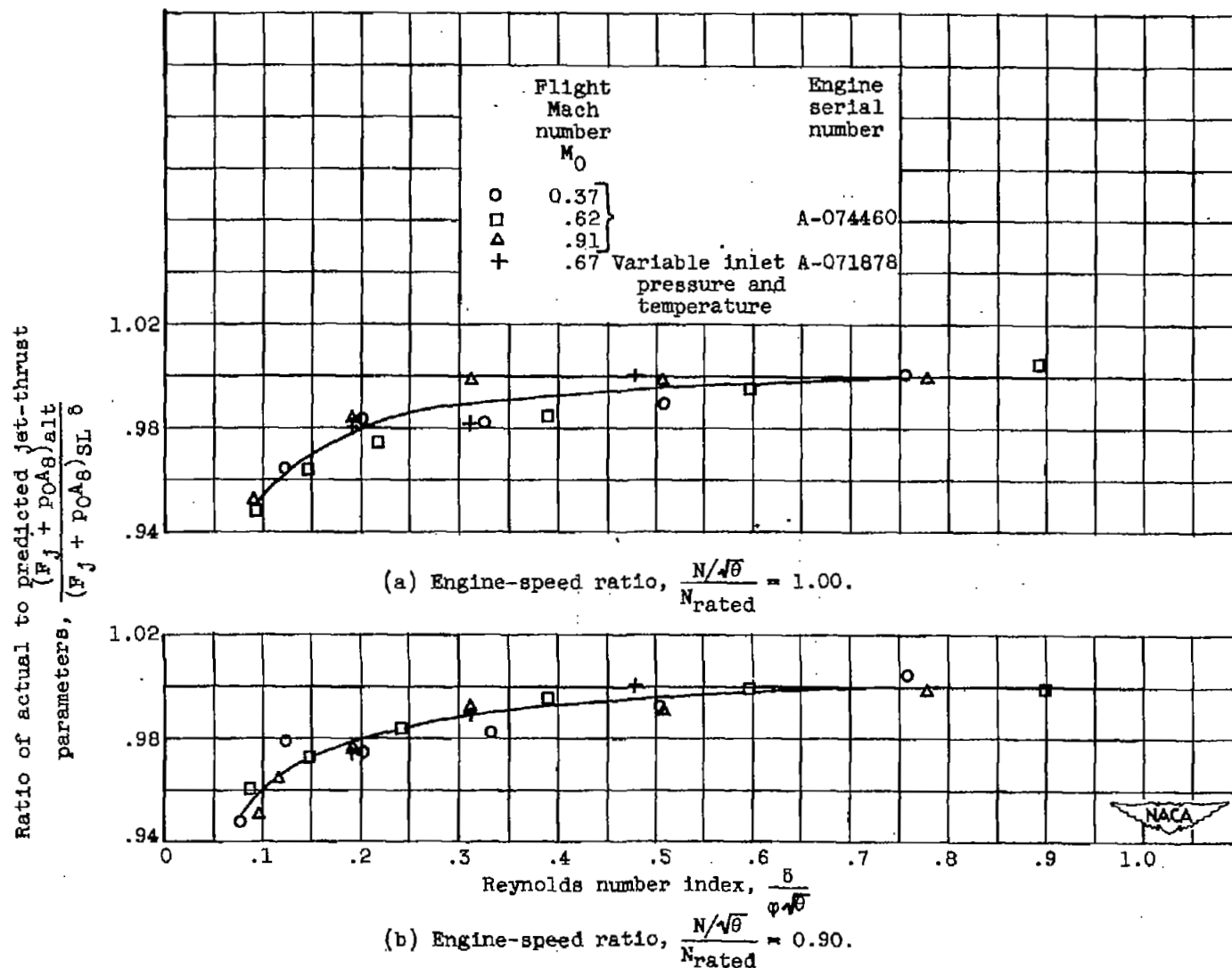


Figure 29. - Ratio of actual to predicted jet-thrust parameters.

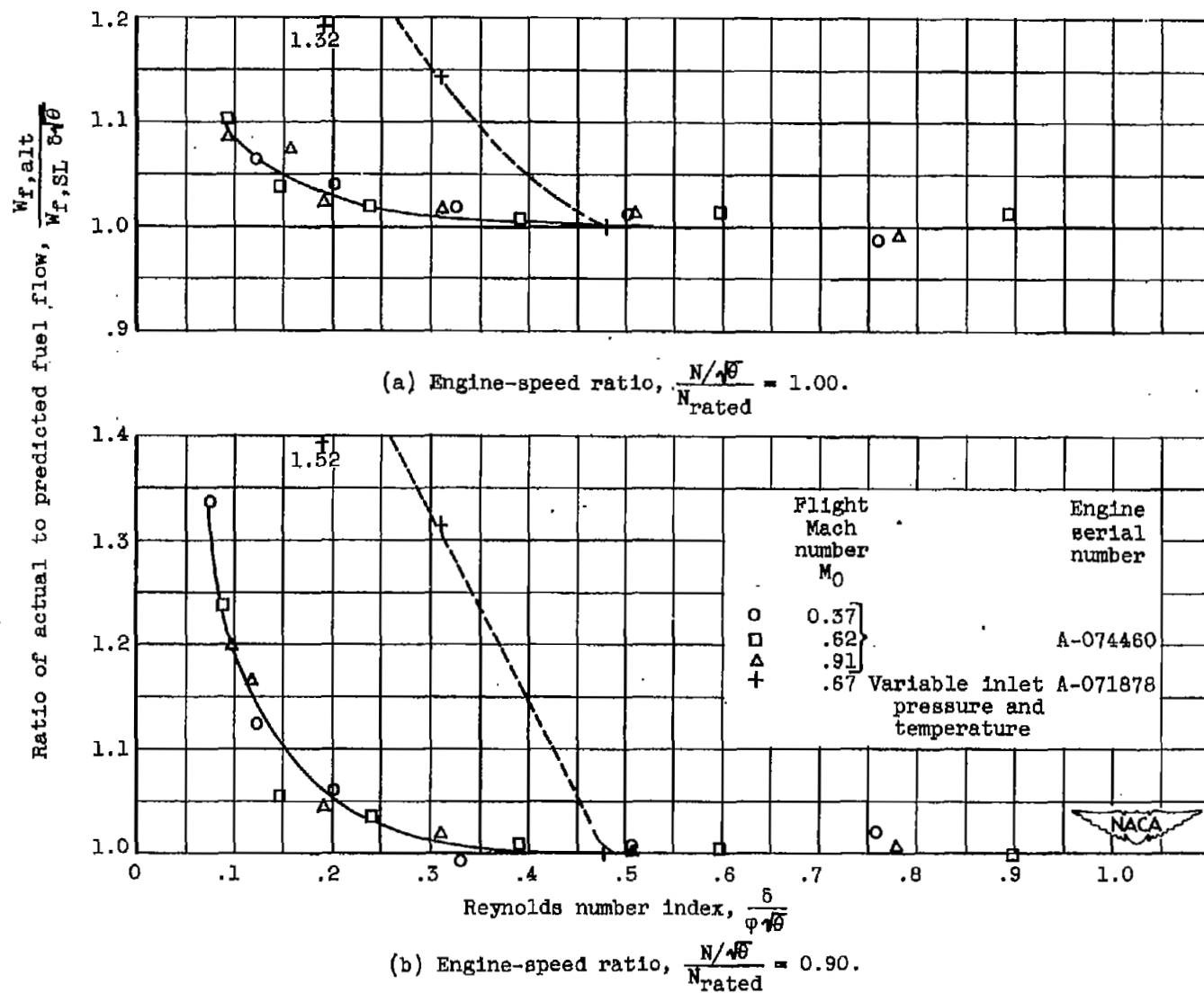


Figure 30. - Ratio of actual to predicted fuel flow.

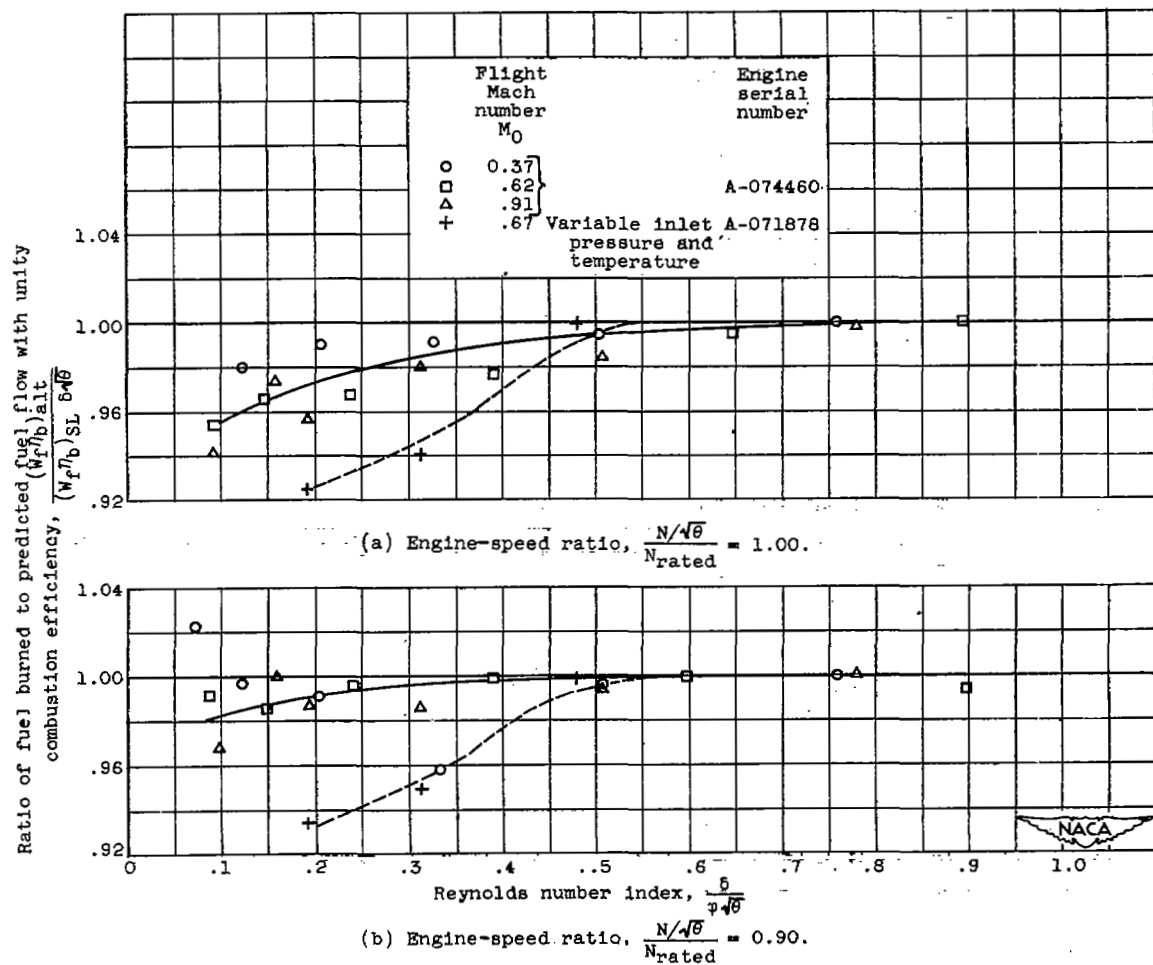


Figure 31. - Ratio of fuel burned to predicted fuel flow with unity combustion efficiency.

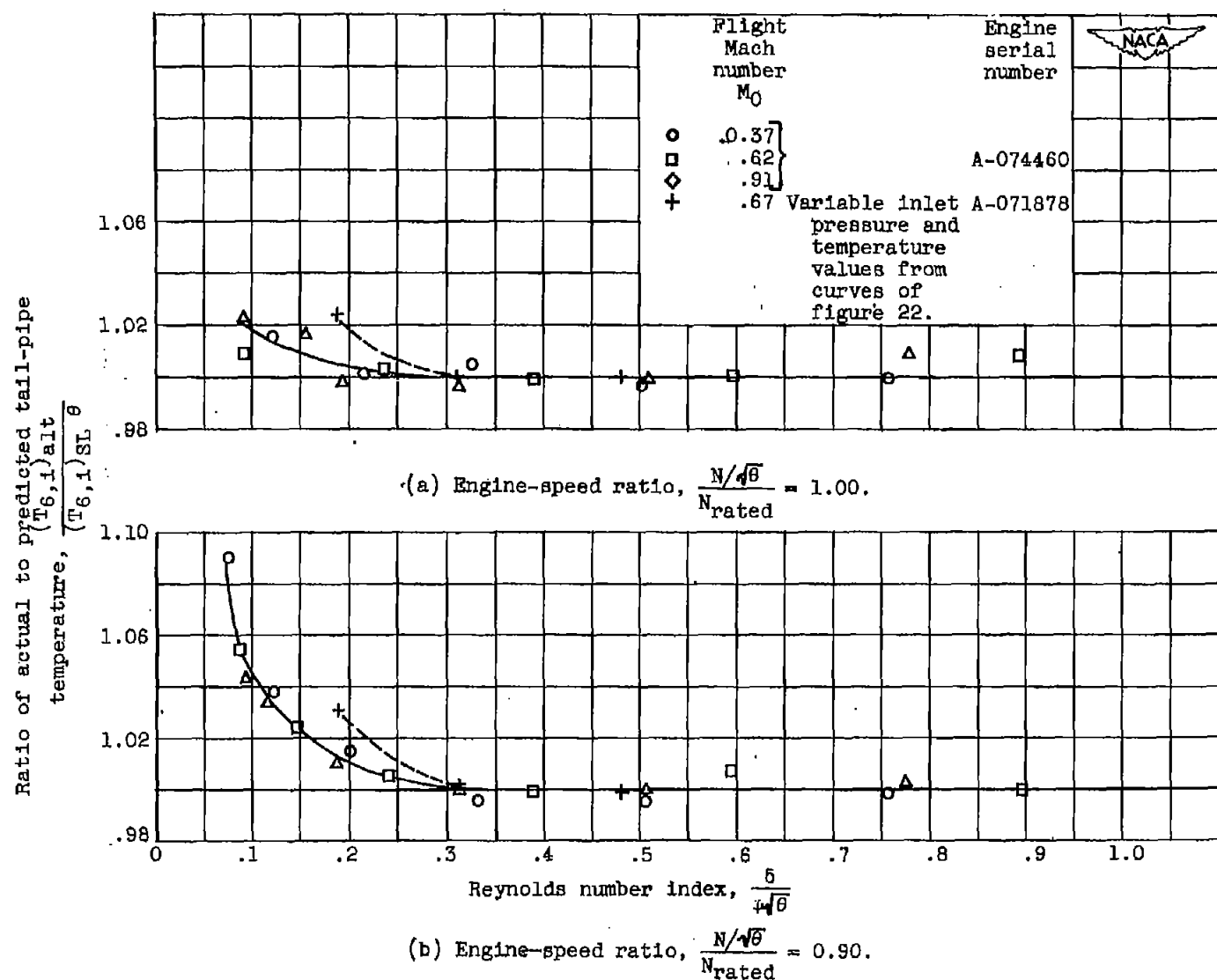


Figure 32. - Ratio of actual to predicted tail-pipe temperature.

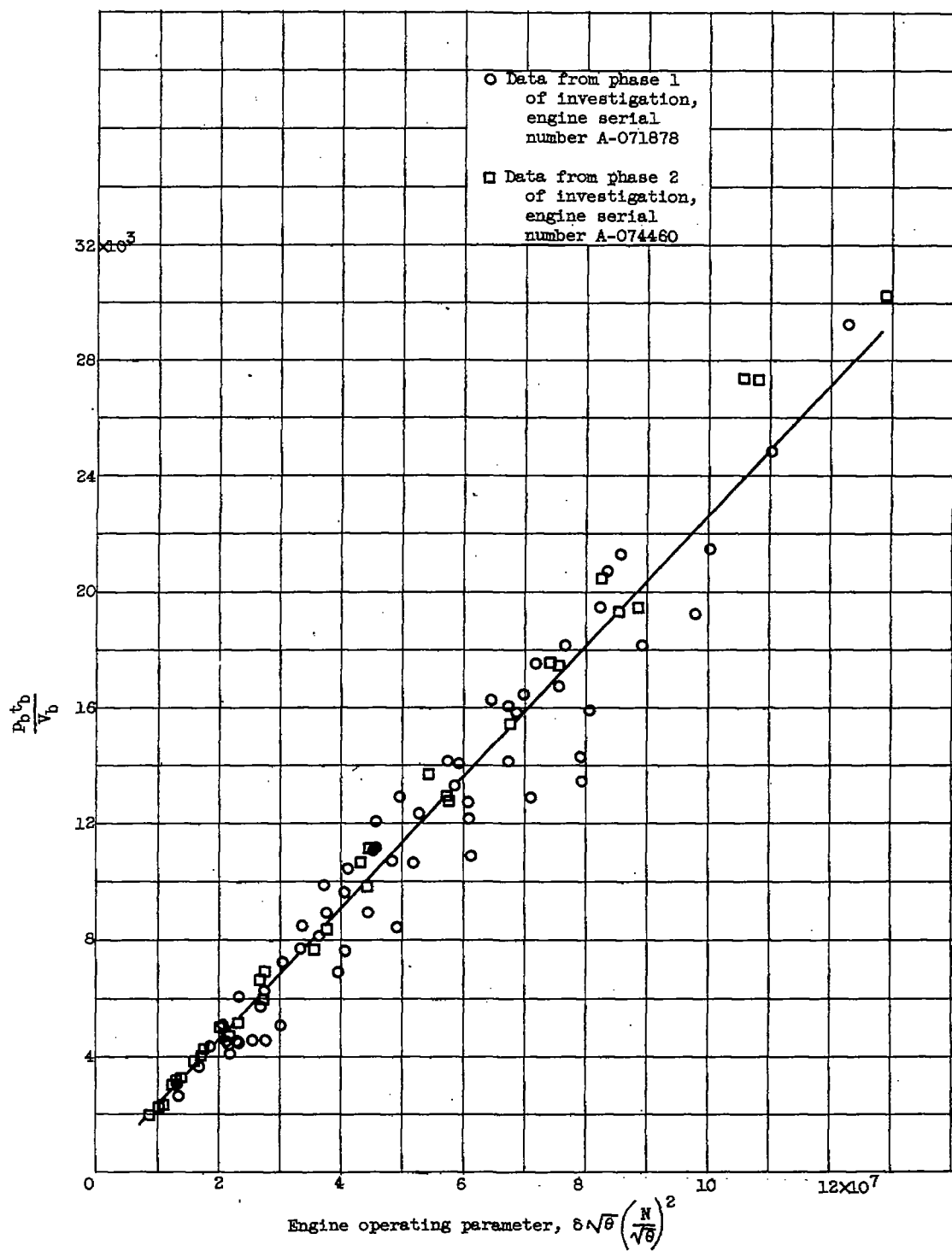


Figure 33. - Correlation of $\frac{P_b t_b}{V_b}$ with engine operating parameter $\delta \sqrt{\theta} \left(\frac{N}{\sqrt{\theta}} \right)^2$

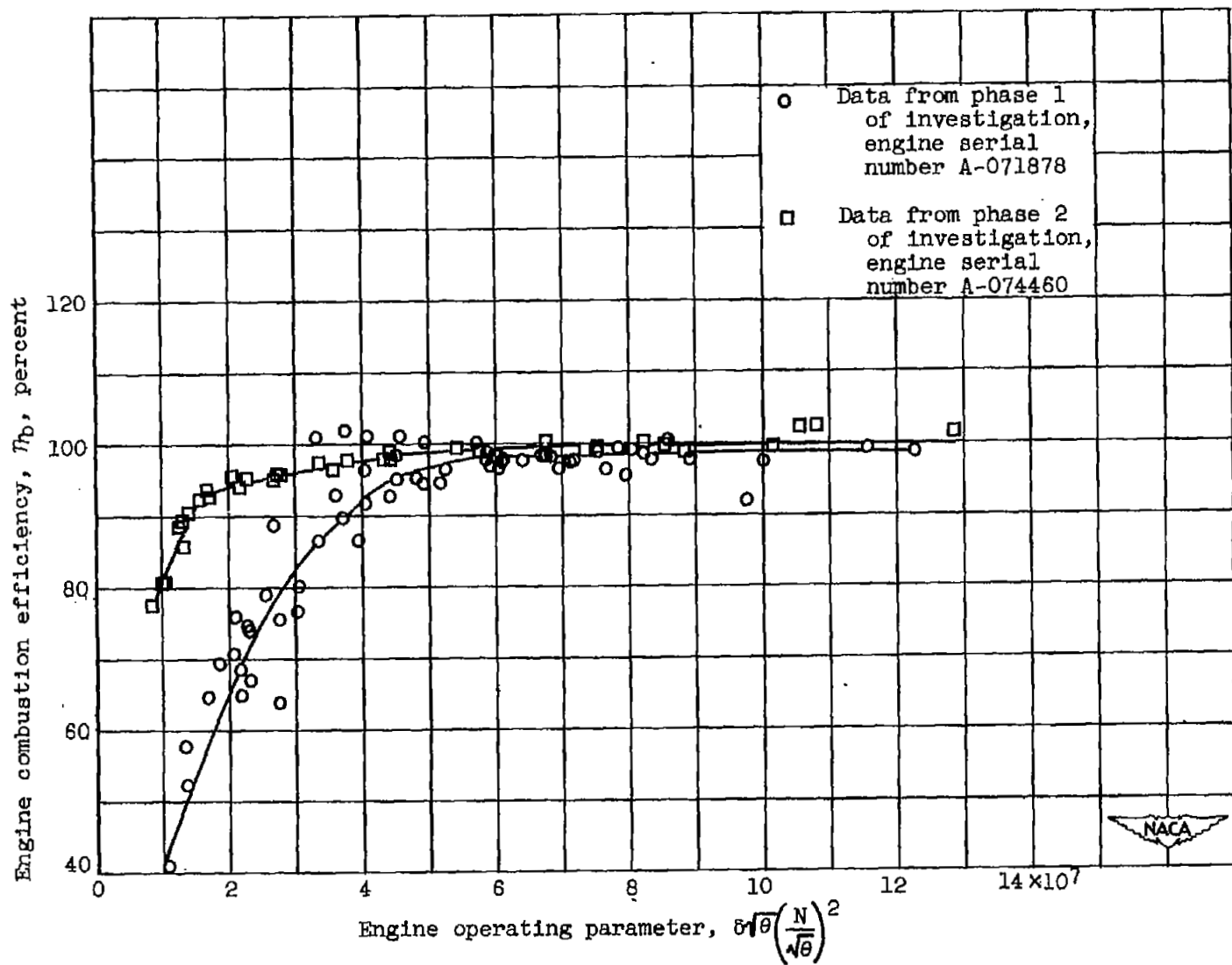


Figure 34. - Correlation of combustion efficiency with engine operating conditions.

NASA Technical Library



3 1176 01435 2182